UNIVERSITY OF CYPRUS
SCHOOL OF PURE AND APPLIED SCIENCES
DEPARTMENT OF BIOLOGICAL SCIENCES
AND
MOLECULAR MEDICINE RESEARCH CENTER

MICRORNAS AS MODIFIERS OF PHENOTYPE IN GLOMERULAR DISEASE AND AS POTENTIAL REGULATORS OF GENE TRANSCRIPTION

GREGORIS PAPAGREGORIOU

PhD THESIS

SUPERVISOR: PROF. CONSTANTINOS DELTAS

NICOSIA, MAY 2012

BOARD OF EXAMINERS

Constantinos Deltas, Professor, University of Cyprus

Antonis Kyrmizis, Assistant Professor, University of Cyprus

Pantelis Georgiades, Assistant Professor, University of Cyprus

Margarita Chatzopoulou-Kladara, Professor, Aristoteleion University Thessaloniki

Jiannis Ragoussis, Reader, Oxford University UK

ABSTRACT

Phenotypic severity in glomerular diseases cannot be usually explained by mutations in relevant genes, thus suggesting the implication of modifier genes which drive the clinical picture towards a milder or a severe course of the disease. We hypothesized that faulty expressional regulation of genes associated with the glomerulus by microRNAs, can be influencing such phenotypic alterations. After performing microRNA 3'UTR and promoter region target prediction analyses using relevant genes, including the Heparin Binding Epidermal Growth Factor (HBEGF) gene, we proceeded in sequencing analysis of the 3'UTR regions in 162 patients having mild or severe thin basement membrane nephropathy (TBMN). HBEGF is expressed in podocytes and was shown to play a role in glomerular physiology. A single nucleotide polymorphism, C1936T (rs13385), was identified at the 3'UTR of *HBEGF* that corresponds to the second base of the seed region of miR-1207-5p. When AB8/13 undifferentiated podocytes were transfected with miRNA mimics and inhibitors of miR-1207-5p, the HBEGF protein levels were reduced by about 50%. A DNA fragment containing the SNP C1936 allele was cloned into the pMIR-Report Luciferase vector and co-transfected with miRNA mimics of miR-1207-5p into AB8/13 podocytes. In agreement with western blot data, this resulted in reduced luciferase expression demonstrating the ability of miR-1207-5p to directly regulate HBEGF expression. On the contrary, in the presence of the T1936 allele, this regulation was abolished. Collectively, these results demonstrate that variant T1936 of this miRSNP prevents miR-1207-5p from down-regulating HBEGF in podocytes. We hypothesized that this variant has a functional role as a genetic modifier. To this end, we showed that in a cohort of 78 patients diagnosed with CFHR5 nephropathy (also known as C3-glomerulopathy), inheritance of the T1936 allele was significantly increased in the group demonstrating progression to chronic renal failure on long follow-up. No similar association was detected in a cohort of patients with thin basement membrane nephropathy, as well as in other cohorts manifesting with primary or secondary glomerulopathy, such as patients with diabetic nephropathy. This is the first report associating a miRSNP as genetic modifier to a monogenic renal disorder.

Prediction analysis of miRNA target sites on DNA regions located up to 10kb upstream of gene transcription start points using the miRWalk algorithm, revealed some interesting results with certain miRNAs having target sites of extended match length on such sites. The hsa-miR-

548c-5p was predicted to target a 21nt long site located more than 8kb upstream of the *FOXC2* gene. An extensive bioinformatic prediction analysis regarding this miRNA and the family it belongs to (miR-548) indicated that miR-548c-5p and the miR-548 family in general are predicted to have more target sites within 10kb upstream of the gene 5'UTRs than in any other gene region. These sites are quite extended in length as regards the actual number of nucleotides hybridizing to the target requence. We hypothesized that this miRNA can target its predicted DNA sequence upstream *FOXC2* and we used luciferase reporter constructs bearing their multiple cloning sites right before a core promoter to prove this direct interaction. The miR-548c-5p DNA target site was cloned into these vectors, while a second plasmid was generated using side directed mutagenesis, which lacked that miRNA target site but preserved ≈200bp of the region flanking the site. Transfection of AB8/13 podocytes with both plasmids showed a significant increase of luciferase expression levels when the miR-548c-5p site was removed, thus suggesting a repressive role for this sequence in transcription. To prove the direct binding of miR-548c-5p on its target sequence, AB8/13 podocytes were transfected with miR-548c-5p mimics and the plasmid bearing the miRNA target site, causing luciferase levels to be significantly reduced. Transfections with miRNA inhibitors showed a boost in luciferase expression levels, as endogenously expressed miR-548c-5p was removed. To support further these results we developed a modified chromatin immunoprecipitation (ChIP) protocol and succeeded in isolating both the DNA region targeted by miR-548c-5p and the miR-548c-5p itself, using an antibody against all Argonaute (AGO) proteins. Specifically, we managed to isolate the endogenously expressed miR-548c-5p from the nucleus of cultured cells, together with its respective predicted target region upstream the *FOXC2* gene. Conclusively, this is the first attempt in showing directly that a specific miRNA may be acting as regulator of transcription in the nucleus.

ΠΕΡΙΛΗΨΗ

Η φαινοτυπική ετερογένεια που παρατηρείται στις σπειραματικές νεφρικές νόσους, δεν μπορεί συνήθως να εξηγηθεί από τις μεταλλάξεις που εντοπίζονται σε γονίδια σχετικά με τις νόσους. Συνεπώς, η εμπλοκή τροποποιητικών γονιδίων στις ασθένειες αυτές είναι ένας σημαντικός παράγοντας για την πρόβλεψη της εξέλιξης της νόσου σε ήπια ή σοβαρή νεφρική νόσο. Υποθέσαμε πως βλάβες στον μηχανισμό ρύθμισης της έκφρασης γονιδίων, που σχετίζονται με την λειτουργία και δομή του σπειράματος, από microRNAs μπορεί να καθορίζει ή να επηρεάζει τις ανομοιομορφίες στην κλινική εικόνα ασθενών με τέτοιες νόσους. Αφού πραγματοποιήθηκαν προβλέψεις στόχων των microRNAs στο 3'UTR και σε μια διευρυμένη περιοχή του προαγωγέα επιλεγμένων γονιδίων, στα οποία περιλαμβανόταν το γονίδιο που κωδικοποιεί για το Heparin Binding Epidermal Growth Factor (HBEGF), προχωρήσαμε σε αλληλούχιση των περιοχών 3'UTR από γονίδια που κρίθηκαν ως καλά υποψήφια σε 162 ασθενείς με ήπια ή σοβαρή νεφροπάθεια των λεπτών μεμβρανών (ΝΛΜ). Το γονίδιο *HBEGF* εκφράζεται στα ποδοκύτταρα και έχει αποδεδειγμένο ρόλο στην διατήρηση της φυσιολογικής λειτουργίας του σπειράματος. Ένας σημειακός πολυμορφισμός, ο C1936T (rs13385), βρέθηκε στο 3'UTR του *HBEGF* ο οποίος αντιστοιχεί στην δεύτερη θέση της ακολουθίας δράσης (seed region) του hsa-miR-1207-5p. Όταν AB8/13 μη-διαφοροποιημένα ποδοκύτταρα επιμολύνθηκαν με μιμητές και παρεμποδιστές του συγκεκριμένου miRNA, τα επίπεδα της πρωτεΐνης HBEGF μειώθηκαν περίπου στο μισό. Ακολούθως, ένα κομμάτι DNA που περιλάμβανε το αλληλόμορφο C1936 κλωνοποιήθηκε στο πλασμίδιο αναφοράς pMIR-Report Luciferase και μαζί με μιμητές του miR-1207-5p μεταφέρθηκε σε AB8/13 ποδοκύτταρα. Όπως παρατηρήθηκε και στα πειράματα αποτύπωσης κατά western, η έκφραση της λουσιφεράσης μειώθηκε καταδεικνύοντας την ικανότητα του miR-1207-5p να ρυθμίζει απευθείας την έκφραση του mRNA του *HBEGF*. Αντιθέτως, στην παρουσία του αλληλομόρφου T1936, η ρύθμιση αυτή καταργήθηκε. Συνολικά, τα αποτελέσματα αυτά αποδεικνύουν πως ο πολυμορφισμός T1936 παρεμποδίζει το miR-1207-5p να μειώνει ρυθμιστικά το HBEGF στα ποδοκύτταρα. Είναι πιθανόν ένας τέτοιος πολυμορφισμός να έχει κάποιο λειτουργικό ρόλο σαν τροποποιητικός παράγοντας. Μετά την γονοτύπηση 78 ασθενών με σπειραματοπάθεια CFHR5, φάνηκε στατιστικά ενισχυμένη η παρουσία του T1936 αλληλόμορφου σε ασθενείς με σοβαρή εξέλιξη της νόσου αυτής σε νεφροπάθεια τελικού σταδίου. Άλλες ομάδες ασθενών οι οποίες εμφανίζουν σπειραματοπάθεια η οποία οφείλεται σε πρωτογενή ή δευτερογενή αίτια, αλλά και ασθενείς

με ΝΛΜ, δεν έδειξαν παρόμοια συσχέτιση. Αυτή είναι η πρώτη αναφορά στην οποία εμφανίζεται συσχέτιση και χαρακτηρισμός ενός πολυμορφισμού σχετικού με microRNA και μιας μονογονιδιακής νεφρικής νόσου.

Η πρόβλεψη στόχων των miRNA που ενδεχομένως βρίσκονται σε ακολουθίες 10kb πριν τα σημεία έναρξη της μεταγραφής γονιδίων (δηλαδή 10 χιλιάδες βάσεις πριν την αρχή του 5'UTR άκρου τους), έγινε με τον αλγόριθμο miRWalk. Τα αποτελέσματα της ανάλυσης αυτής είχαν μεγάλο ενδιαφέρον, αφού φάνηκε πως συγκεκριμένα miRNAs παρουσίαζαν διευρυμένες σε μήκος ακολουθίες στόχους σε τέτοιες περιοχές πριν την έναρξη των γονιδίων που ελέγχθηκαν. Το hsa-miR-548c-5p προβλέφθηκε να στοχεύει μια ακολουθία μήκους 21 νουκλεοτιδίων σε μια περιοχή περίπου 8kb μακριά από την έναρξη του γονιδίου *FOXC2*. Ακολούθησε μια σειρά αναλύσεων προβλέψεων των στόχων του miRNA αυτού και των μελών της οικογένειας στην οποία ανήκει (miR-548), οι οποίες έδειξαν πως τόσο το miR-548c-5p όσο και η οικογένεια miR-548 προβλέπεται να στοχεύουν ακολουθίες μεγάλου μήκους που βρίσκονται κατά προτίμηση σε περιοχές DNA πριν τα σημεία έναρξης της μεταγραφής των γονιδίων, παρά σε οποιοδήποτε άλλο μέρος ενός γονιδίου. Υποθέσαμε πως το miRNA αυτό μπορεί και συνδέεται απευθείας στην DNA ακολουθία στόχο του πριν το γονίδιο *FOXC2*, έτσι χρησιμοποιήθηκε ένα πλασμιδιακό σύστημα αναφοράς με λουσιφεράση, το οποίο φέρει την θέση κλωνοποίησής του ακριβώς πριν τον βασικό υποκινητή του γονιδίου της λουσιφεράσης. Η ακολουθία στόχος κλωνοποιήθηκε στο πλασμίδιο αυτό, ενώ δημιουργήθηκε και ένα δεύτερο πλασμίδιο από το οποίο απουσίαζε η ακολουθία στόχος όμως διατηρήθηκαν οι γειτονικές εκατέρωθεν ακολουθίες. Ακολούθως, επιμολύνθηκαν AB8/13 ποδοκύτταρα με τους πλασμιδιακούς φορείς και δείχθηκε ο κατασταλτικός ρόλος που έχει η ακολουθία στόχος στην έκφραση της λουσιφεράσης, η οποία είχε αυξημένα επίπεδα έκφρασης στην απουσία της ακολουθίας στόχου. Για να δειχθεί περεταίρω η πιθανή απευθείας σύνδεση του miR-548c-5p στην ακολουθία DNA στόχο του, τα μη-διαφοροποιημένα ποδοκύτταρα AB8/13 επιμολύνθηκαν με μιμητές του miR-548c-5p και το πλασμίδιο λουσιφεράσης που έφερε την περιοχή στόχου του συγκεκριμένου miRNA, με αποτέλεσμα να μειωθούν δραστικά τα επίπεδα έκφρασης της λουσιφεράσης. Επιμόλυνση με παρεμποδιστές του miR-548c-5p έδειξαν τα αντίθετα αποτελέσματα, αφού απενεργοποιήθηκαν τα ενδογενώς εκφραζόμενα miRNAs και η περιοχή παρέμεινε ελεύθερη από οποιαδήποτε ρυθμιστική δράση σχετική με το miRNA αυτό. Τα αποτελέσματα αυτά συμπληρώθηκαν με την εφαρμογή ενός τροποποιημένου πρωτοκόλλου ανοσοκαθίζησης χρωματίνης (chromatin immunoprecipitation

- ChIP), με το οποίο έγινε ταυτόχρονη απομόνωση τόσο του miRNA, όσο και της DNA περιοχής στόχου του σε διαλύματα όπου χρησιμοποιήθηκε αντίσωμα που στοχεύει όλα τα μέλη της οικογένειας πρωτεϊνών Argonaute (AGO). Συνολικά, αυτή είναι η πρώτη απόπειρα χρήσης πλασμιδίων αναφοράς λουσιφεράσης για την απόδειξη της πιθανής απευθείας σύνδεσης ενός miRNA σε μια ακολουθία DNA. Ταυτόχρονα, επιτύχαμε την απομόνωση ενδογενώς εκφραζόμενου miR-548c-5p από ποδοκύτταρα σε καλλιέργεια, μαζί με την αντίστοιχη DNA ακολουθία στόχο του.

ACKNOWLEDGEMENTS

This study started as an attempt to incorporate two seemingly independent but equally important research fields at the Molecular Medicine Research Center some years ago: glomerular diseases and microRNAs. Although there was considerable risk in embracing this task, the project proved to be fruitful and a source of scientific excitement and innovation. This work was supported by grants, mainly by the George & Maria Tyrimos endowment through a scolarship by the Pancyprian Gymnasium, Nicosia, and partly co-funding by the European Regional Development Fund and the Republic of Cyprus through the Research Promotion Foundation (Strategic Infrastructure Project ΝΕΑ ΥΠΟΔΟΜΗ/ΣΤΡΑΤΗ/0308/24), to my supervisor and mentor, Prof. C. Deltas.

My biggest gratitude goes to my supervisor Prof. Constantinos Deltas, for his support, his guidance and provision of space and ideas to realize this project and the completion of my PhD thesis. I am deeply grateful to him and like him to know that through the years the Laboratory of Molecular and Medical Genetics, has been both a school and a home away from home to me.

I would also like to thank the person behind this project, Ass. Prof. Kyriacos Felekkis. I am greatly indebted to him for leading me through the project, for sharing his technical expertise and passing me scientific knowledge and culture and by promoting a sophisticated and critical way of thinking to me regarding science.

In addition, I would like to acknowledge our collaborators in this project, Prof. Norbert Gretz and his team at Mannheim, especially Harsh Dweep, for all the support regarding miRWalk prediction analyses and statistics; Prof. Andrew Nicolaides for providing the samples of the "Cyprus Study" cohort; Dr Andrie Panayiotou, for her support and collaborative spirit, Dr Alkis Pierides, Dr Yiannis Athanasiou and all other clinical nephrologists of the public sector in Cyprus, who provided clinical material and information that contributed to this project. I also thank Dr Moin Saleem, Bristol, UK, for providing us with the AB8/13 podocyte cell line.

A big *thank you* must also go to all the members of the Laboratory of Molecular and Medical Genetics, past and present: Dr Konstantinos Voskarides, for sharing his knowledge on genetic analysis, Dr Kamil Erguler, for him being the living proof that Biologists do know their way around statistics, Dr Myrtani Pieri, for her influence and guidance on molecular biology

techniques and for being there when a talk was needed, Louiza Papazachariou, for being a good friend and colleague with always a positive way to look at things, Panagiota Demosthenous, for her stress-relief powers, Charalambos Stefanou, for tolerating me, Andrea Christofides, for her excitement in continuing this project, Demetris Tsiakkis, for his invaluable help and last but not least Dr Panayiota Koupepidou, for her guidance and support.

I could not end without thanking all my other candidate PhD fellows at the University of Cyprus, for working together to make our Department competitive and student-friendly. It is indeed a big challenge to belong in this community and wish them to have the strength and stamina to complete their thesis soon.

Finally, I would like to thank all of my friends, for their support during all these years and for being there for me in good and in bad. Thank you for keeping me balanced and ready to face everything keeping me back.

This work is dedicated to my family. None of this would have been achieved without them and I hope I will be able to return all the love and support I have gratefully received over the years. Even in the hardest of times, they made me understand that I have the strength to overcome and survive. Thank you.

TABLE OF CONTENTS

LIST OF FIGURES

LIST OF TABLES

LIST OF ABBREVIATIONS

ADMA	***Asymmetrical Dimethylarginine***
Ago	***Argonaute Protein***
ANOVA	***Analysis Of Variance***
bp	***Basepairs***
C3	***Complement factor 3***
cDNA	***Complementary DNA***
CDS	***Coding Sequence***
CFHR5	***Complement Factor H-Receptor 5***
ChIP	***Chromatin Immunoprecipitation***
CKD	***Chronic Kidney Disease***
COL4A3	***Collagen type IV chain alpha 3***
COL4A4	***Collagen type IV chain alpha 4***
CP	***Crossing Point***
db	***Diabetic***
DGCR8	***DiGeorge syndrome critical region gene 8***
DN	***Diabetic Nephropathy***
DNA	***Deoxyribonucleic Acid***
ds	***Double Stranded – dsRNA***
DTT	***Dithiothreitol***
E. coli	***Escherichia coli***
ECL	***Enhanced Chemiluminescence***
EDTA	***Ethylenediaminetetraacedic Acid***
ESKD	***End Stage Kidney Disease***
FA	***Folic Acid***
FBS	***Fetal Bovine Serum***
FH	***Familial Hematuria***
For	***Forward***
FOXC2	***Fork-head box C2***
GAPDH	***Glyceraldehyde-3-phosphate Dehydrogenase***
GBM	***Glomerular Basement Membrane***
GFB	***Glomerular Filtration Barrier***
GN	***Glomerulonephritis***
GTP	***Guanosine Triphosphate***
HBEGF	***Heparin Binding Epidermal Growth Factor***
HEK	***Human Embryonic Kidney Cells***
HEPES	***4-(2-hydroxyethyl)-1-piperazineethanesulfonic acid***
HGS	***Hypertensive Glomerulosclerosis***
HREpiC	***Human Renal Epithelial Cells***
HRP	***Horseradish Peroxidase***
Hrs	***Hours***
Ig	***Immunoglobulin – A, G etc***
IgGN	***IgG Nephropathy***
IP	***Immunoprecipitation***
IR	***Ischemia/Reperfusion***
Kb	***Kilobases***
LNA	***Locked Nucleic Acid***
MCS	***Multiple Cloning Site***
MH	***Microscopi Hematuria***
miRNA	***microRNA***
miRNP	***miRNA Ribonucleoprotein Complex***
miRSNP	***microRNA-associated Single Nucleotide Polymorphism***

MMP	***Matrix Metalloproteinase – 1,2,8,9***
MPO	***Myeloperoxidase***
mRNA	***Messenger RNA***
MTHFR	***Methylenetetrahydrofolate Reductase***
NO	***Nitric Oxide***
NP-40	***Nonidet P-40***
nt	***Nucleotides***
PBS	***Phosphate Buffered Saline***
PCR	***Polymerase Chain Reaction***
PI	***Protease Inhibitors***
PVDF	***Polyvinylidene Fluoride***
PVT1	***Plasmacytoma Variant Translocation gene 1***
QTL	***Quantitative Trait Loci***
RASSF3	***Ras-association Factor 3***
Rev	***Reverse***
RI	***RNAse Inhibitors***
RISC	***RNA-induced Silencing Complex***
RITS	***RNA-induced Transcriptional Silencing Complex***
RLU	***Relative Light Units***
RNA	***Ribonucleic Acid***
RNAi	***RNA interference***
RNAP2	***RNA Polymerase II***
rpm	***Rounds Per Minute***
RPMI	***Roswell Park Memorial Institute Medium***
RT	***Reverse Transcription***
s	***Seconds***
SD	***Standard Deviation***
SDM	***Side-directed Mutagenesis***
SDS	***Sodium Dodecyl Sulfate***
SEM	***Standard Error Mean***
siRNA	***Small Interfering RNA***
snoRNA	***Small Nucleolar RNA***
SNP	***Single Nucleotide Polymorphism***
snRNA	***Small Nuclear RNA***
SPP1	***Secreted Phosphoprotein 1***
SRNS	***Steroid-Resistant Nephrotic Syndrome***
TBMN	***Thin Basement Membrane Nephropathy***
TE	***Transposable Element***
TGS	***Transcriptional Gene Silencing***
TIMP	***Tissue Inhibitor Of Metalloproteinase – 1,2***
U	***Units***
UTR	***Untranslated Region***
yo	***Years Old***
β-gal	***Beta-Galactosidase***

1. INTRODUCTION

1.1 Kidney physiology and glomerular function

1.1.1 The human kidney

In order for the human body to preserve its physiological function, internal homeostasis must be preserved. The human kidneys are responsible for controlling fluid homeostasis by constantly actualizing their excretory and secretory properties.[1] Kidneys control the volume and osmomolarity of body fluids, as well as keep a balanced electrolyte load (Na^+, K^+, Cl^-, HCO_3^-, H^-, Ca^{2+}, Mg^{2+}, PO_4^{3-}) in the body in order to preserve homeostasis. In addition, kidneys are responsible for the excretion of metabolic byproducts and toxins, while they can also secrete or activate hormones such as renin, erythropoietin, 1,25-dihydroxyvitamin D_3, prostaglandins and kinins.[2]

Each kidney is estimated to contain 1.5 million nephrons, the units that perform all basic functions of the organ. There are two kinds of nephrons; cortical and juxtamedullary. A nephron consists of the renal corpuscle (with the glomerulus and the Bowman's capsule - Figure 1), the proximal convoluted tubule, the loop of Henle, the distal convoluted tubule and finally the collecting duct.[2] The blood stream enters the kidney through an afferent arteriole, which is further divided into capillaries that form the glomerulus, in order for the primary urine filtrate to be collected into the Bowman's capsule. Then this filtrate travels through the tubular system for water and ions to be re-absorbed and urine is gathered via the collecting duct into the renal pelvis and finally to the urethra through the ureter.[1]

Kidney diseases are usually divided into two main categories that are based on the nephron part being affected; thus nepropathies can be of glomerular (Table 1) or tubular origin.[3] Tubular renal diseases usually manifest with renal cysts and a wide spectrum of extra-renal symptoms, while glomerular diseases are due to defects of the glomerulus and the glomerular filtration barrier and present with hematuria, proteinuria and focal segmental glomerulosclerosis (FSGS).[3,4]

1.1.2 The glomerulus and its filtration barrier

The kidney glomerulus consists of a "tuft", where a capillary is convoluted to introduce the stream of blood to be filtered inside the kidney, surrounded by the Bowman's capsule (Figure 1). [5] This capillary is structurally enforced by the glomerular basement membrane (GBM); hence the GBM serves as the board on which both fenestrated glomerular endothelial cells and podocytes (epithelial cells) are attached to form the glomerular filtration barrier (GFB - Figure 2).[6,7] The GFB is ordered to survey the mobility of the plasma ultrafiltrate towards the urinary space and prevent plasma proteins, albumin and immunoglobulins, from escaping. Molecular and structural defects caused by mutations in genes coding for GFB associated proteins or by the deregulation of protein expression levels can lead to glomerular disease, usually manifesting with proteinuria and hematuria.

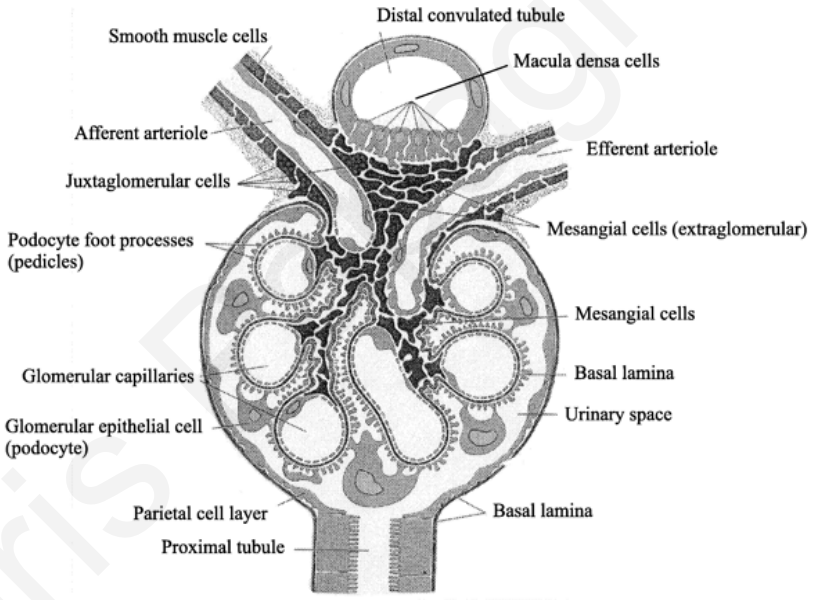

Figure 1: The kidney glomerulus with its filtration barrier surrounded by the Bowman's capsule. The afferent arteriole introduces the blood stream into the glomerulus via capillary arterioles. The blood is then filtered to produce the urine and then exit through the efferent arteriole. Mesangial cells support the structure of the glomerulus, while the juxtaglomerular apparatus, through its macula densa cells, senses the blood flow pressure. Taken from Ross M.H., et al., 1989.[8]

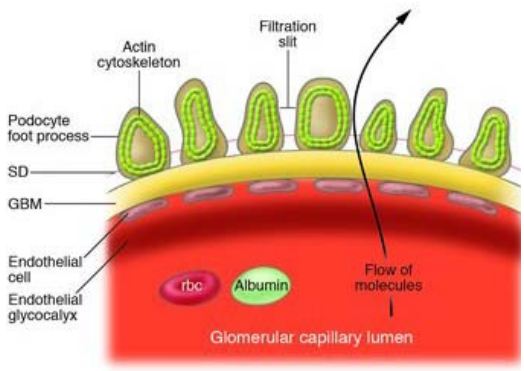

Figure 2: The glomerular filtration barrier (GFB) consisted by the fenestrated glomerular endothelial cells, the glomerular basement membrane (GBM) and the podocyte foot processes. Foot processes of neighboring podocytes communicate through slit diaphragms (SD), which are shaped by protein networks. The GFB acts to prohibit the escape of large molecules, such as albumin, or red blood cells to the urine. Misshaping of the GFB due to mutations in relevant genes, results in hematuria and/or proteinuria and finally renal failure. Taken from Ronco, P. J, 2007.[9]

The cellular components of the GFB are responsible for the maturation, the maintenance and the functional and structural integrity of the GBM.[10,11] The glomerular endothelial cells are lined on the capillary wall having fenestrations with a diameter of 70-100nm.[6] Their surface is covered by a negatively charged glycocalyx acting as a barrier for plasma molecules depending on their charge rather than size.[12]

The GBM is composed of collagen IV molecules winded up in α3α4α5 trimers, together with laminins α5β2γ1, endactin/nidogen and proteoglycans, perlecan and agrin.[13,14] Being a thicker membrane, in contrast with common basement membranes, the GBM is transformed during various glomerular diseases and becomes unusually thin when *COL4A3* and *COL4A4* genes are mutated or serves as the center in which extracellular matrix is deposited during diabetic nephropathy leading to sclerosis.[15,16]

The podocyte is a remarkable, well-differentiated epithelial cell that serves as a trafficking controller between the glomerular capillary lumen and the urinary space of Bowman's capsule. They are polar cells consisting of a cell body sitting on the outer layer of the glomerular basement membrane by using its major processes, which expand and embrace the glomerular capillaries via interdigitating "foot" processes.[5,17] Such foot processes of adjacent podocytes are closely linked by a 40nm-wide network of proteins namely the glomerular slit diaphragm (SD), acting as the ultimate inhibiting guard to the outgo of large molecular weight proteins to the urine ultrafiltrate, while it permits small molecules and water

to flow through.[18] The slit diaphragm and the luminal site of the podocyte are coated by a mix of glycoproteins, such as podocalyxin and podoendin, in order to preserve a strong negative charge functioning as a protein selection barrier.[19,20] Slit diaphragms are organized by intertwining proteins, that control the escape of circulating proteins and are considered as a modified tight junction.[21,22,23] Nephrin is considered as the predominant protein of SD and it is thought to form heterodimers with podocin and NEPH2.[24,25] Mutations in the *NPHS1* gene coding for nephrin, were found to be responsible for the congenital Finnish-type nephrotic syndrome.[26] The SD protein complex also includes the CD2-AP, ZO-1, FAT1, MAGI-1, P-cadherin and LRRC7.[27] Besides *NPHS1*, the *CD2-AP* gene was also found to be mutated in familial and sporadic cases of FSGS, as well as other podocyte specific genes such as ACTN4 and TRPC6.[28,29,30] In addition, mutations in the *NHPS2* gene coding for podocin, have been associated with Steroid-Resistant Nephrotic Syndrome (SRNS).[31] Damage of podocytes leads to nephrotic syndrome, as they are unable to regenerate and recover, therefore their numbers are effectively reduced.[32] Nephrotic syndrome presents with increased proteinuria leading to hypoalbimunuria, oedema, hyperlipidemia and in most cases FSGS, which in turn leads to chronic and soon to end-stage kidney disease (Table 1).

1.2 Inherited glomerulopathies

Clinical phenotypic diversity in inherited glomerular diseases is a frequently observed phenomenon, the molecular pathomechanism of which is rarely explained by researchers. This heterogeneity is exemplified by the observation that not all patients who develop chronic kidney disease (CKD) due to a primary genetic cause will proceed to end-stage kidney disease (ESKD). In such diseases, glomerular defects that include but are not limited to the glomerular basement membrane, the glomerular endothelium and the podocytes can alter the kidney's filtration barrier integrity and lead to an adverse outcome in patients. A subset of glomerular defects emerging from germinal mutations in specific genes or are acquired are directly reflected on podocytes, which may lose their structural integrity and functional properties (Table 1).[33,34]

Table 1: List of monogenic glomerulopathies, together with the gene mutated in each case, their mode of inheritance and characteristic symptoms.[3,35,36]

DISEASE	GENE	INHERITANCE	CHARACTERISTIC PHENOTYPE
Finnish Type Nephrotic Syndrome	NPHS1	AR	Microcystic Nephropathy
Nephrotic Syndrome Type 2	NPHS2	AR	Microcystic Nephropathy FSGS Steroid Resistance
NS Type 3	NPHS3	AR	Diffuse Mesangial Sclerosis FSGS
FSGS Types 1 to 3	ACTN4 CD2-AP TRPC6	AD AD/AR AD	FSGS
Frasier Syndrome	WT1	AD	Diffuse Mesangial Sclerosis FSGS
Alport Syndrome	COL4A3 COL4A4 COL4A5	AR AR XD	Hematuria Proteinuria FSGS Deafness
Alport Syndrome with Leiomyomatosis	COL4A6	XD	
Thin Basement Membrane Nephropathy	COL4A3 COL4A4	AD AD	Hematuria Proteinuria FSGS
CFHR5 Nephropathy	CFHR5	AD	Microscopic Hematuria Proteinuria FSGS
Pierson's Syndrome	LAMB2	AR	Nephrotic Syndrome Microcoria

Microscopic hematuria (MH) of glomerular origin can be a benign condition persisting for life or can be the starting point of a progressive process that may lead many years later to proteinuria and decline of renal function resulting in CKD or ESKD.[37] A prime example is thin basement membrane nephropathy (TBMN) where patients in the same family who bear an identical heterozygous mutation in either the *COL4A3* or *COL4A4* gene that encodes for the α3 or α4 chain of collagen type IV respectively, may follow a quite diverse disease course. In recent studies on a large cohort of patients it was demonstrated that a small percentage of patients will remain for life with benign isolated MH; however a larger fraction of patients will proceed to proteinuria and CKD. Overall 15-20% of patients will have an even worse course and reach ESKD at ages after 50 years of age. In fact, nearly 50% of patients after 50 years will require hemodialysis or a renal transplant.[38]

Similarly, in another recently revisited C3 glomerulopathy that is caused by mutations in the *CFHR5* gene which plays a role in the regulation of the alternative pathway of complement activation, nearly all patients present with MH from childhood, while they may also develop macroscopic hematuria as a response to infections of the upper respiratory tract. Impressively, this disease entity is thus far only recorded in Cyprus, where patients inhabit or originate from mostly some villages in Troodos Mountain, hence called "Troodos Nephropathy". A subset of patients will remain stable but about 15%, predominantly males will develop proteinuria and CKD or ESKD.[39] Female patients appear to have a milder disease progression and according to our recently published work, only 4/18 patients who reached ESKD were females. This variable expressivity might be explained by a number of factors including genetic modifiers through yet unknown molecular mechanisms. MicroRNA (miRNA) regulation of gene expression could be one of these factors.

1.3 microRNAs (miRNAs)

miRNAs belong to the most abundant class of small RNAs in animals. It is a recently discovered class of eukaryotic, endogenous, non-coding RNAs that play a key role in the regulation of gene expression. When mature they are short, single-stranded RNA molecules approximately 21-23 nucleotides in length, and they are partially complementary to one or more messenger RNA (mRNA) molecules.[40] Their main function is to down-regulate gene expression by inhibiting translation or by targeting the mRNA for degradation or deadenylation.[41] The mature miRNA mainly acts by targeting a miRNA recognition element (MRE) on an mRNA's 3'UTR and binding on it through a Watson-Crick base-pairing manner.[42] miRNA target recognition properties depend on its 'seed region', which includes nucleotides 2-8 from the 5'-end of each miRNA.[43] Basepairing between the 3 -segment of the miRNA and the mRNA target is not always essential for repression, but strong base-pairing within this region can partially compensate for weaker seed matches or enhance repression.[44]

miRNAs are thought to finely regulate mRNA translation in almost all cell types and tissues. Landgraf *et al.* performed expression profiling of mammalian miRNAs using small RNA library sequencing from 26 different cell types and organs of both human and rodents.[45]

They found that microRNAs are differentially expressed in almost all tissues and cell types, with certain single miRNAs or miRNA families clustering in specific samples.

1.3.1 Biogenesis

Primary miRNA transcripts (pri-miRNAs) are mostly transcribed by RNA Polymerase II, while in some exceptional cases RNA Polymerase III is used (Figure 3).[46] They are usually polycystronic with a length of more than 1kb. Each miRNA is comprised of a double stranded stem of 33 base pairs, a terminal loop and two flanking unstructured single-stranded segments.[47,48] Pri-miRNAs are cleaved to form pre-miRNAs, which are approximately 60-100 nt long and have a hairpin-like structure.[49] Microprocessors handle this cleavage and are formed by the Drosha protein, an RNAase III endonuclease, and DGCR8/Pasha dsRNA binding protein; they cleave near the hairpin loop base to release both strands of the initial pri-miRNA stem, leaving a 5' phosphate and 3' overhang of 2 nucleotides.[50] Pre-miRNAs are transported into the cytoplasm by Ran-GTP and the export receptor Exportin-5 and then undergo digestion by Dicer ribonuclease to shape a mature double stranded miRNA.[51] Dicer is again an RNAse III enzyme, that was previously shown to be involved in small interfering RNA (siRNA) generation, and is thought to recognize the pre-miRNA through the 5' phosphate and 3' overhang created by Drosha and cuts the terminal base pairs and the loop off the pre-miRNA again by the creation of a 5' phosphate and 3' overhang.[52,53] Finally, miRNAs use the miRNA ribonucleoprotein complex (miRNP), which encompasses RISC-like (RNA-induced silencing complex) structures to form complexes, in order to bind target mRNAs and effectively repress their levels of expression, cleave, deadenylate or destabilize them by decapping.[54,55] The miRNP/RISC complex in humans is formed by proteins like the elF2C2, an Argonaute protein homologue, and the Gemin3 and Gemin4 helicases. Thus far, eight Argonaute proteins have been found in humans and they are thought to perform the cleavage of target mRNAs bound by the RISC through an endonuclease named "Slicer", yet of unknown nature.[56,57]

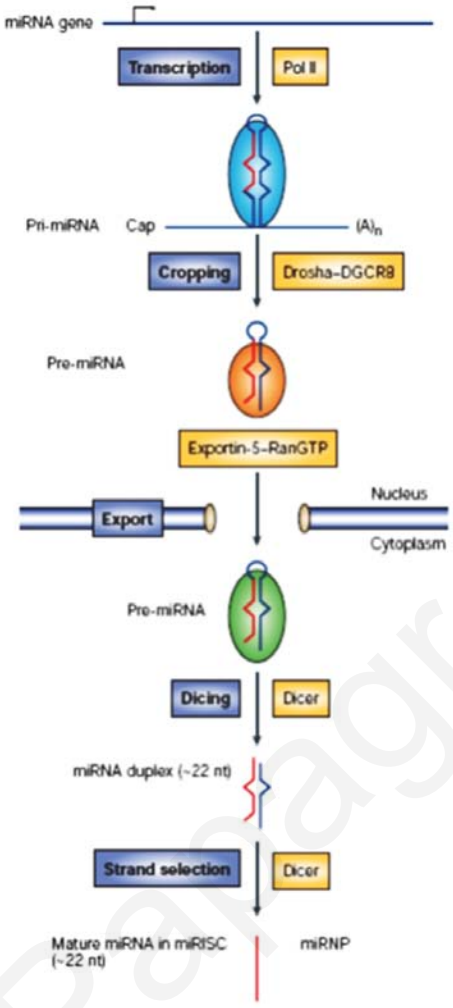

Figure 3: The miRNA biogenesis. See text for a detailed description of this pathway. Adopted by Kim NV, 2005.[58]

1.3.2 Involvement in diseases

In general there are two main mechanisms by which miRNAs can be involved in disease pathogenesis. A mutation on the miRNA itself can render it the primary causative gene. On the other hand, a miRNA can be indirectly involved in disease expression if the gene it targets is defined as the causative gene. The only evidence to our knowledge of a miRNA itself being the primary causative gene came from the work of Mencia et al., in which they identified a point mutation in the seed region of miR-96 which causes autosomal dominant non-syndromic hearing loss.[59] An engineered mouse model with a mutation in the seed region of miR-96, presented a phenotype similar to the human disease confirming the primary role of miR-96.[60] In contrast, a miRNA can be considered as secondary cause to the disease when a genetic variation alters the binding of that miRNA to a causal gene. Evidence for such

mechanism was shown for miR-24 when a point mutation that altered its binding to SLITRK1 gene was identified in patients with Tourette syndrome.[61] Similarly, point mutations on REEP1 which is a candidate gene for hereditary spastic paraplegia were found on the binding sites of two miRNAs (miR-140 and miR-691).[62,63]

Involvement of miRNAs in inherited diseases is not limited to those two mechanisms. Evidence suggests that miRNAs can act as disease modifiers as a result of genetic variations on the precursor molecules or the miRNA-target binding sites. Single nucleotide polymorphisms (SNPs) can affect all states of the miRNA synthesis (pri-, pre-, and mature) and alter the miRNA biogenesis or function. Variations that alter the biogenesis of miRNAs were associated with predispositions to various diseases including congenital heart disease [64], schizophrenia [65], papillary thyroid carcinoma [66] and others. Despite that, it should be noted that genetic variations within the pre-miRNA sequence and specifically within the seed-region are rare and comprise less than 1% of the miRNA-related SNPs.[67]

MicroRNA associated single nucleotide polymorphisms (miRSNPs) found on miRNA target sites within 3'UTRs of mRNAs, are relatively common. A miRSNP can eliminate or weaken the binding of a miRNA to its target site or increase the binding by creating a perfect sequence match to the seed of a miRNA that normally is not associated with the given mRNA, provided that both miRNA and mRNA share the same tissue of expression. In both cases the result will be a significant alteration in protein levels. There are currently three databases available (Patrocles, dbSMR and PolymiRTS) that compile SNPs on the mRNA 3'UTR region of human and mouse genes that create or destroy miRNA binding sites.[68,69,70]

1.3.3 miRNAs in renal diseases

The role of miRNAs in processes such as maturation of the mammalian kidney was recently established by the podocyte-specific inactivation of Dicer, the RNAse III endonuclease responsible for miRNA maturation, in mice.[71,72,73] Podocyte foot processes were consequently depleted, while apoptosis commenced. Animals initially developed albuminuria followed by glomerular sclerosis and tubulo-interstitial fibrosis with acute renal disease progression and eventually death of mice by 6-8 weeks. The pathological phenotype was completed by proteinuria, glomerular basement membrane abnormalities and mesangial expansion, assimilating a congenital glomerulopathy. This proves that miRNAs have a

fundamental role in regulating kidney physiological development; hence they must have a role in renal disease as well.

Implication of miRNA in renal glomerular disease is evident in diabetic nephropathy. The development of glomerular nephropathy in patients diagnosed with type 1 or 2 diabetes is restricted to 30%, with most proceeding to end-stage renal disease depending on their genetic burden or environmental factors.[74] Diabetic nephropathy manifests with proteinuria, thickening of the glomerular basement membrane, expansion of the mesangium and accumulation of the extracellular matrix, where laminin, fibronectin and collagens type I and IV fail to preserve its normal structure.[15] In diabetic mice, miR-192 was found to be elevated in their glomeruli.[75] This miRNA can regulate E-box repressors expression, which in turn regulate Col4a1 and Col4a2 gene expression through TGF-β leading to their accumulation. In addition, hyperglycemia seems to induce the abnormally high expression of miR-377 in mesangial cells, causing the targeted PAK1 and mnSOD mRNA downregulation and finally enhanced production of fibronectin.[76] Furthermore, in early diabetic nephropathy miRNA-21 was found to have reduced levels in db/db mice, while its over-expression paused mesangial cell proliferation and decreased the albumin excretion rate.[77]

In hypertensive nephrosclerosis, a disease where arterial sclerosis leads to glomerular sclerosis and hypertrophy, atrophy of the tubules and interstitial fibrosis, specific microRNAs were found to be highly expressed in a recent study; miR-200a and b, miR-141, miR-429, miR-205 and miR-192 were found in abundance and their levels correlated with proteinuria in patients.[78] Impressively, microRNA expression in patients with IgA nephropathy, revealed the association of miR-192, miR-141, miR-205 and miR-200c with the disease.[79] In this case miR-200c was found to be downregulated with its levels of expression correlating with proteinuria, while the rest were upregulated with miR-192 being associated with glomerulosclerosis and decrease of glomerular filtration rate.

MicroRNAs are also involved in the pathogenesis of polycystic kidney disease (PKD). In ADPKD and ARPKD, miR-15a was found to be downregulated, which in turn influenced the upregulation of Cdc25A, a regulator of the cell cycle, as it was no longer targeting this protein efficiently.[80] In addition, miR-21 was also found to have elevated expression in a PKD rat

model, while other microRNAs such as miR-31, miR-164a and miR-125 were found to be downregulated.[81]

1.3.4 miRNAs as regulators of transcription

RNA interference (RNAi) is a primary epigenetic regulator of gene translational silencing, acting at the chromatin level and transcriptional gene silencing (TGS) is a term introduced to engulf these RNAi properties.[82] Hence, compared to the miRNA/RISC pair, the RNA-induced transcriptional silencing (RITS) complex is build by the cell to assist RNAi mediated TGS. Plant siRNAs do not only have complete complementarity against their targets, but they are usually longer than miRNAs and have been found to repress gene transcription by influencing methylation of promoter sequences at transcription start sites.[83] This is the case in Arabidopsis, where such small RNAs were developed as a response against the invasion of foreign nucleic acids in order for the genome integrity to be preserved.[84] In yeast, the RNAi pathway has been associated with telomere chromatin assembly, as the RITS complex incorporates proteins such as Ago1 which in turn associate with other proteins that cause chromatin modifications to occur.[85] Evolutionarily lower organisms, such as *Saccharomyces pombe* demonstrate the involvement of RNA polymerase-II in TGS and this is suggestive of a strong association between the RISC and RITS acting RNAi molecules; they are both transcribed to serve as regulators of protein synthesis but only by acting on different kinds of targets.[86]

As the miRNA field was evolving, researchers have well suspected that not only siRNAs but also miRNA molecules are entitled to extended roles in regulating gene expression. Not only should they bind on the 3'UTR of mRNAs, but it was inevitable to assume that miRNAs could exert control over gene transcription as well. There are three scenarios as to how miRNAs can preserve such relationships that involve binding onto DNA sequences in order to regulate gene transcription; by interfering with nucleotide methylation of particular promoter sites to enhance or repress transcription, by assisting for chromatin modifications to occur in order to block or release DNA regions or by binding directly onto specific DNA sequences to silence or promote gene expression.[87] If the latter is valid, one must argue on the actual mechanism that leads mature miRNAs back into the nucleus, on the possibility of a miRNA to bind directly on DNA and on the way that transcriptional repression/enhancement occurs. For RNA

to bind on complementary DNA sequences and regulate gene transcription, it is possible that the RNA binds directly onto the DNA molecule or not, as the RNA could bind to other newly synthesized RNA transcripts on specific sequences and influences the creation of an RNA-protein-DNA bundle to inhibit translation.[87]

There have been a number of publications that proved transcriptional regulation by miRNAs. Nevertheless, the published works used only artificially generated miRNA/siRNA LNA molecules and in high concentrations, thus suggesting an effect which cannot be occurring under normal circumstances keeping in mind the low concentration of miRNAs in cells. Kim et al., suggest that miRNAs whose genes are encoded within basal promoters of genes, are related to miRNA-induced transcriptional silencing of "host" genes, via their hybridization on their corresponding complementary regions, thus acting as cis-regulatory elements of transcription.[88] The same study demonstrated that miR-320 regulates the transcription of POLR3D (RNA Polymerase III – subunit D) by this manner. In other cases, there has been an attempt to target specific promoter sequences by using small RNA molecules in order to investigate for their regulatory properties. MiRNA influence on gene transcription was suggested in a study by Younger and Corey (2011), who succeeded in inhibiting the transcription of the human progesterone receptor (PR) gene via miRNA mimics that targeted non-coding RNA transcripts which overlapped with the promoter of the PR gene.[89] Silencing or repression is not always the case, as such antigene RNAs (agRNAs) were also found to promote PR gene expression in a methylation independent manner by targeting sequences on the promoter region of the PR gene in MCF7 cells, which express this protein at low levels.[90]

The possible mechanisms by which a miRNA can pass through the nuclear envelope and enter the nucleus have also been addressed. Hwang et al., found that a miRNA 5'-end hexanucleotide element is responsible for the direction of miRNAs into the nucleus.[91] Furthermore, Argonaute proteins, the primary proteins to shape the miRNP/RISC complex which presumably assist miRNA mediated DNA binding, were found to be imported in the nucleus by importin 8.[92] Both Argonaute 1 (Ago1) and 2 (Ago2) proteins were found to be implicated in TGS.[93,94]

2 HYPOTHESES AND SPECIFIC AIMS

In order to explain the variable course of progression of patients with glomerulopathies to ESKD, researchers are just beginning to focus on the identification of modifier genes. Such modifier genes belong to a category of factors that can alter the phenotypical spectrum in monogenic disorders; one gene bears a mutation that is found segregating in families and is mainly responsible for the pathological phenotype.[95] Furthermore, one should not overlook the pressure exerted from the environment, for example blood pressure control, protein consumption or drug intake.

Governments worldwide are investing great sums of money for cure or prevention of renal disease; by improving prognosis of such diseases, mutation carriers would be able to delay disease progression when they are correctly guided by clinicians and have better lives away from hospitals.[96] Public hospitals in Cyprus have a high turn-over of patients in dialysis and the number of patients is destined to be multiplied. It is a well known fact that three factors contribute to CKD and ESKD, those being increasing trends for hypertension, diabetic nephropathy and aging, with increased life span. On top of these, there are genes contributing to either monogenic or multifactorial diseases and these should be identified and interfered with by various means. Unfortunately, existing clinical interventions cannot always alleviate symptoms effectively and most importantly cannot always prevent the end result and the need for hemodialysis or kidney transplantation.[97,98]

MicroRNAs are an emerging class of molecules that have been implicated in most diseases with complex and non-mendelian inheritance. If the fine tuning they exert on mRNA translation is voided by any means, then a disease/phenotype should follow. Therefore, it is hypothesized that alteration of miRNA physiological control against target mRNAs can turn glomerular disease into more or less severe and this study is designed in a way to prove such interactions. This is the first attempt to associate this otherwise unpredicted deterioration of patients to ESKD with miRNAs.

This study aims to prove that miRNAs play a pivotal role in kidney disease by regulating the normal levels of certain genes expressed in the glomeruli or the podocytes and presumably contribute to disease progression. Single nucleotide polymorphisms in miRNA target regions

of such genes can alter the physiological regulatory properties of a miRNA and thus function as a loss or gain-of-function mutations. In this manner, **we hypothesized that SNPs located in miRNA target sites at the 3'UTRs of such genes could weaken or enhance physiological miRNA binding ability and thereby alter the capacity of miRNAs to regulate gene expression effectively, thus explaining the diverse phenotypic severity in glomerulopathies.** By hypothesizing such a role for miRSNPs, they can be thought of as quantitative trait loci (QTL), acting synergistically with other SNPs or miRSNPs to orchestrate complex phenotypes. In multifactorial diseases, such as diabetes, progressive nephropathy can also be explained by the lack of miRNA tuning attributed to such miRSNPs. Future research will be focused on drug invention to invert the harmful effects of deregulated miRNA translational control and restore physiological mRNA levels in the renal tissue. For the basic workflow of this project, see Figure 4.

In order to test the above hypothesis, the following methodological procedures were realized:

1. **Selection of candidate genes**

   A list of candidate genes was generated which included genes expressed preferably in the kidney glomeruli, the basement membrane, podocytes, focal adhesions, slit diaphragms or genes that have been associated with a disease that manifests with a glomerular deficiency, based on available literature. Such diseases can be thin basement membrane nephropathy, CFHR5 nephropathy, hypertensive nephrosclerosis, diabetic nephropathy and IgA nephropathy.

2. **Prediction of miRNA target sequences at the 3'UTR and the promoter region of candidate genes using algorithms**

   In the past few years target-miRNA prediction algorithms using various criteria and calculation approaches have been used greatly. Predictions in this study were performed using the miRWalk algorithm and for result filtering purposes, predictions were repeated by using four other algorithms available online. A gene target-miRNA pair was considered as a good candidate when it was predicted by all five algorithms.

   For this work, gene promoters were regarded as sequences located up to 10kb upstream of the 5'UTR, in order to explore for the possibility that a miRNA could target sequences that act as enhancer or suppressor elements.

3. **Sequencing analysis of 3'UTR regions of top candidate genes in search for miRSNPs**

   Starting from top candidates, sequencing analysis included patients diagnosed with thin basement membrane nephropathy and classified into one of two distinct classes in terms of severity. Only SNPs located at miRNA target sites and especially into the seed region were selected for further analysis.

4. **Validation of miRNA regulation on predicted target regions at the 3'UTR of candidate genes using "sensor constructs"**

   Luciferase sensor construct assays were used to investigate direct binding and regulation by miRNAs against their predicted target sequences in the AB8/13 podocyte line.

5. **Further analysis of translational regulation of candidate genes using real-time PCR and Western blot analysis**

   In support of luciferase assay data, both real-time PCR and western blots were utilized to evaluate target mRNA and protein levels respectively after experimentally increasing miRNA levels in cultured cells.

6. **miRSNP analysis in patients and examination of its association with the degree of severity in glomerulopathies under study.**

   Patients manifesting the aforementioned glomerular diseases were scrutinized for every SNP that was experimentally proven to alter the binding ability of a certain miRNA to its target. Phenotypic severity was also evaluated for association with miRSNPs using statistical approaches.

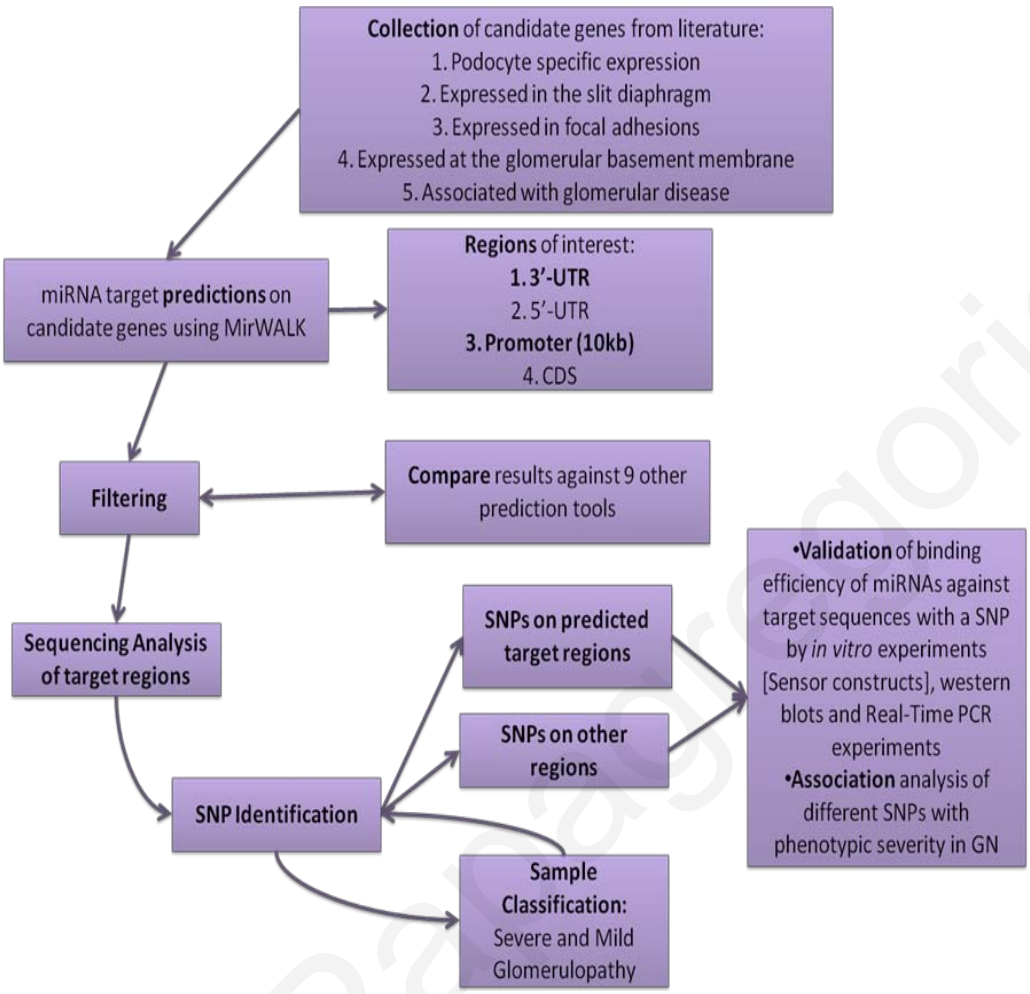

Figure 4: Basic workflow for the identification of miRSNPS that act as genetic modifiers in glomerular diseases

In addition, since preliminary bioinformatic analysis revealed high complementarity between specific miRNAs and promoter regions, we made an attempt to unveil further basic properties of miRNA regulation in terms of DNA transcriptional repression or enhancement. miRNA-DNA coupling relationships have been previously examined and published results are thus far promising that transcription can also be controlled by miRNAs.[92,99,100,101] Herewith, **we hypothesized that specific miRNAs can exert transcriptional regulation by their direct binding on DNA sequence elements located upstream of gene transcription starts.** For this purpose, we aimed at using luciferase reporter constructs for the first time in order to prove direct interaction of miRNAs with DNA sequences and regulation of transcription by miRNAs. We also attempted to support our results by the isolation of endogenously expressed miRNAs and their DNA binding sites by developing a modified chromatin Immunoprecipitation (ChIP) protocol. Further elucidation of miRNA regulatory characteristics

will be an innovative and exceptional advancement in miRNA research. [See Figure 5 for basic workflow].

The specific aims of this part of the project based on the hypothesis are:

1. **Prediction analysis of miRNA targets on DNA sequences upstream of candidate genes.**

   The miRWalk algorithm has the ability to scan genes for miRNA binding sites on regions upstream their 5'UTR regarded as their "promoter". In reality, this region includes the core gene promoter but also genomic elements that enhance transcription. Hence, an extended region of 10kb was scrutinized for miRNA binding sites, based only on the degree of complementarity between the miRNA sequence and the target sequence. In lack of additional algorithms, filtering of results was based on the size of the complementary region and the site of the sequence in respect to its distance from the 5'UTR of the gene.
2. **Use of reporter constructs to investigate for miRNA/DNA target sequence coupling ability.**

   The pGL4.27 vector bears its multiple cloning site right upstream the core promoter of a luciferase gene and it is generally used as a mean of examining the action of transcription factors over promoter/enhancer elements. After cloning the miRNA target site on the multiple cloning site of this vector, AB8/13 podocytes were transfected, together with miRNA mimics and inhibitors. Luciferase level fluctuations reflect the ability of a given miRNA to bind on its target DNA sequence and alter gene transcription.
3. **Chromatin Immunoprecipitation (ChIP) experiments for the isolation of AB8/13 genomic DNA sequences as well as endogenously expressed miRNAs that are bound on these sequences.**

   A modified ChIP protocol was designed and performed for capturing miRNAs, presumably facilitated by the RISC complex to bind directly onto DNA target sequences. These series of experiments were performed in order to evaluate the bionformatic prediction analyses and validate the luciferase experiments. Both DNA and miRNA presence was spotted and relatively quantified with Real-Time PCR experiments, as an altimate proof of our hypothesis.

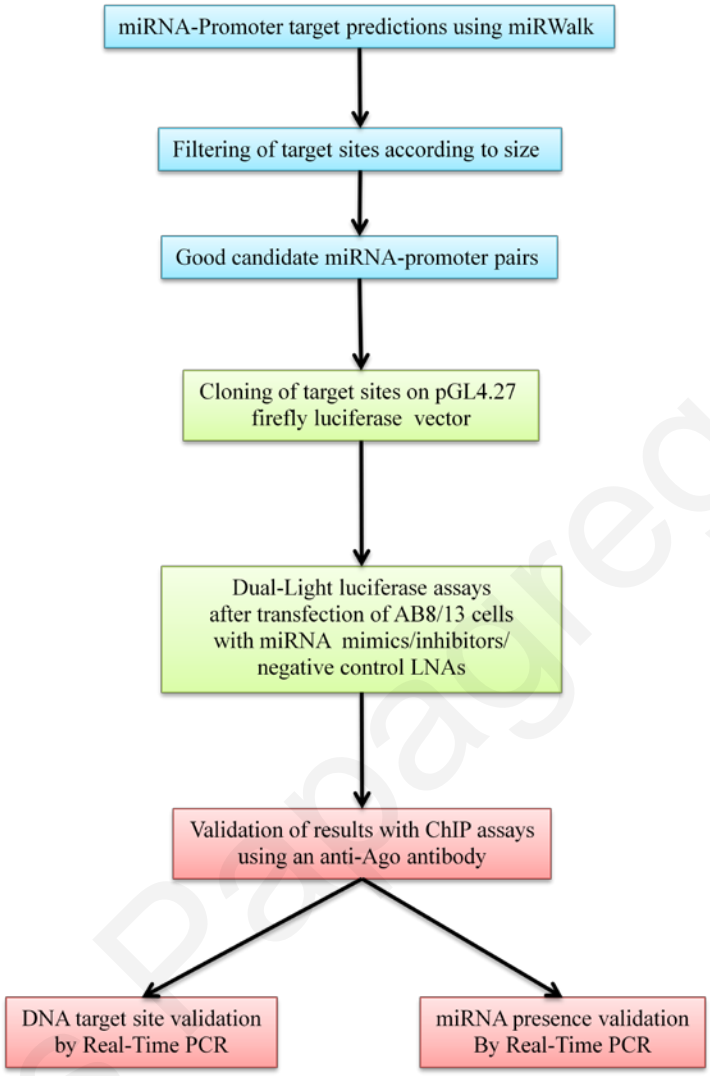

Figure 5: Basic workflow for identifying miRNAs that are able to exert regulation of gene expression via target sites on their extended promoter regions.

3 METHODS

3.1 Identification of miRSNPs that contribute to glomerular pathological phenotypes

3.1.1 Patients

Patients who participated in this study were diagnosed with TBMN or CFHR5 nephropathy and were all shown to have inherited germinal mutations in either the COL4A3/COL4A4 genes or the CFHR5 gene respectively, in heterozygosity. All participants were informed by the clinicians and signed a consent form. The project is approved by the Cyprus National Bioethics Committee. A total of 232 anonymous DNA samples from our DNA bank served as controls.

TBMN patients originate from 16 large Cypriot families. Seventy-eight of 103 patients are heterozygous for the G1334E–*COL4A3* mutation, 19 of 103 are heterozygous for the G871C–*COL4A3* mutation and 6 of 103 are heterozygous for the c.3854delG–*COL4A4* mutation.[98] Due to the slow disease progression patients with "mild disease" (see below) and younger than 48-yo (born before January 1963) were excluded. The CFHR5 nephropathy group was comprised of 45 male and 33 female patients (born before January 1975), all sharing a common exons 2-3 heterozygous duplication in *CFHR5* gene.[39] Pedigrees and analytical clinical data have been published in detail elsewhere.[98,102] For both, TBMN and CFHR5 cohorts, "mildly" affected patients are those having only microscopic or macroscopic hematuria episodes (but no CKD) or hematuria plus low grade proteinuria (<400 mg/24 hrs, but no CKD). "Severely" affected patients are those having hematuria plus proteinuria >500 mg/24 hrs or hematuria plus proteinuria plus CKD or ESKD. CKD was defined as an elevated serum creatinine over 1.5 mg/dl. Patients with remittent or borderline proteinuria were excluded. Patients with a concomitant renal disease (*e.g.*, over five years diabetes, diabetic nephropathy, vesicoureteral reflux) or at the extreme of body weights (outside ±2 SD of the cohort mean) were also excluded (see Table 2).

Table 2: Basic symptoms table for distinguishing between mildly or severely affected patients in TBMN and CFHR5 cohorts.

	Mildly affected patients	Severely affected patients
Hematuria	Microscopic (TBMN and CFHR5) or Macroscopic (only CFHR5)	Microscopic (TBMN and CFHR5) or Macroscopic (only CFHR5)
Proteinuria	<400 mg/24 hrs	>500 mg/24 hrs
CKD/ESKD	NO	YES
Age	Older than 48 years old (TBMN) Older than 36 years old (CFHR5)	

For investigating results in further, additional glomerulopathy patient groups of variable cause were encompassed. Thus, patients diagnosed with IgA nephropathy, hypertensive nephrosclerosis, diabetic nephropathy and glomerulonephritis were also screened for C1936T functional variant of HBEGF.

Control population was expanded to include around 700 samples from the Cyprus Study (Cyprus Cardiovascular Disease Education and Research Trust), which was established in order to study for risk factors leading to atherosclerosis in the Cyprus general population. This sample group was encompassed in order to examine the potential association between the C1936T variant in HBEGF and serum levels of various proteins, aminoacids and chemical substances.[103] Serum creatinine, folic acid, homocystein and B12 vitamin levels, as well as matrix metalloproteinases 1,2,8,9 and metalloproteinase inhibitors 1 and 2 levels, were statistically compared with C1936T genotypes. Correlation with serum level measurements of asymmetrical dimethylarginine (ADMA) – an inhibitor of nitric oxide synthase which is elevated in patients with chronic renal failure and cardiovascular disease, [104] nitric oxide (NO) and myeloperoxidase (MPO), implicated in membranous glomerulonephritis, were also examined.[105]

3.1.2 Gene selection

In accordance with our hypothesis we searched for SNPs in the 3'UTR region of genes and specifically around the putative target regions of respective miRNAs (Appendix I - Table 19). Eighty seven genes were selected based on a wide spectrum of criteria. Candidate genes belong to four general categories based on their glomerular expression, their involvement in monogenic glomerular diseases, whether they were previously associated with a polygenic disease that presents secondary glomerulopathy and other genes expressed in the kidney or elsewhere that were found to be important for renal function or are closely related to genes selected in other categories. Podocyte specific genes, such as NPHS1, NPHS2 or PDPN are considered as good candidates, while polygenic diseases include diabetes, systemic lupus erythematosus, IgA nephropathy, glomerulonephritis and hypertensive nephrosclerosis. Published data regarding kidney or glomerulus specific gene expression microarray experiments enriched the candidate gene list, thus including genes coding for transcription factors, activators, structural proteins etc. In addition, genes implicated in tubular disease like PKD1 and PKD2 were also included.

3.1.3 miRNA target prediction analysis

Candidate gene names were imported into miRWalk algorithm (www.ma.uni-heidelberg.de/apps/zmf/mirwalk) and prediction of miRNA target sequences on their mRNA 3'UTR was performed using 7 nucleotides as the minimum seed number.[106] Multiple comparison using 4 additional algorithms was performed for filtering purposes by encompassing TargetScan, miRanda, miRDB and RNA22 algorithms. These algorithms work in a different way in order to perform prediction analyses. The miRWalk algorithm works by "walking" on the gene sequence in a window of seven or more nucleotides and a miRNA is predicted to target a specific mRNA based only on seed region complementarity. TargetScan on the other hand, is searching for the presence of conserved 8mer and 7mer sites that match the seed region of each miRNA, while it "ranks" a predicted miRNA target based on site length, type, context and accessibility.[107] The miRanda algorithm considers the miRNA sequence as input and searches a sequence dataset for potential target regions and successful predictions are made based on the alignment score and the minimum free energy of the miRNA bound to the potential target sequence.[108] The miRDB algorithm uses a completely

different approach, as it is based on an SVM algorithm which is trained by a wiki database, in which users are able to input sequences of validated miRNA/mRNA couples.[109] Finally, the RNA22 algorithm uses a reverse approach as it first examines gene sequences for putative miRNA binding sites and then identifies a miRNA that could target an identified 3'UTR site.[110] Therefore, algorithms were selected based on how different they performed miRNA/target predictions, as to capture all the possible information as regards our predictions and at the same time to make result filtering stricter.

Table 3: Primer sets and PCR conditions for sequencing analysis of miRNA target regions in mildly or severely affected patients of either the various cohorts.

Pair	Gene	miRNA(s)	Target site location	Primer Sequence	Annealing T°C	Cohort
A	TJP1	hsa-mir-144	6469-6462	5'- GGAGGGTGAAGTGAAGACAA -3' 5'- GCATAGCCAGAAAGAACAGAA -3'	58°C	TBMN
B	PPARA	hsa-mir-223	5877-5868	5'- GTTAGGGCAGGTGGGATG -3' 5'- TGTATGCGGCTGGTAAGTAG -3'	N/A	TBMN
C	SP1	hsa-mir-31	6960-6951	5'- GACTTCCCCAAACCCAGA -3' 5'- CACCCATCCCTTCCAGAG -3'	59°C	TBMN
D	FN1	hsa-mir-96 hsa-mir-144	8340-8332 8331-8322	5'- TTGGGATCAATAGGAAAGCA -3' 5'- GAAGAGATGAAGTGACAAAAACC -3'	58°C	TBMN
E	GJA1	hsa-mir-495	2244-2237	5'- CATCCACTTGCACAATATCA -3' 5'- TTTACTTGCCACAGCAGGA -3'	58°C	TBMN
F	PDPN	hsa-mir-485-5p	1453-1446	5'- GTTAGGGCAGGTGGGATG -3' 5'- TGTATGCGGCTGGTAAGTAG -3'	58°C	TBMN
G	PKD2	hsa-mir-183	4768-4760	5'- TCCAGGTTGAAAGTGAAAC -3' 5'- CAGGGAAAGATAATAGGGAAGA -3'	58°C	TBMN
H	HBEGF	hsa-mir-132 hsa-mir-212	1584-1575 1584-1576	5'- TGAACTGGAAGAAAGCAACA -3' 5'- ACCCCTACATCCTGACCATAC -3'	58°C	TBMN
I	HBEGF	hsa-mir-379	1833-1826	5'- ACTCCTCATCCCCACAATCT -3' 5'- CCCACCTCCAACCTTCTC -3'	58°C	TBMN
J	PKD2	hsa-mir-372	4022-4014	5'- TTCCCATGTGGCTCTACTCA -3' 5'- AGACCCTCTCGTAAAGAAAACA -3'	58°C	TBMN
K	COL4A3	hsa-mir-579 hsa-mir-656	7957-7948 8016-8008	5'- CTCATGTGCATTATTTTCCAG -3' 5'- GGATGGGAGTGAGGATTAGA -3'	56°C	ESKD/CKD
L	COL4A3	hsa-mir-410	6596-6588	5'- TTGATACATTCCCAAGGTTACT -3' 5'- CAGCACCACCAACTCCAC -3'	56°C	ESKD/CKD
M	COL4A3/ COL4A4	Interval sequence	N/A	5'- ACCTCCAGCCCCAATCCAC -3' 5'- CAGCCCCCACTCACCTTG -3'	N/A	ESKD/CKD
N	COL4A1	miRNA target rich region	5133-5324	5'- GACTGATGTGGCGGGACT -3' 5'- TCGCTGTCTTTTTCTCCTTC -3'	N/A	TBMN
O	COL4A2	miRNA target rich region	5446-5668	5'- TGACACTCATGGTTTGCTGT -3' 5'- CTGCTCCTGGCTTTCTGT -3'	60°C	TBMN
P	COL4A5	miRNA target rich region	5303-5715	5'- AAACCATTAAGTCACCAAGAGAG -3' 5'- CGGGATACAGCAGGATTAG -3'	59°C	TBMN

In search for polymorphic variants by DNA sequencing around the miRNA target sequences, our attention was restricted only to pairs of miRNA-mRNA targets that were predicted by all five algorithms and gave a p-value<0.05. This p-value was automatically calculated by the miRWalk algorithm by using Poisson distribution and depicts the distribution of the probability of a miRNA 5'-end sequence to be randomly paired with a given 3'UTR mRNA sequence. On a later stage, prediction analysis was repeated using the same selection of genes but encompassing 5 additional algorithms to confirm initial predictions; DIANA-mT, RNAhybrid, PITA, PICTAR4 and PICTAR5.

3.1.4 DNA sequencing analysis of miRNA target regions

DNA sequencing of predicted target regions (Table 3) was performed using BigDye™ V3.1 chemistry on an ABI Prism™ Genetic Analyzer (Applied Biosystems, Foster City, CA, USA). Sequencing primers (all supplied by MWG, Ebersberg, Germany) were designed to flank the target region but also included an additional 300 bp on average on each side. Sequence electropherograms were obtained from the ABI Sequencing Analysis™ V5.2 Software (Applied Biosystems, California, USA) and sequences were imported into BioEdit™ Software to be aligned against a reference sequence with ClustalW algorithm.[111] SNPs that were identified in positions other than the predicted ones were evaluated using the miRanda tool (http://www.microrna.org) and cross-referenced with initial predictions.

3.1.5 Expression reporter system constructs

To evaluate the binding efficiency of miRNAs onto predicted target sequences, the pMiR-REPORT™ miRNA Expression Reporter Vector System (AMBION, Texas, USA) was used (Figure 6). For the case where we identified a SNP in the 3'UTR region, each allele was obtained with a polymerase chain reaction (PCR) amplification from two patients, each one homozygous for either allele and primers were designed to introduce a *SpeI* and a *HindIII* restriction enzyme sites to be cloned into the pMiR-REPORT™ Luciferase vector. Ligation products were transformed into competent DH5a *E. coli* cells (Takara, Japan). Insert verification included a restriction reaction with *SpeI* and *HindIII* and sequencing using 100ng of DNA.

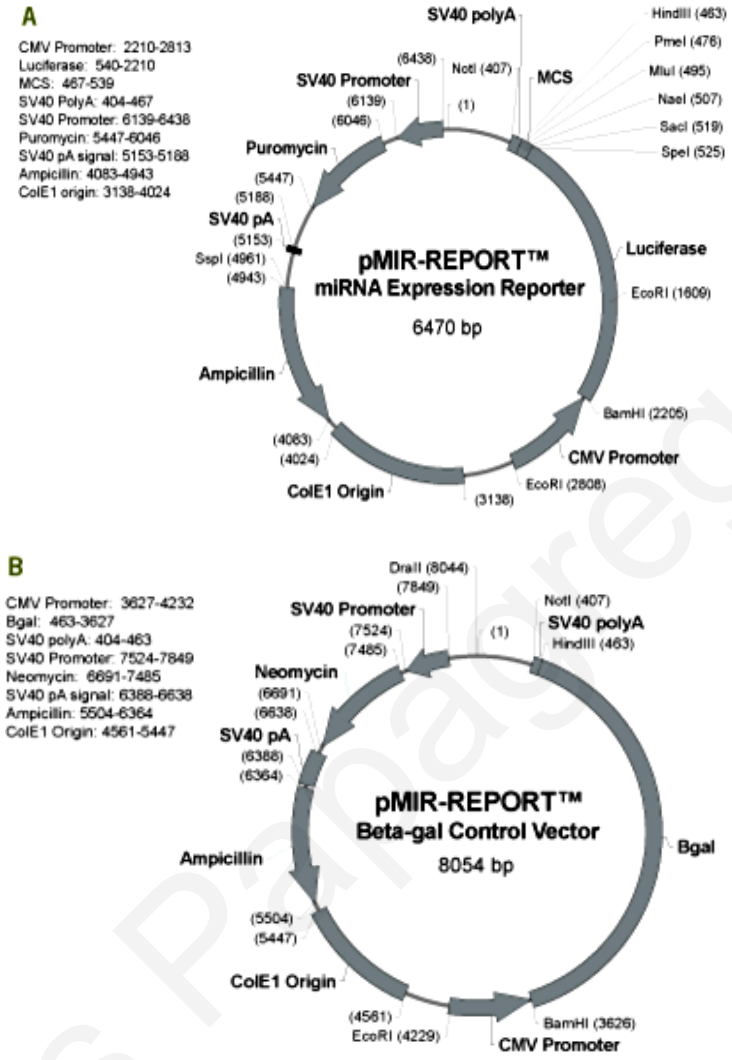

Figure 6: The pMIR-REPORT™ kit vectors by Ambion (Texas, USA). A. The luciferase vector, B. The β-gal vector [Taken from the Ambion website – www.ambion.com]

3.1.6 Transfection of AB8/13 podocytes

The AB8/13 undifferentiated podocyte cells, supplied by Dr Moin A. Saleem,[112] were incubated at 33°C at 5% CO_2 and cultured in RPMI medium, supplemented with 10% Fetal Bovine Serum (FBS) (Invitrogen, Carlsbad, CA, USA), 1% of 100 units/ml Penicillin/Streptomycin (Invitrogen, Carlsbad, CA, USA) and 1% Insulin-Transferrin-Selenium (Invitrogen, Carlsbad, CA, USA). AB8/13 cells were triply transfected with equal amounts of the pMIR-REPORT™ Luciferase and β-gal vectors and 25nM of miScript™ hsa-miR-1207-5p mimic (QIAGEN, West Sussex, UK) or the AllStars™ Negative Control

scrambled sequence LNA (QIAGEN, West Sussex, UK), using Lipofectamine 2000 (Invitrogen, Carlsbad, CA, USA). The β-gal vector was used for normalization (see Table 4). Every experiment was performed in triplicates in 6-well cell culture plates with the appropriate controls. Cells were harvested 12h after transfection. The Dual-Light Assay™ Kit (Applied Biosystems, Foster City, CA, USA) was used for the quantification of both luciferase and β-gal in an automated luminometer (Sirius, Berthold Detection Systems, Pforzheim, Germany).

Table 4: Series of experiments in AB8/13 undifferentiated podocyte cells using luciferase sensor constructs and miRNA mimics or inhibitors in order to examine direct binding of miRNAs on the HBEGF mRNA* 3'UTR *target site.

Experiment / Additive	A	B	C	D	E	F	G	H	I	J	K
pMiReport- Luciferase vector	-	+	-	+	+	-	-	-	-	-	-
pMiReport- β-gal vector	-	-	+	+	+	+	+	+	+	-	-
pMiReport- Luciferase vector w/C1936	-	-	-	-	-	+	+	-	-	+	-
pMiReport- Luciferase vector w/T1936	-	-	-	-	-	-	-	+	+	-	+
AllStars miRNA negative control	-	-	-	+	-	+	-	+	-	-	-
miRNA mimic	-	-	-	-	+	-	+	-	+	-	-

3.1.7 Western blot experiments

AB8/13 cells were lysed in equal volumes of pre-heated 2xSDS loading buffer (Sodium Dodecyl Sulphate–125mM Tris-HCl pH 6.8, 20% Glycerol, 2% SDS, 2% β-mercaptoethanol and bromophenol blue) and homogenized using a 2ml syringe. Whole cell lysates were subsequently electrophoresed in a 12% SDS-Polyacrylamide gel. Gel transfer was held in a wet transfer system on Hybond Polyvinylidene Fluoride (PVDF–Millipore, Massachusetts, USA) membranes. Membranes were blocked with 5% non-fat dry milk in PBS/0.01% Tween20 for 1 hour at room temperature. Primary antibody was diluted in milk and added to the membrane for one hour. HBEGF protein was detected with the murine primary monoclonal antibody G-11 (SantaCruz Biotechnology, California, USA) at around 24kDa. β-Tubulin was used as loading control by using the T-4026 primary antibody (SIGMA,

Taufkirchen, Germany). As secondary antibody we used the rabbit anti-mouse antibody (SantaCruz Biotechnology, California, USA), conjugated with Horseradish Peroxidase (HRP). Proteins were detected using the Enhanced ChemiLuminescence (ECL) Plus Blotting Detection system (Amersham Biosciences, Buckinghamshire, UK) and were visualized by autoradiography on photographic film (KODAK X-OMAT, New York, USA). Band density was defined by ImageJ Software (http://imagej.nih.gov/ij).

3.1.8 microRNA specific Real-Time PCR

To investigate whether AB8/13 podocytes endogenously express miRNAs of interest miRNA specific Real-Time PCR was performed. Real-Time PCR involves two main steps; miRNA specific reverse transcription and subsequently real-time PCR. In lack of biopsies from patients, mature miRNA levels were comparatively investigated in both differentiated and undifferentiated podocytes, in HEK293 cells, in SHSY-5Y neuroblastoma cells and in miRNA enriched RNA extracted from human renal epithelial cells (HREpiC - supplied from ScienCell, Carlsbad, CA, USA).

For miRNA detection, the miScript Reverse Transcription Kit (QIAGEN, West Sussex, UK) was used for reverse transcription. This kit includes the miScript™ Reverse Transcriptase Mix and the miScript™ RT Buffer. The first is a mix of enzymes comprised of a poly-A polymerase and a reverse transcriptase, while the buffer contains Mg^{2+}, dNTPs, oligo-dT primers and random primers. The poly-A polymerase introduces a poly-A tail to miRNAs, which are not naturally polyadenylated, while the reverse transcriptase converts all RNAs, including miRNAs, into cDNA. Template RNA was thawed on ice and the RT mix was added in tubes right before adding the RNA (10pg to 1μg of RNA). After incubation for 60min at 37^{o}C, inactivation of the RT mix followed by incubating for 5min at 95^{o}C. Samples were kept on ice until they were used for Real-Time PCR.

Real-Time PCR to detect mature miRNA levels was performed using the miScript™ Primer Assay Kit (QIAGEN, West Sussex, UK) and the miScript™ SYBR Green PCR Kit (QIAGEN, West Sussex, UK), on the Roche LightCycler® available in our lab. miScript™ Primer Assay Kit includes both a universal primer that helps amplify miRNAs and the miRNA specific primer.

Each Real-Time PCR reaction was set up in a 20 μl reaction volume, by adding 10μl of 2x SYBR Green PCR Master Mix, 2μl of 10x miScript™ Universal Primer and 2μl of 10x miScript™ Primer Assay miRNA specific primer, 2μl of cDNA and RNase-free water. Cycling starts with an initial activation step at 95°C for 15 minutes in order to activate the HotStar™ DNA polymerase contained in the PCR Master Mix and 40 cycles will follow, with the denaturation step at 94°C for 15 seconds, the annealing step at 55°C for 30 seconds and the extension step at 70°C for 30s. A small nucleolar RNA (snoRNA) was used as a reference. A calibrator sample was also used for each experiment for the relative quantification of each sample. The calibrator cDNA was a pool of randomly selected cDNAs from every experiment and was used for normalization when comparing target and reference samples.

3.1.9 Genotyping of miRSNP C1936T

Genotyping for the C1936T SNP was performed in all samples, either by direct re-sequencing (TBMN samples) or by restriction reaction analysis (CFHR5 and healthy control samples). For this purpose, a restriction recognition site for *BsrI* was engineered in the forward PCR primer, by substituting the penultimate T by an A (Forward primer: 5'- CAA AGT GTA ACA GAT ATC AGT GTC TCC CCG TGT CCT CTC CCA G – 3', Reverse Primer: 5'- GCT TTG CTA ATA CCT TCT CCA GAC TGT CCT CTG CTG CAC TGA -3'). The recognition site is created upon PCR amplification of the T allele (Figure 7).

3.1.10 Statistical analysis

Genotyping results were statistically evaluated using two-sided Barnard's unconditional test of superiority, as it was shown that it is more powerful for 2x2 contingency tables with limited observations than conventional conditional tests.[113,114,115] The reported Wald statistic is the standardized difference between the two binomial proportions of each category.[113] For the analysis of contingency tables we used StatXact 9 (Cystat, Cambridge, MA, USA).[116] as suggested in a publication by Ludbrook J. (2008).[117] In order to provide an open-source alternative for performing the Barnard's test, the "Barnard" package has been developed for the statistical scripting language R, by Dr Kamil Erguler. The package is currently waiting to be included in the Comprehensive R Archive Network (http://cran.r-project.org). C1936T was tested for Hardy-Weinberg equilibrium using Pearson's chi-square test in controls. Luciferase

expression levels were analyzed using one-way non-parametric ANOVA after being normalized against β-gal expression levels.

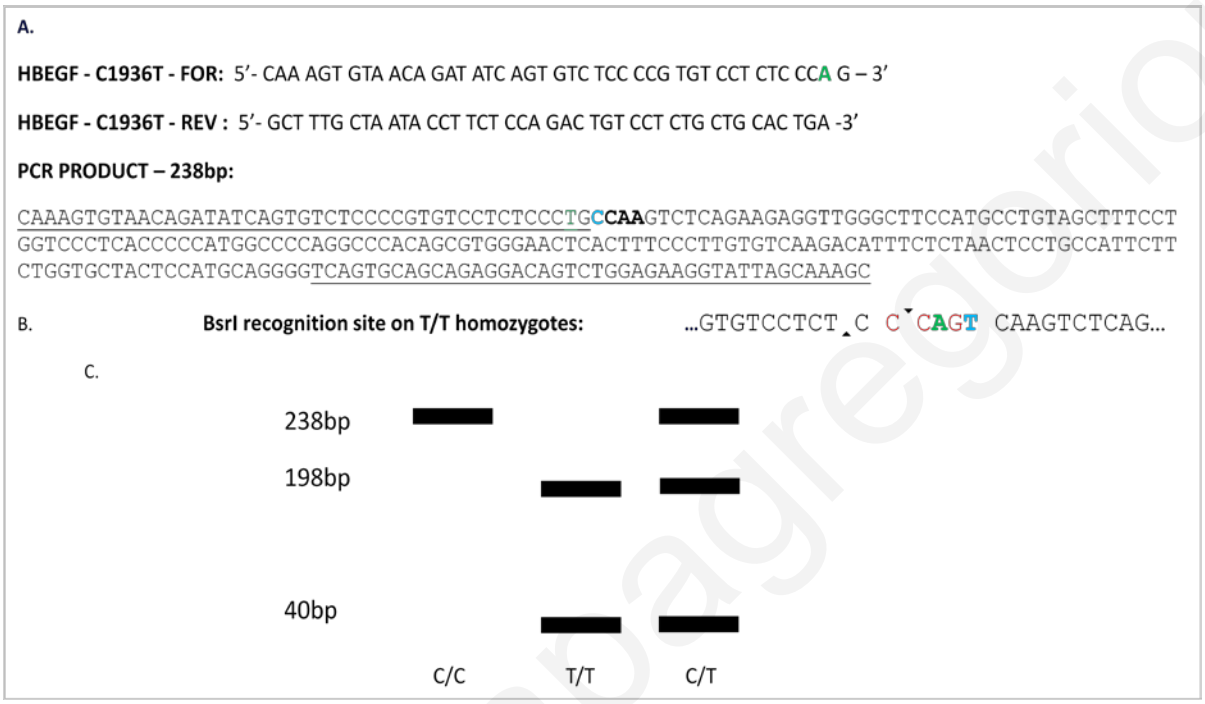

Figure 7: A. Primer pairs for introducing an A at position 1936 of the HBEGF 3'UTR, in order to create a restriction site for BsrI restriction enzyme. Bases colored in green, are the ones changing after the PCR (transversion of a T to an A). Bases colored in blue, indicate the C1936T SNP position. B. The BsrI restriction site. BsrI will only digest the PCR product if the sample is homozygous for the T1908 allele. Homozygous C1936 PCR products will remain undigested. C. Schematic of agarose gel electrophoresis following BsrI digestion of PCR products. C/T heterozygotes will be presented as having 3 bands, sized 238bp, 198bp and 40bp respectively.

3.2 Investigation of the role of miRNAs as regulators of transcription

3.2.1 Prediction analysis of miRNA targets at DNA regions up to 10kb upstream of gene transcription start points

3.2.1.1 Prediction analysis for hsa-miR-548c-5p

The miRWalk miRNA prediction algorithm was used for the prediction analysis of miRNA targets. Target predictions of the 3'UTR of candidate genes (Appendix I - Table 19) was supplemented with predictions concerning the "promoter" region for each gene, which was regarded as the first 10kb immediately upstream their transcription start. Interesting results concerning the sequence upstream the *FOXC2* gene and miRNA hsa-miR-548c-5p as well as the sequence upstream the *SPP1* gene and miRNA hsa-miR-548d-5p, re-directed this project to study in depth the putative regulatory roles of miRNAs in gene transcription. Hence, a concise list of gene promoter targets of miR-548c-5p was compiled after bioinformatic analysis using the MiRWalk algorithm. In addition, miR-548-5p mature sequence was aligned against all mature sequences of all other members of the miR-548 family (Appendix II - Figure 24).

3.2.1.2 Bioinformatic examination of miR-548 family

As preliminary results were indicative of putative lengthy target sites in the first 10kb sequence upstream of gene transcription start points, further predictions were performed using the MiRWalk algorithm. Predictions aimed at examining the recurrence of such sites, targeted by the miR-548 family members. The miR-548 family of consists of 69 miRNA stem loop sequences, among which only 56 mature miRNA sequences are non redundant. In other words, 13 of the miRNAs share the same mature sequence, but are encoded from different genomic loci. Predictions included 20.728 genes, which were scanned for miRNA binding sites on their 5'UTR, their coding sequence, their 3'UTR, and their "promoter" regions which were regarded as the first 10kb upstream their transcription start.

3.2.2 Cloning of miRNA target sites into the pGL4.27 luciferase vector

The pGL4.27 firefly luciferase vector, together with the pGL4.74 renilla luciferase vector was supplied from Promega (Fitchburg, WI, USA). This vector system is widely used in studies examining the role transcription factors exert on transcription enhancer elements. The pGL4.27 vector has a basal promoter sequence right before a gene encoding for the firefly luciferase protein, which keeps a minimal level of gene transcription (Figure 8). A multiple cloning site positioned upstream of the basal promoter is used for the introduction of a sequence of interest, tested by its influence on luciferase expression levels. Hence, the predicted target sequences of miR-548c-5p found more than 8kb upstream the transcription start of the *FOXC2* gene was cloned on the multiple cloning site, using specific PCR primers (For: 5'-**GCT AGC TGG AAG GAA TAG CGT AGA**-3', Rev: 5'-**AAG CTT GAA AAT AAC AAT GCC CAC AG**-3') bearing restriction sites for enzymes *NheI* and *HindIII*. PCR products were first subcloned in the pGEM-T Easy vector supplied by PROMEGA, and then in the pGL4.27.

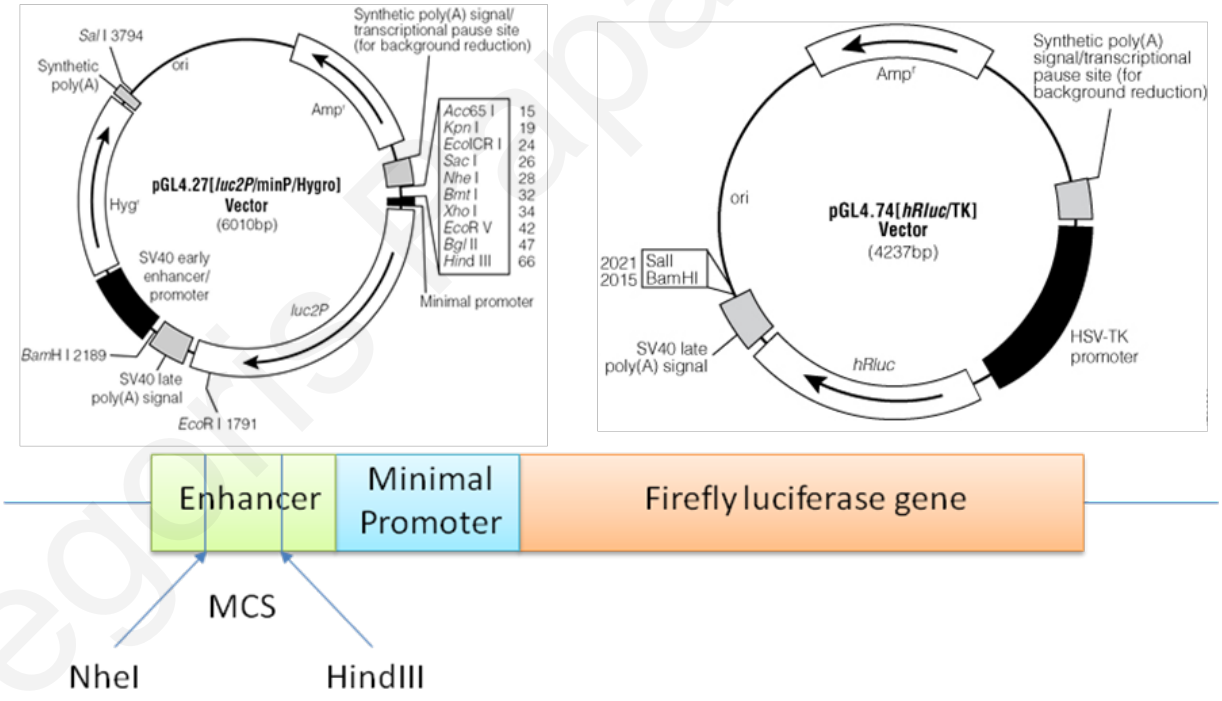

Figure 8: The pGL luciferase reporter vector system. The upper panel depicts plasmid maps for the pGL4.27 firefly luciferase vector and the pGL4.74 renilla luciferase vector. The lower panel demonstrates the multiple cloning site for pGL4.27 in relation to the firefly luciferase gene minimal promoter and gene.

3.2.2.1 Site directed mutagenesis (SDM)

A pGL4.27 vector lacking the miR-548c target site was generated in order to check for target site specificity on luciferase gene expression. For this purpose, a set of primers were designed for the removal of 23 nucleotides from the *FOXC2*-pGL4.27 vector. The primers used were: *FOXC2*-548rem2-F: 5'-**AAG TTG GTT GGT G**CA TTA CTT TGA ATG TAG ATT GAA AGT-3' and *FOXC2*-548rem2-R: 5'-**CTA CAT TCA AAG TAA TG**G CAC CAA CCA ACT TAA CAA AAT G-3'. Sequence in bold represents primer overhangs for the easier re-ligation of the vector. The PCR was performed on the pGEM-T Easy vector bearing the *FOXC2*-miR-548c insert and then cloned in the pGL4.27 vector. PCR was performed using the *Pfu* Polymerase from Agilent (Santa Clara, CA, USA) together with 100ng of template DNA. The SDM cycling protocol started with 2 minutes denaturation at 95^{o}C, followed by 20 cycles of 95^{o}C for 1 minute, 63^{o}C for 1 minute and 3 minutes at 72^{o}C and completed with 10 minutes incubation at 72^{o}C. Products were treated with DpnI, activated for 1h at 37^{o}C and deactivated for 20 minutes at 80^{o}C.After PCR purification of products with the NucleoSpin Extract II kit (Macherey Nagel, Düren, Germany), products were ligated using the T4 DNA Ligase (Promega, Fitchburg, WI, USA) for 1 hour at room temperature and transformed into DH5a E. coli competent cells (Invitrogen, Carlsbad, CA, USA). Colonies were checked with sequencing analysis after colony PCR and the plasmid was purified using the Nucleospin Plasmid Mini kit (Macherey Nagel, Düren, Germany). Inserts were digested out of the vector with the NheI and HindIII restriction enzymes for 1 hour and 30 minutes and purified with the Nucleospin Extract kit to be cloned into the pre-digested pGL4.27 vector.

3.2.3 Transfection of AB8/13 and luciferase assay experiments

The AB8/13 undifferentiated podocyte cells were triply transfected in 6-well plates with the pGL4.27 vector, the pGL4.74 vector and 25nM of miRNA mimics/inhibitors/AllStars Negative control LNAs, all supplied from QIAGEN (West Sussex, UK), using Lipofectamine 2000 (Invitrogen, Carlsbad, CA, USA). Cells were scraped off the plate 12 hours after transfection using the 5X Passive Lysis buffer (Promega, Fitchburg, WI, USA), and lysate was collected in a 1.5ml amber coloured tube (Eppendorf, Hamburg, Germany) and kept frozen at -80^{o}C until its use or was used directly. Transfection conditions are described in Table 5. The Dual-Light Assay™ Kit (Applied Biosystems, Foster City, CA, USA) was used for the

quantification of both luciferase and β-gal in an automated luminometer (Sirius, Berthold Detection Systems, Pforzheim, Germany).

3.2.4 Chromatin Immunoprecipitation (ChIP) experiments

In general, Chromatin Immunoprecipitation (ChIP) assays are useful tools in molecular biology and epigenetic research, in terms of discovering protein-DNA interactions. To undoubtedly verify direct functional interaction between **endogenously** expressed miRNAs in cell cultures, and their gene promoter target sites, we will attempt to isolate miRNA/DNA complexes using a novel protocol. We hypothesize that miRNAs which target promoter-localized DNA sequences can be isolated together with their target sequence. The miRNA is postulated to hybridize with its target sequence using the RISC complex; for this purpose the Anti-pan Ago (clone 2A8) antibody from Millipore (Temecula, CA, USA) was used in order to isolate this complex by immunoprecipitation while bearing the miRNA bound on its target DNA sequence. ChIP experiments were performed using the EZ-ChIP Kit supplied from Millipore (Temecula, CA, USA), which was modified to include miRNA isolation and analysis.

Table 5: Series of experiments in AB8/13 cells using luciferase sensor constructs and miRNA mimics or inhibitors in order to examine direct binding of miRNAs on predicted target sites.

Experiment / Additive	A	B	C	D	E	F	G	H	I	J	K	L
pGL4.24 – Firefly Luciferase vector	-	+	-	+	+	-	-	-	-	-	-	-
pGL4.74 – Renilla Luciferase vector	-	-	+	+	+	+	+	+	+	-	-	-
pGL4.24 – Firefly Luciferase vector FOX2-548c-5p+SITE	-	-	-	-	-	+	+	-	-	+	-	-
pGL4.24 – Firefly Luciferase vector FOX2-548c-5p-SITE	-	-	-	-	-	-	-	+	+	-	+	-
miR-410 mimic (Negative Control)	-	-	-	+	-	+	-	+	-	-	-	-
miRNA mimic/inhibitor	-	-	-	-	+	-	+	-	+	-	-	-

Additionally, in order to isolate miRNAs acting in the nucleus, there has been an attempt to design and perform a modified custom-made ChIP protocol. For this purpose a series of buffers, reagents and protocols were unified, modified and tested for the successful isolation of such miRNA-DNA couples and are reported throughout the text. Nevertheless, this protocol has to be tested thoroughly and repeatedly in a large number of samples and have consistent results. Protocols and reagents are documented as the ChIP protocol is analyzed below.

3.2.4.1 Crosslinking and lysis of AB8/13 undifferentiated podocytes

AB8/13 undifferentiated podocytes were cultured in RPMI 1640 medium in a 150mm dish, as described above. After reaching a confluency of around 90%, cells were washed with 1x PBS on ice and growth medium was replaced over cells after washes. Cells were then crosslinked with 1% formaldehyde (final concentration) and after 10 minutes incubation in room temperature, 10X Glycine was added. The plate was then placed on ice and the medium was removed for the cells to be washed twice with ice cold 1XPBS. Cells were then scraped off the culture plate, in 20ml 1XPBS containing 0.1U of Protease inhibitors (PIs) and RNase inhibitors (RIs) and were harvested in a sterile falcon tube. Cells were then pelleted by centrifugation and were subsequently lysed in 1ml lysis buffer containing SDS, PIs and RIs which was included in the EZ ChIP kit. For cell lysis we used a lysis buffer which consisted of 25mM Hepes pH 7.8, 1.5mM $MgCl_2$, 10mM KCl, 0.1% NP-40, 1mM DTT and 0.1U of PIs and RIs. Culture plates were found to have at least $1x10^7$ AB8/13 cells, therefore reagent volumes were calculated accordingly. Lysed cells were then aliquoted in microfuge tubes (300μl of lysate per tube and 3 tubes per culture plate). Lysates were kept at -80^oC until they were used as required in downstream experimentation.

3.2.4.2 DNA shearing by sonication

Crosslinked DNA was sonicated using the Diagenode BioRuptor (Diagenode, Denville, NJ, USA) with a protocol optimized for AB8/13 cells. Prior to sonication 20μl of cell lysate was removed from tubes in order for the sonication procedure to be tested by agarose gel electrophoresis. Podocyte cell lysates were sonicated in 13 cycles - 30s of High Power sonication followed by 30s of rest. Tubes were immersed in circulating cold water during the whole procedure and were constantly rotated to keep a uniform low temperature in the lysate

solution. Specialized RNase and DNase free microfuge 2ml tubes were used, that had a straight body ending to a conical bottom. After sonication, lysates were centrifuged at 10.000 rpm at 4^{o}C for insoluble material to be removed. Consequently, 20μl of sonicated lysate was removed from tubes and was compared with non-sonicated lysate after being de-crosslinked with 5M NaCl. Lysates were tested with 2% agarose gel electrophoresis and sonication was considered as successful if a smear sized from 1000-200bp was observed in the sonicated sample. DNA that failed to be sonicated appeared as band at around 10kb.

It was important at this stage to be able to isolate only the nuclear fraction and discard cytoplasmic debris, as we aim at reducing cytoplasmic contamination for miRNA isolation. Hence, successful isolation of nuclei by the kit was tested with western blot analysis of a number of samples. A rabbit antibody against Lamin A/C, supplied from SantaCruz Biotechnology (Santa Cruz, CA, USA) was used in a working concentration of 1:3000 to detect for the nuclear fraction, while a mouse β-tubulin was selected as a cytoplasmic marker supplied from SantaCruz Biotechnology (Santa Cruz, CA, USA) in a working concentration of 1:2000. Lysates were de-crosslinked prior to western blotting to release proteins, by adding 8μl 5M NaCl in 200μl of lysate and incubating at 65^{o}C overnight. The desired result in every case would be minimal levels of β-tubulin and enhanced levels of Lamin A/C compared to controls. Controls were both a non-treated lysate and a sonicated non-decrosslinked lysate. When DNA shearing was considered as successful per batch of samples, sonicated lysates were aliquoted in 100μl aliquots to be used in Immunoprecipitation experiments and were kept frozen at -80^{o}C until they were used.

3.2.4.3 Immunoprecipitation (IP)

It is possible that if miRNAs are able to re-enter the nucleus after their maturation in the cytoplasm, the RISC complex might be used as their vehicle as it normally is when they are active in the cytoplasm. Therefore, the Anti-pan Ago (clone 2A8) antibody from Millipore (Temecula, CA, USA) was used in order to immunoprecipitate the Ago2 protein and hence the RISC complex together with the miRNA it carries and the DNA piece bound on that miRNA. As a positive control, an antibody against the Anti-RNA Polymerase II (Millipore, Temecula, CA, USA) was used as well as a negative control, a normal mouse anti-IgG antibody (Millipore, Temecula, CA, USA). Prior to IP, sonicated lysates were defrosted on ice and

diluted in Dilution Buffer, enforced with PIs and RIs, up to 1ml. Homemade IP Dilution Buffer consisted of 0.01% SDS, 1.1% Triton X-100, 1.2mM EDTA, 16.7 mM Tris-HCl pH 8.0 and 150mM NaCl. Lysates were pre-cleared using 60μl of Protein G Agarose beads (included in the kit) or Protein A/G Agarose beads (Santacruz, CA, USA) for the homemade protocol, for 1h rotating at 4^{o}C. Agarose beads were then pelleted by centrifugation at 3000rpm for 1 minute and the supernatant was collected. Right before the IP, 20μl of the supernatant were removed to be used as the "Input" control in end-point or real-time PCR. For every IP, 1-2μg of every antibody used were added in the supernatant and left rotating overnight at 4^{o}C. Then, 60μl of agarose beads were added and left rotating for one hour more. Each IP was centrifugated and the supernatant was removed and subsequently washed once in Low Salt Immune Complex Wash Buffer, once in High Salt Immune Complex Wash Buffer, once in LiCl Immune Complex Wash Buffer and twice in TE buffer, after been let rotating in room temperature for 5 minutes. Homemade buffer recipes were the following: a. Low salt buffer contained 50mM Hepes pH 7.8, 140mM NaCl, 1mM EDTA, 1% Triton-X 100, 0.1% Na-deoxycholate and 0.1% SDS, b. High salt buffer contained 50 mM Hepes pH 7.9, 500 mM NaCl, 1 mM EDTA, 1% Triton X-100, 0.1% Na-deoxycholate and 0.1% SDS, c. LiCl wash buffer contained 20mM Tris pH 8.0, 1mM EDTA, 250mM LiCl, 0.5% NP-40 and 0.5% Na-deoxycholate, d. TE buffer contained 50mM Tris pH 8.0, 1mM EDTA and 1% SDS.

3.2.4.4 Elution of Protein/DNA/miRNA complexes

Protein, DNA and miRNAs were eluted using 200μl of freshly prepared elution buffer (10μl 20% SDS, 20μl 1M $NaHCO_3$ and 170μl ddH_2O) added to all IP pellets and Input samples. For IP pellets, 100μl of elution buffer were added followed by 15 minutes incubation at room temperature and collected after centrifugation for 1 minute at 3000 rpm, repeated twice to obtain a final volume of 200μl. All samples were reverse crosslinked with 8μl of 5M NaCl at 65^{o}C overnight. Tubes to be used for DNA extraction were treated with RNaseA for 30 minutes at 37^{o}C, followed by incubation in Proteinase K solution (4μl 0.5M EDTA, 8μl 1M Tris-HCl, 1μl Proteinase K) for 1 hour at 45^{o}C. DNA was purified with spin columns, following the EZ-ChIP kit manufacturer's protocol, buffers and columns. The miRNA fraction was extracted from IP and Input samples with the miRNeasy Kit from QIAGEN (West Sussex, UK) and the mirVana Kit from AMBION.

3.2.4.5 Validation and enrichment analysis of DNA target regions and miRNAs

DNA target regions and miRNAs were investigated using real-time PCR, using both IP and Input samples. For miRNA specific Real-Time PCR procedure see paragraph 3.1.8. DNA and a miRNA enriched fraction of the input and IP samples were isolated from each sample using the NucleoSpin miRNA Kit (Macherey-Nagel, Düren, Germany) partnered with the NucleoSpin RNA/DNA buffer (Macherey-Nagel, Düren, Germany) simultaneously.

For DNA targets, primers were specifically designed to flank the desired target region and giving a product of 100-200bp (Table 6). Control primers amplified for *GAPDH* promoter, which should give an enriched DNA fraction in RNA Polymerase II IPs, while the same product should be absent or non-enriched in mouse IgG ChIPs. If a ChIP experiment worked appropriately and efficiently, then control primer sets should not amplify the respective genomic region or the region should be under-represented in ChIPed samples. In addition, two primer sets were designed, one to amplify the miR-548c-5p target region on the *FOXC2* promoter and a second amplifying a different region closer to the gene that is not targeted by this miRNA (Figure 9). Real-Time PCR experiments were performed in a Roche LightCycler with glass capillaries, using the QIAGEN SYBR Green PCR Kit (West Sussex, UK) and the running protocol was prescribed by the manufacturer. As regards microRNA analysis, miScript Primer Assays that detect mature miRNAs were supplied by QIAGEN (West Sussex, UK) for miR-548c-5p, the U6b small nuclear RNA (snRNA) and the miR-23b, which was previously demonstrated to have enhanced expression in podocytes.[73]

Table 6: Primer sequences for different DNA regions examined in Real-Time PCR experiments after ChIP assays.

GENE	PRIMER SEQUENCES	SITE
GAPDH	5'-TACTAGCGGTTTTACGGGCG-3' 5'-TCGAACAGGAGGAGCAGAGAGCGA-3'	Proximal Promoter
FOXC2	5'-GAATCTCCAAGCTGTGTTCC-3' 5'-ACATTTTGTTAAGTTGGTTGGT-3'	miR-548c-5p
FOXC2	5'-GGTTAGAAAAAGAGCCCAGAA-3' 5'-CCAATAAAAGAACAGAAGACGA-3'	Non miR-548-5p

Results in each case are depicted as the immunoprecipitated enrichment of a product versus the Input. For this purpose, dCPs were calculated for every pair by detracting the CP of the ChIPed sample from the CP of its Input. Furthermore, ddCPs were calculated using the equation dCP_{sample}-$dCP_{negative\ control\ (mouse\ IgG)}$ and finally the fold change for every product is demonstrated as $2^{-ddCP_{sample}}$. Fold change ratios were statistically analyzed with t-test using GraphPad Prism 5.

Figure 9: Placement of primers used for Real-Time PCR experiments after ChIP assays. The first set (blue arrows) amplifies the region predicted to target the miR-548c-5p, while the second set (red arrouws) a non-miR-548c-5p target region on the promoter of FOXC2.

4 RESULTS

4.1 Identification of miRSNPs that contribute to glomerular pathological phenotypes

4.1.1 Bioinformatic analysis for identification of miRNAs as modifiers of glomerulopathies

Heritable monogenic glumerulopathies that present with MH display interfamilial and intrafamilial phenotypic heterogeneity, thereby suggesting the involvement of modifier genes in disease progression.[118] We herewith hypothesized the putative role of miRNAs as disease modifiers and we searched for functional polymorphic variants in the predicted target sites of miRNAs for genes expressed or located in the glomerulus. To this end, we guided our search for SNPs within the miRNA target sites of genes selected as described in Methods. Expression in podocytes, localization in the slit diaphragm and the glomerulus basement membrane rendered genes as good candidates for our study.

Table 7: Prediction results using five different miRNA-target prediction tools. Ticks under algorithm names indicate the successful prediction of each miRNA-mRNA pair per prediction tool. "Start" and "end" columns state the exact position of the putative miRNA target region on the 3'UTR of the respective mRNA. Numbering refers to position from the start of the mRNA 3'UTR. For sequencing analysis, pairs that had p-values of less than 0.05 were selected.

GENE	miRNA	RNA22	miRANDA	miRDB	miRWalk	TargetScan	SEED LENGTH	START	SEQUENCE	END	p-VALUE
PDPN	hsa-mir-485-5p	✓	✓	✓	✓	✓	8	1453	AGAGGCUG	1446	0.031
HBEGF	hsa-mir-212	✓	✓	✓	✓	✓	9	1584	UAACAGUCU	1576	0.0056
HBEGF	hsa-mir-132	✓	✓	✓	✓	✓	10	1584	UAACAGUCUA	1575	0.0014
HBEGF	hsa-mir-379	✓	✓	✓	✓	✓	8	1833	UGGUAGAC	1826	0.0223
FN1	hsa-mir-96	✓	✓	✓	✓	✓	8	8340	UUUGGCAC	8333	0.0169
FN1	hsa-mir-144	✓	✓	✓	✓	✓	9	8331	UACAGUAUA	8323	0.0042
GJA1	hsa-mir-495	✓	✓	✓	✓	✓	8	2244	AAACAAAC	2237	0.0261
PKD2	hsa-mir-183	✓	✓	✓	✓	✓	8	4768	UAUGGCAC	4761	0.0315
PKD2	hsa-mir-372	✓	✓	✓	✓	✓	9	4022	AAAGUGCUG	4014	0.008
PPARA	hsa-mir-223	✓	✓	✓	✓	✓	9	5877	UGUCAGUUU	5869	0.0314
SP1	hsa-mir-24	✓	✓	✓	✓	✓	7	5240	UGGCUCA	5240	0.2725
SP1	hsa-mir-31	✓	✓	✓	✓	✓	9	6960	AGGCAAGAU	6952	0.0197
SP1	hsa-mir-105	✓	✓	✓	✓	✓	7	5548	UCAAAUG	5542	0.2725
SP1	hsa-mir-155	✓	✓	✓	✓	✓	8	2560	UUAAUGCU	2553	0.0764
TJP1	hsa-mir-144	✓	✓	✓	✓	✓	8	6469	UACAGUAU	6462	0.0218

With the use of miRWalk (http://www.ma.uni-heidelberg.de/apps/zmf/mirwalk) and four other prediction algorithms (miRANDA, TargetScan, miRDB and RNA22), we looked for validated miRNAs that target the candidate genes. We narrowed down the candidates of interest by selecting only miRNA-mRNA pairs that were predicted by all five algorithms (Table 7).

Table 8: Results after re-sequencing of 103 samples with mutations in COL4A3 or COL4A4 genes and thin basement membrane nephropathy. Sequencing primers were designed to flank the predicted target sites and also include about 300bp on either side.

GENE	miRNAs	SNPs FOUND	NOTES
PDPN	hsa-mir-485-5p	T1226A G1545A G1262A 1251DEL-G	SNPs not on miRNA target sites
HBEGF	hsa-mir-132 hsa-mir-212	None	No SNPs found
HBEGF	hsa-mir-379	C1936T	SNP found at neighboring position, which is target for hsa-miR-1207-5p
FN1	hsa-mir-96 hsa-mir-144	None	No SNPs found
PKD2	hsa-mir-183	None	No SNPs found
PKD2	hsa-mir-372	G4003A G4210A	SNPs not on miRNA target sites
PPARA	hsa-mir-223	None	No SNPs found
SP1	hsa-mir-31	None	No SNPs found
TJP1	hsa-mir-144	A6485C	SNPs not on miRNA target sites

4.1.2 Identification of candidate SNPs by sequence analysis

A segment of about 500-600 nt encompassing the miRNA binding site in the 3'UTR of selected genes, was re-sequenced in 103 patients with TBMN, classified as severe or mild. Table 8 summarizes the results of the sequencing analysis depicting the gene sequenced, the miRNA predicted to bind to the 3'UTR of that gene and the SNPs identified. Although various SNPs were identified in the group of patients sequenced, none was located on the predicted miRNA binding sites. However, a SNP was identified in the binding site of another miRNA that was originally excluded due to a lower significance compared to top candidates. Specifically, while sequencing around the hsa-miR-379 target site in the *HBEGF* 3'UTR, we identified a biallelic variation of C or T at position 1936 (C1936T) in the target region of hsa-miR-1207-5p which is also predicted to target *HBEGF*. The C1936T SNP is found at what corresponds to position 2 of the 'seed' region of hsa-miR-1207-5p (Figure 10) suggesting a possible elimination or severe compromise of the ability of this miRNA to bind on *HBEGF* mRNA. Phylogenetic alignment of this SNP using the Ensembl genome browser (http://www.ensembl.org) in 10 eutherian animals, demonstrated in Table 9, shows a conservation of the C1936 allele in all aligned species, with the exception of the primate *M. mulatta* in which the T1936 allele is predominant. This region is absent from non-mammalian species such as *Xenopus*, *Zebrafish*, *Zebrafinch* and *Gallus*.

Table 9:Multiple phylogenetic alignment of the C1936T SNP. All species appear to have this position conserved, except M. mulatta, which has the T allele in the same position. Shown is the sense sequence of the region examined. By definition, the miRNA hybridizes to the anti-sense sequence.

SPECIES	CHROMOSOME	ALIGNMENT
Homo sapiens	5	CTGAGACTTGGCAGGGAGAGG
Pan Troglodytes	5	CTGAGACTTGGCAGGGAGAGG
Gorilla gorilla	5	CTGAGACTTGGCAGGGAGAGG
Macaca mulatta	6	CTGAGACTTGACAGGGAGAGG
Mus musculus	18	CTGGGATTTGGCAGGAAGAGG
Rattus norvegicus	18	CTGAGATTTGGCAGGGAGAGG
Bos taurus	7	CTGGGATTGGGCAGGGAGAGG
Sus scrofa	2	CCGAGATGGGGCAGGGAGAGG
Canis familiaris	2	AGGAGATTTGGCAGGGAGAGG
Equus caballus	14	CTGAGATTTGGCAGGGAGAGG

4.1.3 Verification of functional significance by *in vitro* experimentation

In order to verify whether HBEGF is a true target of hsa-miR-1207-5p and that the presence of C1936T SNP alters the binding and regulation incurred by the miRNA, we performed luciferase 'sensor' assays. A segment of the HBEGF 3'UTR containing the 1936C (pMIR-REPORT-HBEGF-1936C) or 1936T (pMIR-REPORT-HBEGF-1936T) variant was cloned into the 3'UTR of the luciferase gene in pMIR-REPORT plasmid. Reporter plasmids and β-gal reference plasmid were co-transfected in AB8/13 podocyte cell line with either hsa-miR-1207-5p mimic or negative control mimics for 12 hours followed by luciferase and β-gal measurement. Co-transfection of hsa-miR-1207-5p mimics with the pMIR-REPORT-HBEGF-1936**C** resulted in significant reduction in luciferase expression (47.14% +/- 0.42 SEM of normalized RLU relative to control) demonstrating that this miRNA directly binds on HBEGF 3'UTR region (Figure 11).

In agreement, transfection of hsa-miR-1207-5p mimics in AB8/13 cells significantly reduced the endogenous levels of HBEGF protein as demonstrated by Western blot analysis at about 20% of total expression, while hsa-miR-1207-5p inhibitors boosted HBEGF levels by reducing the endogenously expressed miRNA levels (Figure 12 – upper panel). Densitometry of western blots revealed a significant decrease or increase of HBEGF levels on mimic or inhibitor transfection respectively. (Figure 12 – lower panel).

Figure 10: Schematic depicting the position of miRSNP C1936T on the target region of hsa-miR-1207-5p on HBEGF. This miRSNP corresponds to the second base of the seed region of hsa-miR-1207-5p, underlined C.

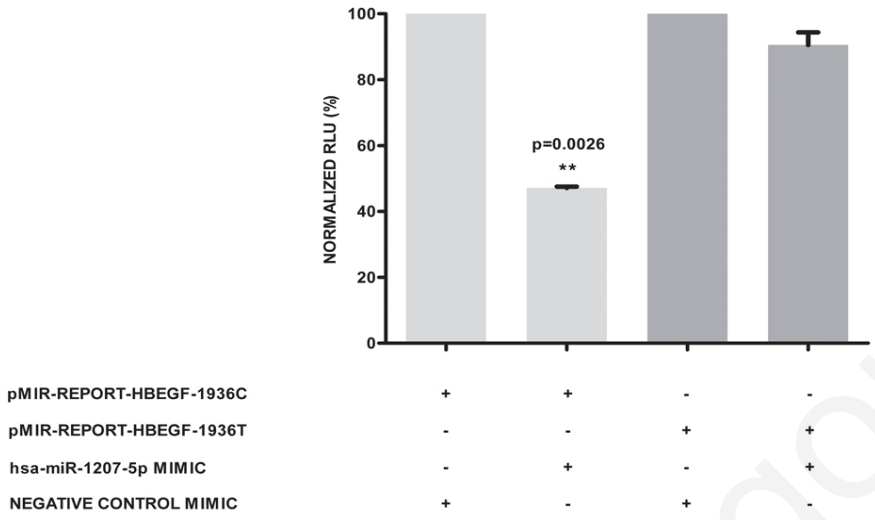

Figure 11: Normalized luciferase relative light units (RLUs) in AB8/13 cell lysates after transfection with sensor constructs. Co-transfection of the pMIR-REPORT- HBEGF -1936C with hsa-miR-1207-5p miRNA LNA mimics resulted in significant reduction of luciferase expression, with a p-value of 0.0026 using one-way non-parametric ANOVA test. In contrast, the pMIR-REPORT construct bearing the 1936T allele (pMIR-REPORT- HBEGF -1936T) abolished the hsa-miR-1207-5p binding site as demonstrated from the loss of RLU reduction. Results represent mean values of triplicates ± SEM.

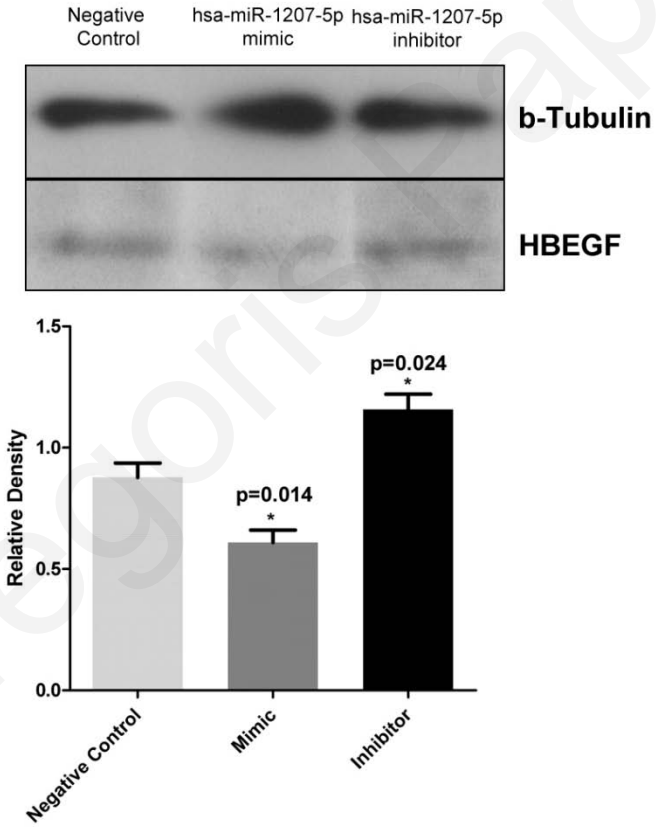

Figure 12: Western blot of HBEGF from AB8/13 cells after transient transfection with hsa-miR-1207-5p miRNA LNA mimics, inhibitors and the AllStars™ Negative Control scrambled sequence LNA. This is a representative of six experiments. Lower panel presents the statistical analysis of western blot densitometry results, normalized against the Negative Control. Values represent the mean ± SEM. Results illustrate the reduction of HBEGF protein levels at the presence of hsa-miR-1207-5p mimics (p=0.014), while miRNA inhibitors significantly increased HBEGF levels (p=0.024).

On the contrary, in the presence of pMIR-REPORT- HBEGF -1936**T**, transfection of hsa-miR-1207-5p mimics did not significantly alter luciferase expression (90.56% +/- 3.8 SEM of normalized RLU relative to control) in AB8/13 cells (Figure 11). Combined these results demonstrate that hsa-miR-1207-5p can directly regulate HBEGF expression and this regulation is abolished if there is a T nucleotide at position 1936 of HBEGF's 3'UTR.

The hsa-miR-1207-5p is highly enriched in podocytes as demonstrated by miRNA specific Real-Time PCR experiments. Specifically, miR-1207-5p is expressed 2-fold higher in differentiated AB8/13 podocytes, compared to undifferentiated cells (Figure 13). In addition, human renal epithelial cells express 4-fold higher miR-1207-5p than differentiated AB8/13 cells. Other cell lines, such as HEK293 and SHSY-5Y demonstrate limited expression levels of miR-1207-5p when compared to podocytes.

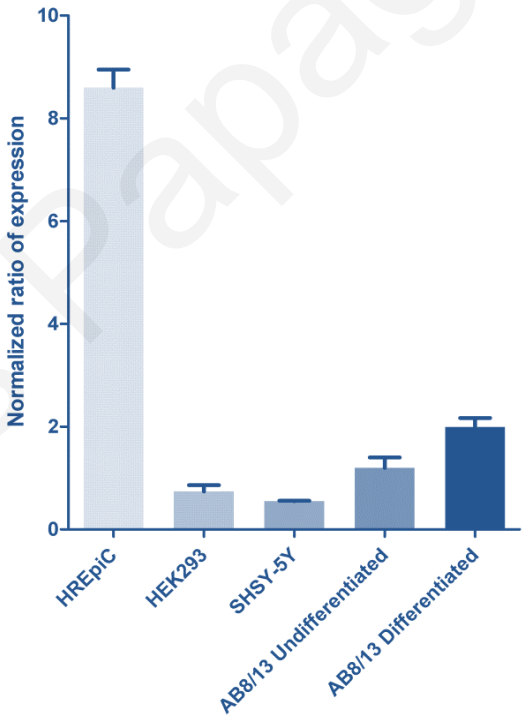

Figure 13: Relative expression analysis of mature hsa-miR-1207-5p levels in various cell types, as tested by miRNA specific Real-Time PCR experiments. Both AB8/13 differentiated and undifferentiated podocytes revealed significantly high expression levels of miR-1207-5p, compared to HEK293 and SHSY-5Y neuroblastoma cells. Further examination of miR-1207-5p levels in human renal epithelial cells (HREpiC), recorded 4-fold higher mature miRNA than the AB8/13 differentiated podocyte cell line. Results represent the mean of quadruplicate values ± SEM.

4.1.4 C1936T genotyping in various cohorts including control samples

4.1.4.1 Control samples

A total number of 232 control samples, was genotyped in order to test for general population frequency of the C1936T miRSNP genotypes and 70% were CC homozygotes, 27% CT heterozygotes and 3% TT homozygotes. The control population obeys the Hardy-Weinberg equilibrium (p = 0.772), as tested by the Pearson's chi-square test. Allele frequencies are C: 83.4% and T: 16.6%.

4.1.4.2 TBMN and CFHR5 cohorts

Sequencing analysis showed that 68.2% of patients having mild TBMN are homozygous for the C allele, 6.8% are homozygous for the T allele and 25.7% CT heterozygotes (Table 10). Concerning patients with severe TBMN disease, 76.3% were CC homozygotes, 1.7% TT homozygotes and 22% CT heterozygotes. There was no statistical significance between the two groups, upon two-sided Barnard's testing (p-value = 0.368).

Table 10: Genotype and allele frequencies in TBMN and CFHR5 groups. Under each group label, left columns demonstrate the number of subjects for each genotype and allele, while right columns the respective percentages.

GENOTYPE	MILD TBMN (COL4A3/COL4A4 MUTATIONS)		SEVERE TBMN (COL4A3/COL4A4 MUTATIONS)		MILD CFHR5 NEPHROPATHY		SEVERE CFHR5 NEPHROPATHY	
CC	30	68.2%	45	76.3%	39	86.6%	21	63.6%
CT	11	25%	13	22%	6	13.4%	12	36.4%
TT	3	6.8%	1	1.7%	0	0%	0	0%
CT/TT	14	31.8%	14	23.7%	6	13.4%	12	36.4%
MILD vs SEVERE	p=0.368				p=0.018			

In a separate cohort of 78 patients diagnosed with CFHR5 nephropathy, among 45 CHFR5 patients with milder disease progression, 86.6% are homozygous for the C allele, while the remaining are CT heterozygotes. In contrast, 63.6% of the 33 severely affected CFHR5 patients are CC homozygotes and 36.4% are CT heterozygotes. Barnard's test with a 95% confidence interval revealed an association between mild CFHR5 and the CC genotype, with a p-value of 0.018 and Wald statistic of -2.385 (Figure 14). Further grouping of TT homozygotes and CT heterozygotes, indicated a significant difference between mild CFHR5 patients and mild TBMN patients with a p=0.038 after Barnard's test with a Wald statistic of 2.089. The corresponding frequencies did not differ significantly between severe CFHR5 and severe TBMN patients. Collectively, evidence suggests that the CT/TT genotype has no significant effect on the severity of TBMN, but it increases the risk for a severe outcome in patients with CFHR5 nephropathy, by 3.7 times.

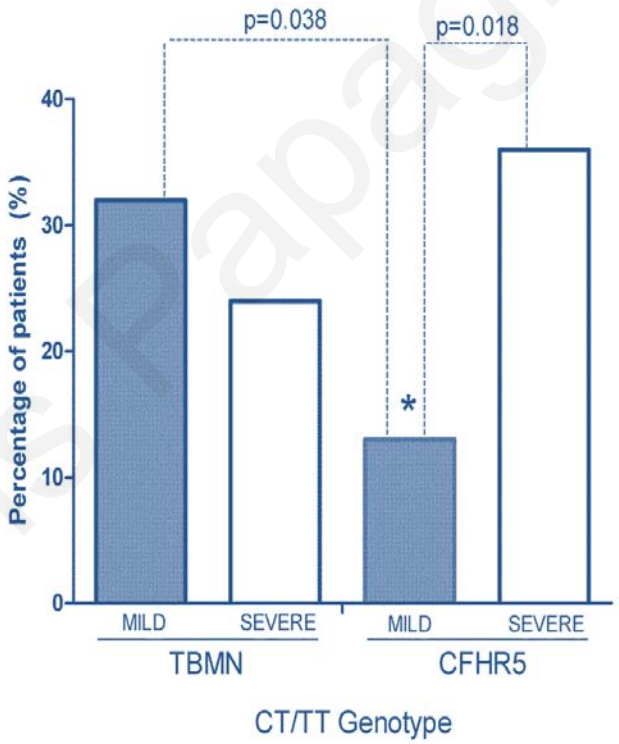

Figure 14: Mildly affected CFHR5 patients have lower occurrence of the 1936T allele. Graphical representation of both TBMN and CFHR5 nephropathy cohorts used in this study in relation to the number of CT and TT patients. Nephropathy patients with mild CFHR5 have significantly lower percentage of the CT genotype when compared with severe CFHR5 patients (p=0.018), indicating a protective effect of the CC genotype. Statistical comparison between mild TBMN and mild CFHR5 patients demonstrated a significant underrepresentation of the 1936T allele in mild CFHR5 patients (p=0.038). Mild TBMN patients did not differ from severe TBMN patients (p=0.368). All statistical analyses were performed using two-sided Barnard's test.

A separate evaluation of women in our CFHR5 cohort, revealed significance between mildly and severely affected women with a p-value of 0.035 and a Wald statistic of -2.234 (Figure 15). As women are known to have a milder course of the disease, it is 8 times more likely to have a severe phenotype if the patient is a female and a carrier of a CT/TT genotype.

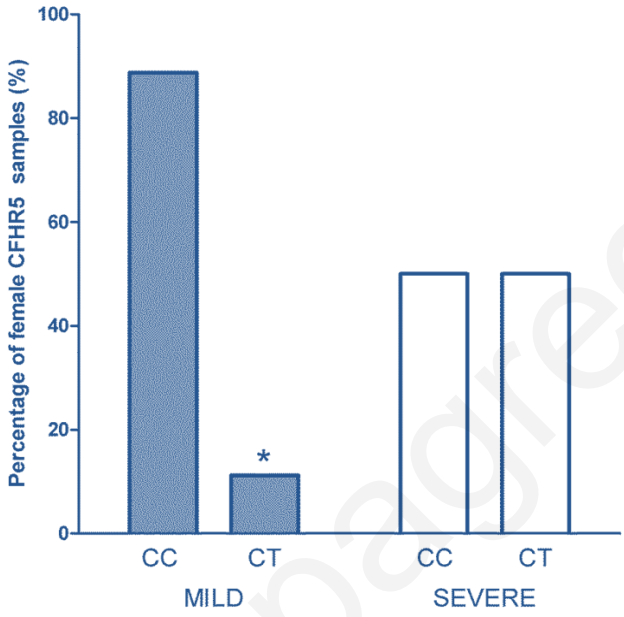

Genotype \ CFHR5 Phenotype	Mild	Severe
CC	24	3
CT	3	3
p-value	0.035	

Figure 15: The 1936T HBEGF genotype is overrepresented in women affected with severe CFHR5. Comparison of C1936T genotypes in women manifesting CFHR5 nephropathy. Women are known to have a milder course of the disease when compared to men and this is also demonstrated when they are statistically compared with severe CFHR5 women as regards the C1936T SNP. The 1936C allele has a significantly lower representation in severe CFHR5 women, compared to mild women, thus suggesting a protective effect for this allele (p=0.035).

4.1.4.3 Genotyping of additional groups of patients

4.1.4.3.1 CKD and ESKD cohort

The CKD and ESKD cohorts include two phenotypically distinct groups of patients that are diagnosed with CKD or progressed to ESKD and belong to three disease groups, hypertensive glomerulosclerosis (HGS), glomerulonephritis (GN) and diabetic nephropathy (DN). From 17 patients diagnosed HGS and having CKD, 76.5% have CC genotype, 17.6% have CT and

5.9% have the TT genotype. Respectively, 76.9% of ESKD HGS patients have CC genotype and the remaining 23.1% have CT. The two groups do not appear to differ on Barnard's two-sided testing with p=1, after grouping of CT heterozygotes and TT homozygotes (Table 11).

From patients presenting GN and a mild course of renal disease, 57.1% are CC homozygotes, 33.4% CT heterozygotes and 9.5% TT homozygotes, while from GN patients proceeding to ESKD, 67.9% have a CC, 28.6% CT and 3.5% TT genotype. When CT heterozygotes and TT homozygotes were grouped, groups did not differ upon Barnard's two-sided test, with p=0.569 (Table 11).

In DN patients, 83.3% of CKD patients and 71.4% of patients with ESKD have CC genotype, while 16.7% and 25.7% have CT genotype respectively. TT homozygotes are absent from the CKD DN group, while one patient (2.9%) appears to have this genotype in the ESKD DN group. These two groups did not differ on Barnard's two-sided test with p=0.674, after CT and TT grouping (Table 11).

Table 11: Results of genotyping of patients with either CKD or* ESKD*, diagnosed with mild or severe GN, HN and DN, for the C1936T miRSNP of HBEGF.

GENOTYPE	MILD GLOMERULONEPHRTIS		SEVERE GLOMERULONEPHRITIS		MILD HYPERTENSIVE NEPHROSCLEROSIS		SEVERE HYPERTENSIVE NEPHROSCLEROSIS		MILD DIABETIC NEPHROPATHY		SEVERE DIABETIC NEPHROPATHY	
CC	12	57.1%	19	67.9%	13	76.5%	10	76.9%	5	83.3%	25	71.4%
CT	7	33.4%	8	28.6.%	3	17.6%	3	23.1%	1	16.7%	9	25.7%
TT	2	9.5%	1	3.5%	1	5.9%	0	0%	0	0%	1	2.9%
CT/TT	9	42.9%	9	32.1%	4	23.5%	3	23.1%	1	16.7%	10	28.6%
MILD vs SEVERE	p=0.569				p=1				p=0.674			

Collectively, when C1936T genotype results from CKD patients from all groups were statistically compared to ESKD patient results by using Barnard's two-sided test, they appear not statistically different with p=0.795. This is proving that in these specific disease groups, the de-regulation of HBEGF expression by miR-1207-5p due to the C1936T miRSNP is not implicated in the disease severity.

4.1.4.3.2 IgA nephropathy and familial hematuria cohorts

The IgA nephropathy (IgAN) cohort is composed of 24 patients with CKD and 25 patients with ESKD, while the familial hematuria (FH) cohort consists of 35 patients with CKD and 43 patients with ESKD. Genotyping of the IgAN CKD cohort revealed that 54.2% of patients have CC genotype, while the remaining 45.8% are CT heterozygotes. Absence of TT homozygotes was also observed in IgAN ESKD patients, with 68% of them being CC homozygotes and 32% CT heterozygotes. These two groups did not differ statistically upon Barnard's testing, with p=0.397 (Table 12).

The FH cohort alone was genotyped in the same way as the IgAN cohort and results showed that 74.3% of FH patients having a milder disease course have a CC genotype, while in the same group of patients 17.1% have a CT genotype and 8.6% are TT homozygotes. In FH patients that progressed to ESKD, 74.4% are CC homozygotes, 18.6% are CT heterozygotes, while 7% are TT homozygotes. Similarly, these two FH groups did not differ statistically, with p=0.999 after tested with Barnard's two-sided test (Table 12).

Table 12: Genotyping and allele frequencies of IgAN and FH cohorts, for the C1936T miRSNP.

GENOTYPE/ ALLELE	MILD IgA NEPHROPATHY		SEVERE IgA NEPHROPATHY		MILD FAMILIAL HEMATURIA		SEVERE FAMILIAL HEMATURIA	
CC	13	54.2%	17	68%	26	74.3%	32	74.4%
CT	11	45.8%	8	32%	6	17.7%	8	18.6%
TT	0	0%	0	0%	3	8.6%	3	7%
CT/TT	11	45.8%	8	32%	9	25.7%	11	25.6%
MILD vs SEVERE	p=0.397				p=999			

4.1.4.3.3 The “Cyprus Study” cohort

This cohort was provided to us, by the Cyprus Cardiovascular Disease Education and Research Trust, through Dr Andy Nicolaides. A significant number of subjects participating in the “Cyprus Study” cohort were genotyped for the C1936T miRSNP on HBEGF, in an attempt to spot a differentially expressed protein, aminoacid or substance in the serum of patients, which is implicated in pathology of renal function. Expression levels of different proteins were previously identified in this cohort, using commercially available biochemical assays. Matrix metalloproteinase expression levels, together with their inhibiting enzymes TIMP1 and TIMP2, were the first to be studied. Statistical analysis with Kruskal-Wallis test for independent samples did not reveal any significance among groups (genotyping results with mean serum levels of proteins are reported in Table 13).

Table 13: Genotyping results and mean serum levels for each group for MMP1, MMP2, MMP8, MMP9, TIMP1 and TIMP2 proteins.

GENOTYPE OF C1936T	MATRIX METALLOPROTEINASE 1 SERUM LEVELS		MATRIX METALLOPROTEINASE 2 SERUM LEVELS		MATRIX METALLOPROTEINASE 8 SERUM LEVELS		MATRIX METALLOPROTEINASE 9 SERUM LEVELS		TIMP1 SERUM LEVELS		TIMP2 SERUM LEVELS	
	N	RANKMEAN	N	RANKMEAN	N	RANK MEAN	N	RANKMEAN	N	RANKMEAN	N	RANKMEAN
CC	284	217.38	284	212.38	284	222.53	284	219.42	284	212.33	251	194.42
CT	135	209.14	135	225.36	135	208.57	135	211.58	135	223.52	115	178.92
TT	14	285.04	14	226.04	14	186.11	14	220.07	14	248.93	11	170.73
p	0.096		0.597		0.364		0.832		0.433		0.384	

The contribution of homocysteine levels in renal decline has been well investigated in the past. Thus, it was inevitable to compare C1936T to serum homocysteine levels, supplemented by serum levels of folic acid and vitamin B12, both known to alleviate symptoms of renal disease. Genotyping results and serum level means for all these proteins are recorded in Table

14 – Panel a. Statistical analysis using Kruskal-Wallis test for independent variables, revealed weak statistical significance between the CT genotype and lower levels of folic acid with p=0.047, while B12 and homocysteine levels did not. Further analysis regarding the same proteins was performed, by performing statistics after filtering for samples having both high homocysteine and low folic acid levels, a combination known to increase the risk for developing renal disease. Under these circumstances, subjects having the CC genotype demonstrated statistically significant higher levels of homocysteine when compared to subjects having CT or TT C1936T genotypes, suggesting a protective effect for the 1936T genotype with p=0.027 (Table 14 – Panel b). Kruskal-Wallis testing for both folic acid and B12 levels did not reveal any statistical significance for the C1936T genotype distribution.

Table 14: Association of the C1936T miRSNP in subjects of the "Cyprus Cohort" and serum levels of folic acid, vitamin B12 and homocysteine. Panel (a) includes all samples, while panel (b) includes only samples belonging to the upper quartile of homocysteine levels and the lower of folic acid.

a.

GENOTYPE OF C1936T	FOLIC ACID SERUM LEVELS		B12 SERUM LEVELS		HOMOCYSTEINE SERUM LEVELS	
	N	RANK MEAN	N	RANK MEAN	N	RANK MEAN
CC	399	306.80	445	322.12	379	279.68
CT	171	268.32	188	340.25	164	281.71
TT	20	302.35	19	293.05	18	302.39
p	**0.047**		0.843		0.398	

b.

GENOTYPE OF C1936T	FOLIC ACID SERUM LEVELS		B12 SERUM LEVELS		HOMOCYSTEINE SERUM LEVELS	
	N	RANK MEAN	N	RANK MEAN	N	RANK MEAN
CC	47	38.77	41	30.49	47	41.14
CT	26	37.85	22	35.57	26	32.92
TT	2	22.00	1	47.50	2	6.75
p	0.566		0.422		**0.027**	

Furthermore, serum creatinine, ADMA, NO and myeloperoxidase levels in subjects of the same cohort were also correlated with C1936T miRSNP. After Kruskal-Wallis testing, MPO levels were found to be strongly associated with C1936T, with CC homozygotes having significantly lower serum levels of MPO compared with CT heterozygotes and TT

homozygotes (p=0.0001). Neither creatinine, nor NO or ADMA levels showed any statistical association with the C196T miRSNP on HBEGF (Table 15).

Table 15: Correlation of ADMA, NO, creatinine and MPO serum levels with the C1936T genotype in subjects of the "Cyprus Study" cohort.

GENOTYPE OF C1936T	ADMA SERUM LEVELS		NITRIC OXIDE SERUM LEVELS		CREATININE SERUM LEVELS		MYELOPEROXIDASE SERUM LEVELS	
	N	RANK MEAN	N	RANK MEAN	N	RANK MEAN	N	RANK MEAN
CC	108	76.33	173	133.15	445	326.51	119	75.08
CT	40	77.31	82	127.43	194	338.06	43	105.78
TT	4	73.00	8	153/94	20	329.43	5	108.90
p	0.980		0.606		0.780		**0.001**	

4.2 Investigation of the role of miRNAs as regulators of transcription

4.2.1 Bioinformatic analysis of gene "promoter" regions

Genes listed in Appendix I were initially tested using the miRWalk algorithm for miRNA target regions, defined only by their degree of complementarity against mature miRNA sequences, located at their promoter regions. "Promoter" regions were considered as the first 10kb immediately upstream the 5'UTR of any gene. Surprisingly, miR-548c-5p and miR-548d-5p appeared to have almost complete complementarity with sequences located upstream genes *FOXC2* and *SPP1* respectively (Table 16). In other upstream gene sequences, such as of *HBEGF* and *TCF21* lengthy target sites were also observed that corresponded to miR-1273 and miR-1285 respectively. Target site position upstream *FOXC2* and *SPP1* are demonstrated on Figure 16. The miRWalk algorithm displays results in reverse numbering, therefore a "start" site of 1310 for miR-548c-5p target site upstream *FOXC2* implies that the site is located upstream the 10kb region and far away from the 5'UTR of the gene.

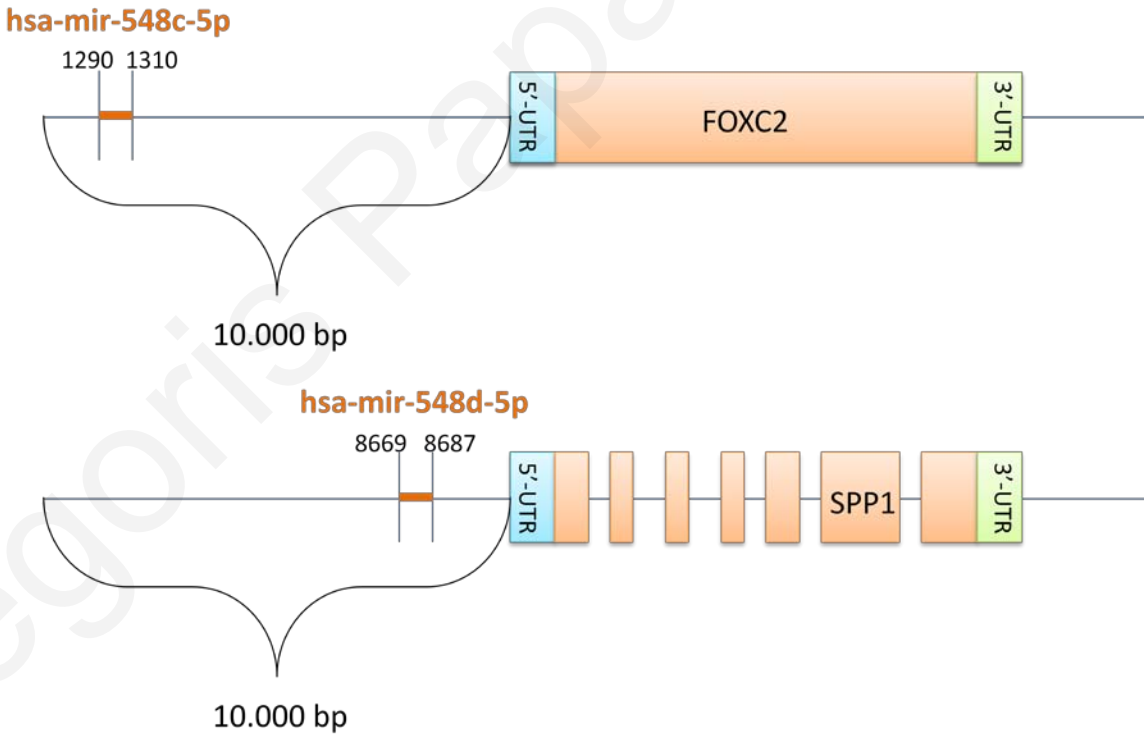

Figure 16: Position of the miRNA target sites on FOXC2 (upper panel) and SPP1 (lower panel) genes. Position 1 is the first nucleotide 10 kb upstream and numbering continues in the right direction until it reaches the transcription start at 5'UTR.

In order to investigate whether this kind of target side length is a widespread phenomenon observed amongst genes, a reverse prediction approach was carried out by importing all validated mature miRNAs into miRWalk and searching for target sites in the same regions of all known genes. The genes presenting the highest length of miRNA complementary sequences appear on Table 17. The hsa-miR-548c-5p seems to have a high number of lengthy target sites in intergenic regions with proximity to gene transcription start sites, while other miRNAs did not.

Pathway analysis using the DAVID algorithm (http://david.abcc.ncifcrf.gov/), did not reveal any functional correlation between these genes. This result led us to assume that this specific miRNA, miR-548c-5p, can potentially bind to such sequences and we decided to further investigate its putative binding and regulatory properties. In order to investigate the miR-548c-5p predicted target site region further, we used the Blat algorithm from the UCSC Genome Browser (http://genome.ucsc.edu). It appears that this sequence is located downstream of a non-coding RNA gene and upstream the *MTHFSD* gene, which is transcribed in an anti-sense direction. In addition, testing of this target sequence demonstrated that it is non palindromic nor similar to a MADE1 type transposable element nor located on any kind of a transcript.

Table 16: The lengthiest target sites on the promoter region of candidate genes using the miRWalk algorithm

GENE	miRNA	Seed Length	Start	Sequence	End
FOXC2	hsa-miR-548c-5p	21	1310	AAAAGUAAUUGCGGUUUUUGC	1290
SPP1	hsa-miR-548d-5p	19	8687	AAAAGUAAUUGUGGUUUUU	8669
HBEGF	hsa-miR-1273	19	5113	GGGCGACAAAGCAAGACUC	5095
TCF21	hsa-miR-1285	19	181	UCUGGGCAACAAAGUGAGA	163

Table 17: List of genes that contain the lengthiest target sites for hsa-miR-548c-5p, in the sequence 10kb upstream of their 5'UTR. Prediction analysis included all human genes.

Gene	Seed Length	Start	Sequence	End
CDC23	21	3638	AAAAGUAAUUGCGGUUUUUGC	3618
ASB5	21	6948	AAAAGUAAUUGCGGUUUUUGC	6928
NSUN5	21	3023	AAAAGUAAUUGCGGUUUUUGC	3003
RBP4	21	3050	AAAAGUAAUUGCGGUUUUUGC	3030
NR0B1	21	4270	AAAAGUAAUUGCGGUUUUUGC	4250
EBI2	21	1515	AAAAGUAAUUGCGGUUUUUGC	1495
FGF23	21	140	AAAAGUAAUUGCGGUUUUUGC	120
ANXA3	21	9753	AAAAGUAAUUGCGGUUUUUGC	9733
PLAC1	21	8757	AAAAGUAAUUGCGGUUUUUGC	8737
ATHL1	21	7462	AAAAGUAAUUGCGGUUUUUGC	7442
ZNF418	21	9269	AAAAGUAAUUGCGGUUUUUGC	9249
PSTPIP2	21	9206	AAAAGUAAUUGCGGUUUUUGC	9186
FOXC2	21	1310	AAAAGUAAUUGCGGUUUUUGC	1290
LBP	21	3246	AAAAGUAAUUGCGGUUUUUGC	3226
UBQLN2	21	8250	AAAAGUAAUUGCGGUUUUUGC	8230
C11orf65	20	8063	AAAAGUAAUUGCGGUUUUUG	8044
SSH1	20	4823	AAAAGUAAUUGCGGUUUUUG	4804
AOX1	19	9533	AAAAGUAAUUGCGGUUUUU	9515
HRK	19	212	AAAAGUAAUUGCGGUUUUU	194
PTER	19	9160	AAAAGUAAUUGCGGUUUUU	9142

4.2.2 Bioinformatic investigation of the promoter targeting properties of the miR-548 family

After demonstrating that miR-548c-5p has lengthy target sites on a number of different genes, we examined further the binding properties of the miR-548 family members by using the miRWalk algorithm. The miR-548 family consists of 68 mature miRNAs emerging from different premature transcripts that eventually give 56 non-redundant sequences, as it is recorded by miRBase. This implies that some miRNAs that belong to this family have the same mature sequence, with one of them being miR-548c-5p sharing the exact same sequence with miR-548o-5p and miR-548am-5p. Furthermore, a number of miRNAs that are classified into the miR-548 family have a mature sequence that differs from miR-548c-5p in one, two or more nucleotides (Table 18).

Table 18: List of miRNAs that belong to the miR-548 family and share extended similarities in their sequence with miR-548c-5p. The difference in base numbers between each miRNA and miR-548c-5p is also displayed, together with a rough grouping depending on how they differ.

miRNA Name	Start	End	Seed Length	Difference in Bases from miR-548c-5p	Group
548c-5p	1310	1289	21	0	1
548am-5p	1310	1289	21	0	1
548o-5p	1310	1289	21	0	1
548au-5p	1310	1289	21	-1	1
548j	1310	1296	15	3	2
548as-5p	1310	1297	14	1	2
548i	1310	1297	14	1	2
548a-5p	1210	1298	13	3	2
548ar-5p	1310	1299	12	1	2
548ab	1310	1300	11	3	3
548b-5p	1310	1200	11	2	3
548d-5p	1310	1300	11	1	3
548h-5p	1310	1302	9	2	4
548y	1310	1302	9	3	4
548aj-5p	1313	1299	15	1 (+3,-2)	5
548n	1311	1300	12	3 (+1,-1)	5
548aq-5p	1309	1299	11	2	3
548aw	1314	1305	10	3(+4,-6)	6

The length of target sites in accordance to their location (Promoter region, 5'UTR, coding sequence and 3'UTR of all human genes) was also examined by miRWalk. Target sites of 25-15 complementary nucleotides clustered in the promoter region of genes (10kb upstream the 5'UTR), while hits on the 3'UTR remained low in number, thus indicating a specificity of miR-548 family members for promoter sequences (Figure 17).

In general, most predicted target sites (Figure 18) by miRWalk regarding the miR-548 family are located on the promoter regions of genes (44.13%), followed by the 3'UTR (34.39%), the coding sequence (16.02%) and finally the 5'UTR (5.46%). This analysis included only target sites that had a pValue of equal or less than 0.05 after an automatic statistical analysis performed by the miRWalk algorithm and targets are defined by their complementarity against the mature sequence of miRNAs as they appear in miRBase.

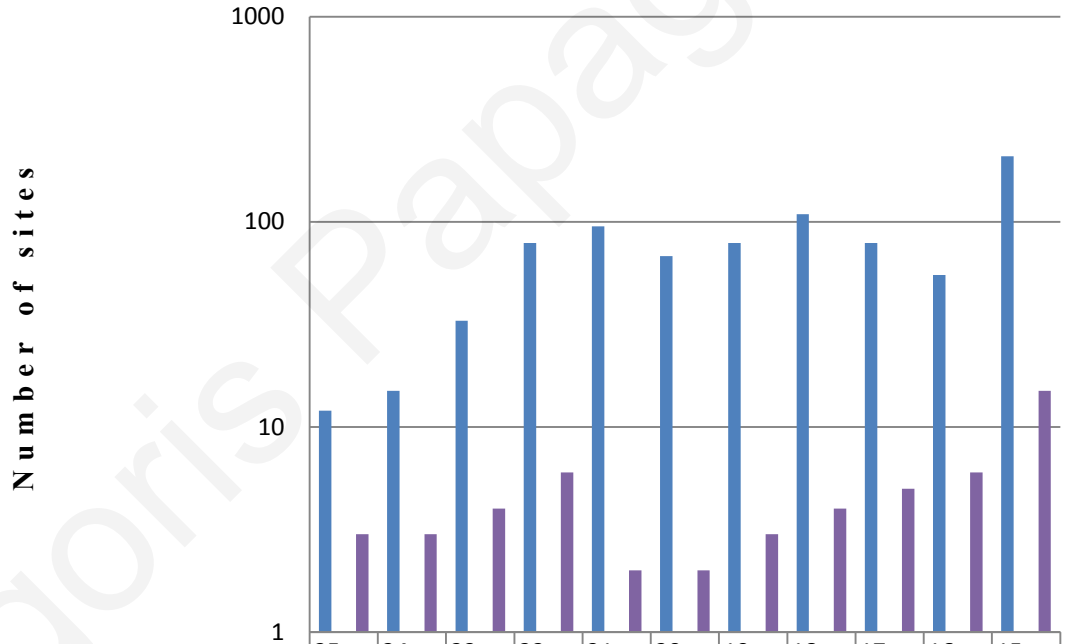

	25nts	24nts	23nts	22nts	21nts	20nts	19nts	18nts	17nts	16nts	15nts
10kb upstream region	12	15	33	79	95	68	79	109	79	55	209
5'UTR	0	0	0	0	0	0	0	0	0	0	0
Coding Sequence	0	0	0	0	0	0	0	0	0	0	1
3'UTR	3	3	4	6	2	2	3	4	5	6	15

Figure 17: Distribution of target site length for miR-548 family members in relation to all human protein coding genes as predicted by the miRWalk algorithm. The promoter region seems to have more sites than any other region, as target sites remain extended in length. Each site is unique for a specific miRNA and the lengthiest target site was always taken into account.

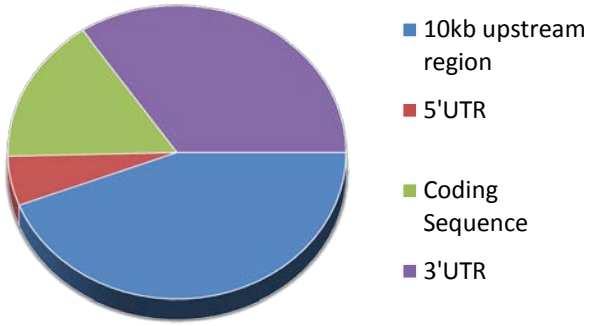

Figure 18: Pie chart displaying the distribution of predicted target sites of miR-548 family members throughout the human genome genes. Prediction analysis demonstrated an enrichment of target sites at the promoter regions of genes, termed as the first 10kb located upstream the 5'UTR. The predicted target sites include sites with at least seven complementary nucleotides in the seed region.

4.2.3 Experiments with reporter constructs

Reporter constructs bearing a multiple cloning site at the promoter's enhancer element of the firefly luciferase gene were encompassed in order to investigate for the binding properties of miRNAs against their predicted promoter target sites. Affinity of miRNA mimics and removal of endogenously expressed miRNAs by inhibitor LNAs was demonstrated by the determination of luciferase expression levels with a luminometer. The lengthy binding site of miR-548c-5p located more than 8kb upstream the 5'UTR of the *FOXC2* gene was firstly examined.

The significance of miR-548c-5p binding site upstream *FOXC2* was demonstrated by transfecting AB8/13 podocytes with equal amounts of reporter plasmids. Each plasmid either had (548c-5p+SITE) or not (548c-5p-SITE) the target site, as it was previously removed with side-directed mutagenesis from the pGL4.27 vector. The 548c-5p-SITE vector only carried the flanking sequence of the miR-548c-5p target site upstream the *FOXC2* gene. The luciferase vector without an insert was used as a control. ANOVA with Tuckey post-testing was used to test for trend significance, with $p<0.0001$. Statistical analysis of luciferase expression levels with t-test demonstrated that cells transfected with the plasmid having the miR-548c-5p target site on the promoter enhancer element of the luciferase gene, expressed significantly more

luciferase compared to the empty vector (p=0.002). The transcriptional suppression caused by the miRNA target site was eliminated after determining luciferase expression levels in cells transfected with the plasmid lacking the site, with p=0.0006 compared to the plasmid bearing the target site with t-test (Figure 19). These results suggest that the specific region flanking the target site could be acting as a transcription enhancer element, while the miRNA target site itself limits this effect possibly via the hybridization of miR-548c-5p miRNA on its respective target sequence.

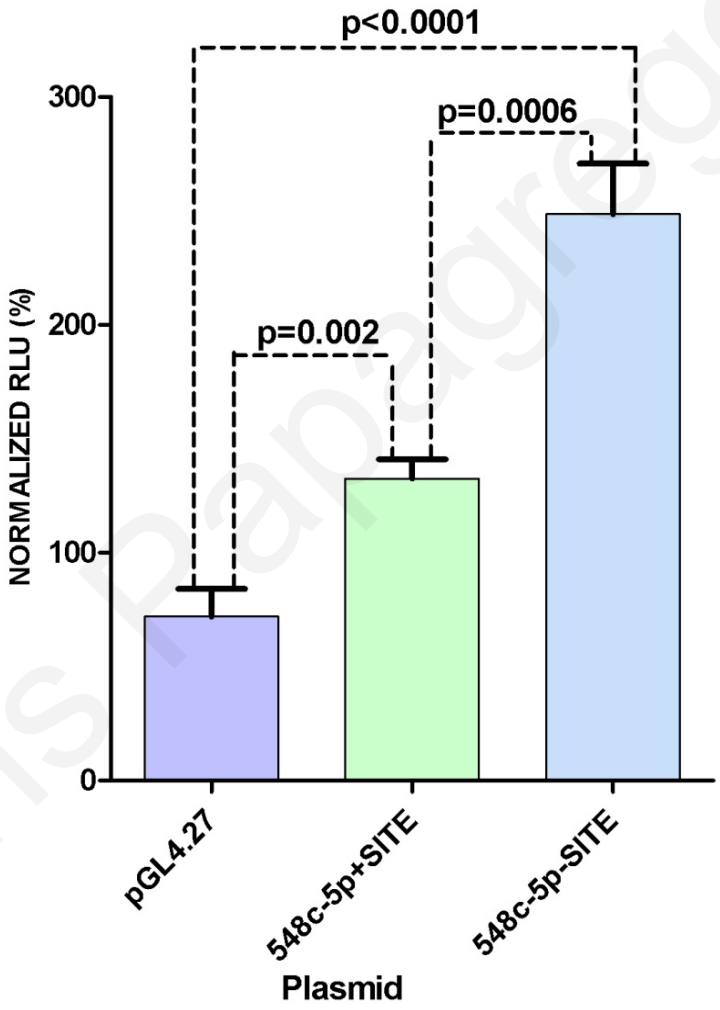

Figure 19: Luciferase expression levels after transfection of AB8/13 podocyte cells with luciferase reporter plasmids. The plain vector (pGL4.27) kept a minimal rate of transcription for the luciferase gene, while the miR548c-5p target site boosts luciferase expression (548c-5p+SITE). When the site was removed (548c-5p-SITE), repression is released and luciferase levels increase at least 2.5 times more than in cells transfected with the plain vector. Firefly luciferase expression levels were normalized against renilla luciferase levels, expressed by the pGL4.74 reporter vector. Results represent the mean of values from 6 experiments ± SEM.

Binding properties of miR-548c-5p were then examined using miRNA mimics, inhibitors and Negative Control scrambled sequence LNA in AB8/13 undifferentiated podocytes. Initial experiments demonstrated significant reduction of luciferase levels in cells transfected with the 548c-5p+SITE vector and the Negative Control LNA, probably caused by the non-specific binding of the Negative Control LNA on the firefly luciferase plasmid. Therefore, we made an effort to replace the Negative Control LNA by a different miRNA mimic, which would keep normalized luciferase levels the same as when the 548c-5p+SITE plasmid is not co-transfected with any LNAs. ANOVA with Tuckey post-testing was used to test for trend significance, with p=0.004. The miR-410 mimic demonstrated good resemblance, with p=0.205 after t-testing, to the non-LNA transfected cells (Figure 20) and replaced the negative control in mimic/inhibitor transfection experiments.

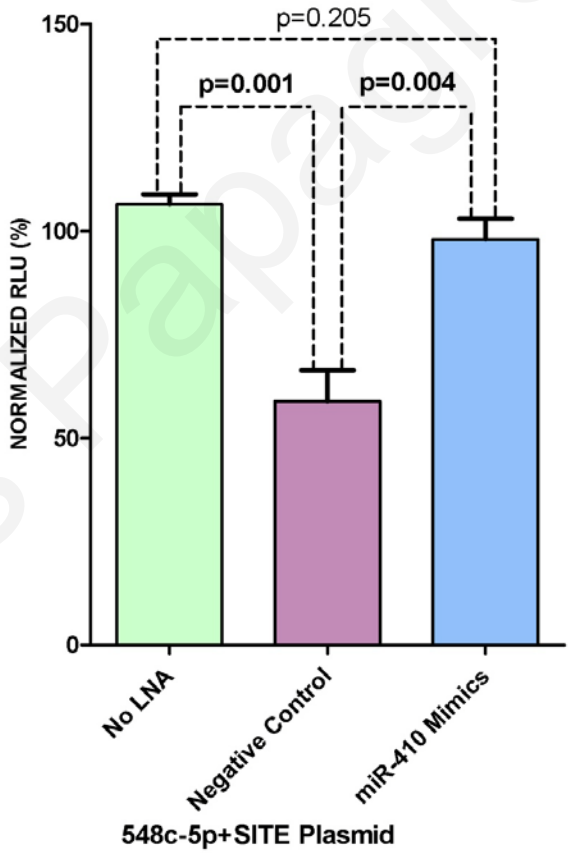

Figure 20: Normalized luciferase relative light units (RLUs) in AB8/13 cell lysates after transfection with sensor constructs. AB8/13 cells transfected with the pGL4.27 plasmid bearing the 548c-5p site together with negative control scrambled sequence LNA, miR-410 mimics or no LNA. The negative control LNA demonstrated a significant reduction in luciferase levels and was excluded from future experiments as the negative control. The miR-410 mimic showed no difference when compared to the non-LNA containing samples and was considered as having no effect over the pGL4.27luciferase vector. Results represent mean values of triplicates ± SEM.

After transfecting AB8/13 cells with miR-548c-5p mimics and inhibitors and the firefly luciferase expressing plasmid with the miR-548c-5p target site, luciferase expression was affected. ANOVA with Tuckey post-testing was used to test for trend significance, with $p<0.0001$. MiR-548c-5p mimics managed to significantly reduce luciferase levels, compared with cells transfected with miR-410 mimics, with $p=0.02$ after t-testing. As expected, miR-548c-5p inhibitors boosted luciferase levels compared to cells transfected with miR-410 mimics, with $p=0.005$. In addition, miRNA mimics of miR-548c-5p appeared to have significantly reduced luciferase levels compared to miRNA inhibitors, with $p<0.0001$ after t-testing (Figure 21).

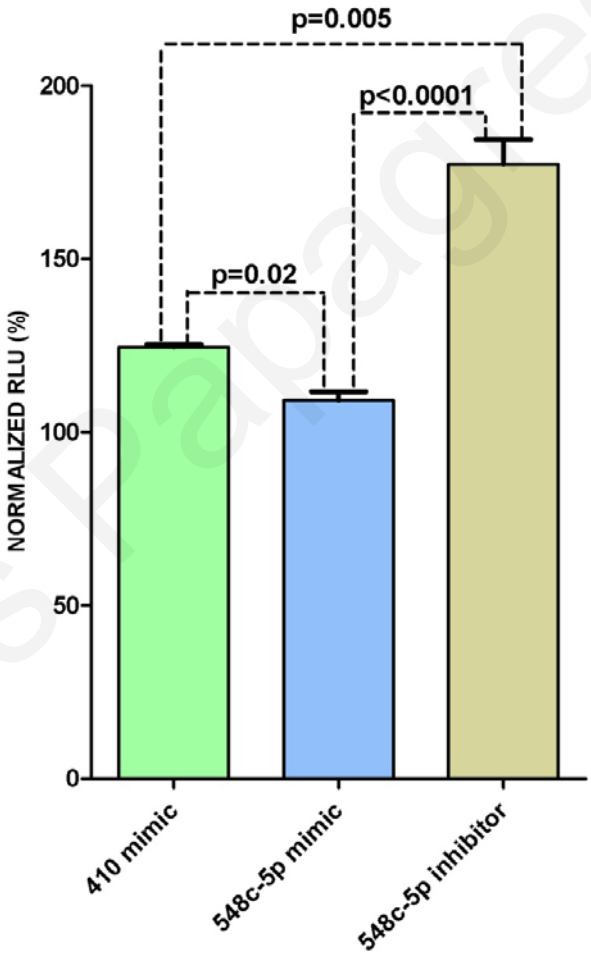

Figure 21: Normalized luciferase relative light units (RLUs) in AB8/13 cell lysates after transfection with sensor constructs. AB8/13 cells transfected with the pGL4.27 plasmid bearing the 548c-5p site and miR-548c-5p mimics demonstrated reduced luciferase expression, while miR-548c-5p inhibitors boosted luciferase levels compared to miR-410 mimics. Results represent mean values of triplicates ±SEM

4.2.4 Examination of endogenously expressed miRNA binding efficiency on predicted DNA target sites using ChIP experiments

A modified ChIP protocol was developed in order to isolate DNA that is potentially bound on the RISC complex, via a miRNA which is targeting a specific site located upstream the transcription start of a given gene. Hence, the final eluate after the IP was analyzed by using Real-Time PCR. Analysis involved the degree of enrichment of a specific piece of DNA precipitated with each antibody, normalized against the background signal given by the negative control anti-mouse IgG antibody. The *GAPDH* proximal promoter site was considered as the positive control for RNA Polymerase II (RNAP2) and the negative control for the anti-mouse IgG antibody.

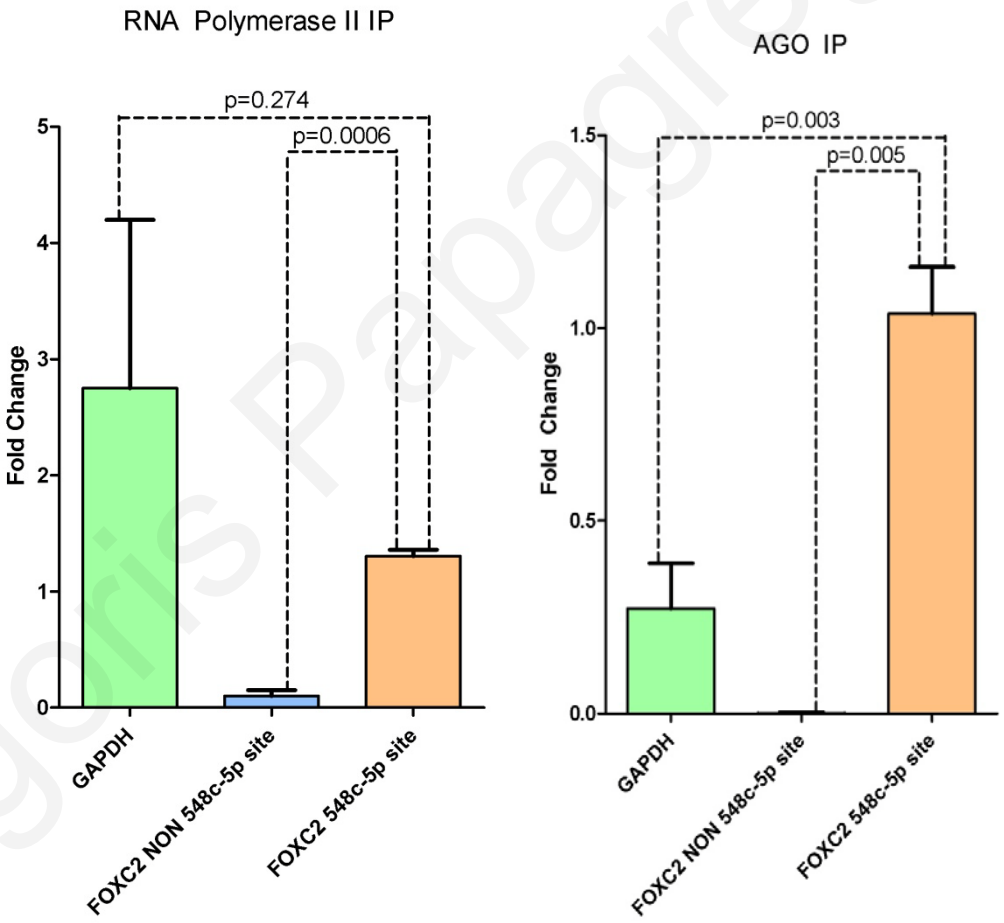

Figure 22: Real-time PCR results after ChIP assays for RNA Polymerase II and AGO. Both proteins appear to be precipitated together with the predicted miR-548c-5p DNA target region compared to a different nearby DNA region without a miR-548c-5p binding site (p=0.0006 and p=0.005 respectively). Results represent the mean of normalized fold change values from 3 experiments ± SEM.

The target site of miR-548c-5p appeared to be enriched in AGO processed samples (Figure 22). ANOVA with Tuckey post-testing was used to test for trend significance, with p=0.0014. Region specificity is demonstrated by the statistically significant under-representation of a neighboring DNA region that did not have a miR-548c-5p target site (Figure 9), with p=0.005 after t-testing.

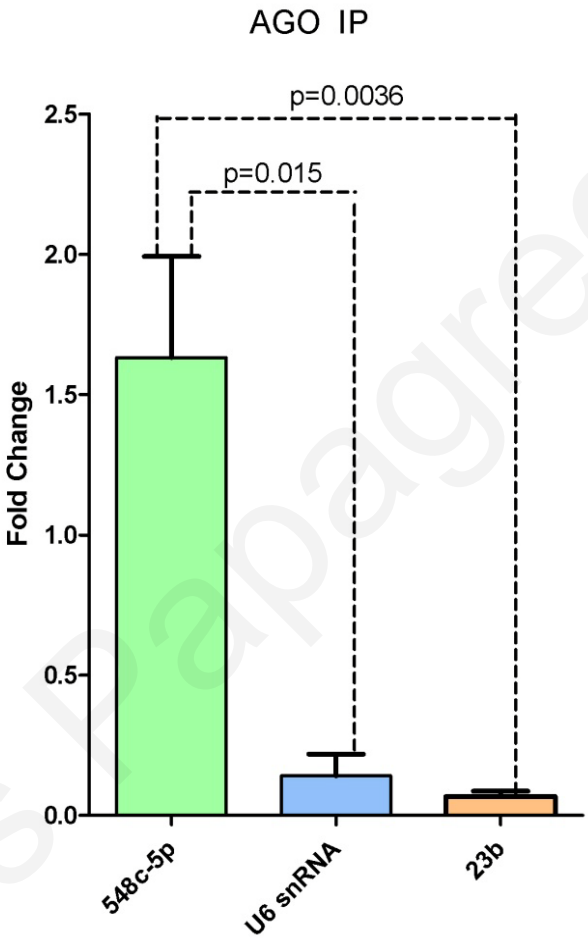

Figure 23: Real-time PCR results after ChIP assays for the miR-548-5p. This miRNA appears to be enriched in AGO ChIPed samples, with statistically significant differences when compared to the U6b snRNA (p=0.015) and the podocyte specific miR-23b (p=0.0036). Results represent the mean of normalized fold change values from 3 experiments ± SEM.

A miRNA enriched fraction of ChIPed samples was extracted using commercially available kits and analyzed with Real-Time PCR. After AGO ChIP, the miR-548c-5p was found to be highly enriched compared to the podocyte specific miR-23b and the U6b small nuclear RNA. ANOVA with Tuckey post-testing was used to test for trend significance, with p<0.0011.

Statistical examination with t-test of these results demonstrated an enhanced representation of the miR-548c-5p with p=0.0036 compared to miR-23b and p=0.015 compared to the U6b snRNA (Figure 23). These results indicate that miR-548c-5p has increased levels of presence in the nucleus of AB8/13 cells.

5 DISCUSSION

5.1 A miR-1207-5p binding site polymorphism abolishes regulation of HBEGF and is associated with disease severity in CFHR5 nephropathy

The phenotypic heterogeneity and variable expression, exemplified as a broad spectrum of symptoms in a cohort of patients, is the norm in many monogenic disorders including renal conditions, such as glomerulopathies. The role of genetic modifiers, at least partly, is frequently invoked as they are hypothesized to act in symphony with a validated mutation in a single gene. For example, recent publications have reported several occasions where SNPs in genes confer a higher risk for progression of pathology, for example a SNP in the DKK3 gene or in the eNOS gene in polycystic kidney disease.[119,120,121]

Having in mind recent advances in our understanding of molecular pathogenetic mechanisms, it is reasonable to expect that a class of modifiers, among others, could be sequence variations on the target sites of miRNAs, in genes whose function relates to the disease under study. Inheritance of such variants is not expected to cause a disease in a Mendelian fashion; however their stochastic co-segregation with a primary disease-causing mutation may affect the risk for slower or faster progression of the phenotype. A mutation in a miRNA gene itself that is responsible for a Mendelian phenotype has been reported once, to our knowledge, whereas several publications report on the presence of pathology-associated variants in the target sites of known miRNAs. At the same time miRNAs can act as disease modifiers as a result of genetic variations on the precursor molecules. Specifically, SNPs may occur at the level of the pri-miRNA, pre-miRNA or mature miRNA. Such SNPs may affect either the biogenesis or the action of the mature miRNA, contributing to deregulation of target gene expression and consequently to disease development.[122] Notwithstanding this situation, most common are the miRNA-associated single nucleotide polymorphisms (miRSNPs) that are located in the miRNA target sites within the 3'UTRs of corresponding mRNAs. Several studies have identified associations of miRSNPs with complex trait diseases such as diabetes [123], asthma [124], Parkinson [125], hypertension [126], breast cancer with early age at onset [127] and others.

In this study, we show data according to which a reduction of hsa-mir-1207-5p binding ability on its target site in the 3'UTR of HBEGF due to the presence of C1936T SNP, is associated with the severity of CFHR5 nephropathy in patients inheriting the pathogenic *CFHR5* gene duplication of exons 2-3. To our knowledge this is the first time a miRSNP is shown to be correlated with the phenotypic manifestation of a monogenic glomerular disease. Specifically, we showed that in a cohort of patients inheriting this CFHR5 nephropathy, the 1936C allele at the binding site for miRNA hsa-miR-1207-5p is associated with a less severe phenotype, as this is exemplified in patients who are protected from the development of high grade proteinuria and CKD ($p=0.018$, Figure 14). When concentrating on the subgroup of women, only three of 27 with mild disease inherited the T allele, compared to three of six women with severe disease (Figure 15). This finding obtains particular significance in view of the fact that women follow a much milder course of disease compared to men, according to previous work of our group.[39,102] The exact mechanism by which HBEGF can alter disease phenotype is currently unknown and under investigation. However, we hypothesize that the role of HBEGF in proliferation and fibrosis of mesangial cells is very critical to this end. In support of its functional significance, we showed in cell culture experiments that the presence of the T allele eliminates the binding of the miRNA, thus resulting in higher HBEGF protein levels (Figure 11).

This is a rather reverse approach for identifying such a SNP, by first collecting genes from the literature known to be involved in glomerular structure and function and then examining SNPs for functional significance. In order to narrow down our search, we utilized prediction algorithms to filter out the best candidate genes for sequencing analysis. In our case, the miR-1207-5p was predicted to target HBEGF by two out of five algorithms. Although not a top candidate, luckily enough hsa-miR-1207-5p target site is positioned nearby a site for an alleged good candidate miRNA (hsa-miR-379). As a result, we managed to prove the functional interaction of hsa-miR-1207-5p with HBEGF; cell culture experiments as well as the statistical evaluation in our cohort of patients supported its implication in gene regulation at post-transcription level. This case is a prime example where despite the improvement in bioinformatics tools and methods for predicting miRNA targets, some valuable information can still escape. The systematic approach we used, along with the flexibility of our tools, enabled us to identify a functional SNP that otherwise would have been missed.

HBEGF belongs to the epidermal growth factor superfamily. It is also known as the Diphtheria toxin receptor since it is required for the surface binding of diphtheria toxin and entry into the cell.[128] This growth factor is expressed at high levels in podocytes, tubular epithelial cells and mesangial cells.[129] Several studies have emphasized the role of HBEGF in kidney function under normal or pathologic conditions. Ischemia/reperfusion (IR) injury was shown to be mediated by HBEGF, as the reduction in expression of this protein has protective effect in various IR models.[128,130,131] As a member of a growth factor family, HBEGF can promote cellular proliferation in both mesangial and renal epithelial cells. Specifically, studies using renal proximal tubular cells revealed that proliferation in this cell type is mediated by HBEGF through an autocrine/paracrine mechanism, which antagonizes the action of Src kinases.[132] In addition, *HBEGF* is expressed in mesangial cells and is involved in their proliferation in glomerulonephritis. Also, it contributes to lesion formation in focal glomerular sclerosis through stimulation of mitogens at those sites.[133,134] Similarly, HBEGF participates in renal fibrosis by regulating both TGF-β-mediated fibronectin expression and collagen expression in mesangial cells.[135]

Further analysis of this miRSNP in additional groups manifesting with glomerular disease of a variable cause, did not show any significance between mildly and severely affected patients. In addition, the 1936T allele appeared to have a relatively high appearance in healthy controls, which led in deciphering its role regarding the expression levels of other genes implicated in renal disease. For this purpose, we gained access to data and samples from the Cyprus Study cohort, in which more than 1000 healthy population individuals originating from two villages in Cyprus take part in order for several genetic, pathological and lifestyle factors influencing atherosclerosis to be studied. After a careful examination of data available, we performed statistical analysis by comparing the C1936T genotype of 700 samples to serum levels of proteins involved in renal disease such as MMP1,2 and 9, TIMP1 and 2, as well as MTHFR, B12, folic acid, creatinine, ADMA and NO and MPO1. With a marginal statistical significance ($p=0.047$), the 1936CT genotype appeared to have the lowest serum levels of folic acid. To further explain this, we selected cases that had low folic acid and high MTHFR levels in order to include samples with increased risk of developing renal disease. Results demonstrated a significant reduction of MTHFR, with $p=0.027$ after Kruskal-Wallis testing, in 1936TT homozygotes. Still, no useful information can be extracted after this test, as sample

numbers dramatically dropped and perhaps interfered with the statistical testing. Furthermore, higher levels of serum MPO1 were statistically correlated with the 1936T allele in homozygotes, with p=0.001 after Kruskal-Wallis testing (Table 15). Myeloperoxidase is involved in antimicrobial immune responses and is expressed in neutrophils and identified in phagocytes, where it participates in various biochemical reactions but most importantly serves as a substrate for chloride to form hypochlorous acid; the latter acts as a chlorination agent in response to bacterial infection.[136,137] It is also contained in atherosclerotic lesions and has been implicated in kidney IR injury, while it is highly expressed in kidney inflammatory lesions.[136,138,139] Tissue damage following ischemic episodes, promotes the venular permeability to leucocytes, where activated neutrophils interact and adhere to endothelial cells and downstream expression of pro-inflammatory agents is induced to extend the initial damage.[140] In glomeruli, tissue degradation can be extended to the basement membrane through the generation of reactive oxygen species, thus implicating MPO in this procedure.[141] HBEGF on the other hand, is highly expressed by differentiated macrophages in response to conditioned media cultures.[142] Under IR conditions, HBEGF was found to repress the expression of neutrophil adhesion molecules, such as selectins, and other pro-inflammatory proteins, thus limiting neutrophil activation and damage expansion at the endothelium.[143] Collectively, MPO and HBEGF potential interaction during IR injury cellular responses, requires further understanding and elucidation. In addition, proof of this interaction could assist in a better comprehension of the variable phenotypic severity recorded in CFHR5 nephropathy, where complement deposits in the glomerulus are evident in biopsies and could contribute in ischemic episodes.[102,144]

In humans, the miR-1207-5p is transcribed from the PVT1 locus on chromosome 8q24.[145] The *PVT1* gene encodes for a non-translated RNA and has been found to be implicated in diabetic nephropathy, breast and colon cancer and in translocations related to Burkitt's lymphoma and associated with Hodgin's lymphoma.[146,147,148,149] Interestingly, end-stage renal disease occurring in patients with type 2 diabetes has been associated with *PVT1*, while variants in the same gene were associated with ESKD in patients with type 1 diabetes.[150,151] A recent study by Alvarez and DiStefano investigated PVT1 properties in depth and confirmed its high expression in mesangial cells. Moreover, an up-regulation in the levels of the miRNAs emerging from *PVT1* was proposed, by elevated glucose in the

mesangium.[146] These findings can supplement the results of our study and together are suggestive of novel roles for *PVT1* influenced miR-1207-5p expression and translational regulation of *HBEGF* in terms of maintaining the physiological function of the mesangium or the glomerulus in general.

In conclusion, this study presented evidence for the novel genetic modifier role of miRNA hsa-miR-1207-5p in predisposing patients with CFHR5 nephropathy, to more severe phenotype. At the same time *HBEGF* is implicated as the gene through which this miRNA exerts its effect. Further work at the cellular level and perhaps with the use of animal models will help elucidate in more detail the exact mechanism by which this hsa-miR-1207-5p/HBEGF pair plays its role. This work has been partially published by Papagregoriou G. et al, 2012.[152]

5.2 Investigation of the role of miRNAs as regulators of transcription

It is believed that miRNAs have additional regulatory roles that are not constrained in the cytoplasm and mRNA translational repression, but also extend inside the cell's nucleus and target DNA to regulate transcription. This kind of properties for miRNAs is suggested by quite few publications in regards to mammalian cells. Nonetheless, direct interactions between DNA sequences and miRNAs remain elusive as the literature presents an artificially evoked regulation of gene transcription by miRNA mimics. Initial predictions of miRNA target sequences on the 10kb upstream region of candidate genes demonstrated an extended degree of complementarity between a number of miRNAs and DNA sequences. Therefore, we hypothesized that miRNAs are able to directly interact with predicted DNA target sequences and regulate gene transcription levels and used luciferase expression vector systems to prove that.

Preliminary miRNA-10kb upstream sequences of genes recorded in Appendix I (Table 19) were performed using the miRWalk algorithm and had at least one interesting outcome (Table 16): the miR-548c-5p had almost complete complementarity with 21 out of 22 nucleotides of its mature molecule against its predicted target sequence, found more than 8kb away from the 5'UTR of the *FOXC2* gene (Figure 16). Such lengthy sites are rarely observed in 3'UTR sites; hence we decided to perform further prediction analyses to eliminate the possibility of them

occurring by chance or being a frequent phenomenon. For this purpose, all validated miRNAs listed in miRBase at the time were imported into miRWalk and prediction analysis against the 10kb upstream sequences of all known genes was performed. As reported in the results section, a significant number of lengthy target sites were observed, but they all corresponded to the sequence of miR-548c-5p, thus establishing this miRNA as a strong contender in miRNA induced transcriptional regulation. Target sites were spread out in the region under investigation from some bases upstream the 5'UTR up to almost 10kb (Table 17). It was expected that miRNAs able to act as siRNAs would have extended complementarity to their target sequences, hence miR-548c-5p seemed like a good candidate miRNA to start with. If the latter is valid, then miR-548c-5p could be regulating but perhaps not silencing the expression of its target genes, and therefore cause at least subtle changes in gene transcriptional levels. Such changes could be the outcome of a miRNA binding on a DNA enhancer/repressor element rather than the proximal core promoter, assisted by the RISC complex. Furthermore, if a transcription factor binds on such sites, then its binding would be either impeded or enhanced. Hence, an extended region (10kb) upstream the 5'UTR of genes under study was taken into account rather than the first bases, as to look for transcription regulatory elements as well.

An extended site containing the miR-548c-5p target site was cloned into the pGL4.27 luciferase vector. This particular vector is usually used in studies examining transcription regulatory elements by bearing a MCS right upstream the basal promoter of the firefly luciferase gene. A different construct was assembled by specifically removing the miRNA target site, which succeeded in characterizing this sequence as a repressor of transcription (Figure 19). Co-transfection of AB8/13 podocytes with the pGL4.27 vector bearing the miR-548c-5p target site together with miR-548c-5p mimics demonstrated a statistically significant reduction of luciferase levels. In the same manner, when miR-548c-5p inhibitors were used, luciferase levels were enhanced; hence miR-548c-5p can target its predicted target sequence and regulate luciferase expression levels (Figure 21). Collectively, results demonstrated the transcriptional regulation exerted by the direct binding of miR-548c-5p on this specific predicted sequence located more than 8kb upstream the *FOXC2* gene. This study is the first to encompass such reporter constructs for miRNA research and it is anticipated that they will be broadly used in the future to prove such direct interactions. Further elucidation of miR-548c-

5p binding properties on this site, will be examined in the future using a site-specific mutation on the pGL4.27 miR-548-5p+SITE plasmid and/or with the use of mimics that differ from miR-548c-5p in a number of residues, such as miRNAs that belong to the miR-548 family (Table 18). For example, the significance of the miRNA target site will be further investigated, by generating luciferase plasmids bearing mutations at various target site positions. In addition, the potential regulation exerted by miR-548c-5p on the levels of transcription of various genes, such as *FOXC2* or *MTHFSD*, which is located 3kb upstream the miRNA target sequence will be investigated with Real-Time PCR experiments after the transfection of AB8/13 cells with miRNA mimics and inhibitors. This study provides preliminary data regarding the potential role of miR-548c-5p in transcriptional regulation and supportive experiments are required in order to verify our hypothesis.

The miR-548c-5p belongs to the miR-548 family, together with other 69 miRNAs. The miR-548 family of miRNAs is believed to have originated from transposable elements (TE) that at some point of the primate evolution were placed into various places and supposedly have regulatory roles.[153] Family members preserve the TE architecture by having palindromic DNA sequence elements, from which each miRNA is generated. The cell's response against TE assisted the RNA interference pathway to be evolved as a protection mechanism against these rather malignant molecules.[154] We investigated this family in further by implementing prediction analyses with the miRWalk algorithm. Impressively, only 56 out of 69 members have a "unique" sequence. Concerning the miR-548c-5p, two other miRNAs, miR-548am-5p and miR-548o-5p, appear to have exactly the same mature sequence although they are encoded from different premature transcripts (Table 18). Therefore, they share the same target sequences and given that the mature miRNA molecule drives all the way to the nucleus to be functional, any one of these three miRNA transcripts could be functioning in that sense. In addition, by performing a multiple sequence alignment of the miR-548 family members (Appendix II - Figure 24) it was observed that there are two distinct groups of miRNAs: each group has miRNAs that have more or less similar mature sequences, but when groups are compared to each other they seem to have complementary sequences. This can be explained by considering that for any given miRNA, its 3p and 5p strands emerge from the same RNA hairpin premature molecule and at least partial complementarity was expected.

Furthermore, in support to the luciferase assay data presented above, we aimed at isolating endogenously expressed miR-548c-5p, together with other miRNAs, by capturing them using Chromatin Immunoprecipitation. Various recent publications have elaborately examined the role of siRNA or miRNA induced transcriptional silencing in mammalian cells; nonetheless, all this work is based on synthetic siRNA mimics, a parameter which is usually overlooked. For this purpose, a ChIP analysis protocol corresponding to our goal in isolating a nuclear enriched miRNA fraction was generated. In agreement to our luciferase reporter vector results, both the predicted DNA target region and the miR-548c-5p were found to be significantly enriched, when compared to a different DNA sequence region located nearby and the *GAPDH* proximal promoter (Figure 22 and Figure 23). This protocol was developed after combining different kinds of ChIP protocols, with emphasis on transcription factor associated ChIPs and was finalized after several trials resulting in isolating both DNA and miRNAs from the same tube by the successful combination of different commercially available kits. Future projects should be revolved around the isolation of nucleus-acting miRNAs. Also, the possible formation of a genomic library of miRNAs being able to exert transcriptional regulation is important, in order to study this phenomenon in depth. It could be possible that miRNAs other than miR-548c-5p have similar properties and should be efficiently isolated. Furthermore, it is essential to elucidate the functional mechanism assisting miRNAs to interact with DNA target sequences in a direct manner. miRNA targeted DNA regions positioned upstream of gene transcription start points, are not necessarily expected to be located near or at the transcription start, but at distal spots which are used as transcriptional repressors or enhancers; thus target prediction algorithms would be effectively used or developed for the recognition and documentation of such sites.

The miR-548c stem loop is encoded by a gene located in the first intron of *RASSF3*, which is coding for a Ras association factor considered to suppress tumor generation by controlling apoptosis and the cell cycle.[155] The same first intron codes for the miR-548z stem loop, which coincidentally expresses miR-548z which has the exact complementary mature sequence as 548c-5p. This fact is suggestive for a common role between these two miRNAs: they both target the same sequence but in complementary strands perhaps in a *cis*- and/or *trans*- manner of transcriptional regulation of gene expression.

Collectively, we provided data which suggest that miRNAs are able to bind directly onto DNA target sequences and regulate gene transcription by encompassing bioinformatics, luciferase reporter constructs and a novel modified ChIP protocol. The exact mechanism assisting the miR-548c-5p to act as a transcriptional repressor through its binding onto DNA target sequences remains to be established, as well as the role of the RISC complex and the RNA Polymerase II in this procedure. It is possible that this miRNA influences the methylation of its target sites or blocks the attachment of other protein complexes that enhance transcriptional levels. In addition, as the miR-548 family members exhibit high sequence similarity for sequences at the promoter region of genes, they could act preferably in the nucleus and be of great importance in buffering gene transcription in a direct manner rather than targeting secondary elements in a siRNA similar fashion. Further examination of miR-548c-5p targeting ability against other sequences upstream of genes, as well as the establishment of a strong context in which this regulation takes place in the cell and the proteins involved, are required in order to expand our understanding in such basic cellular functions that involve miRNAs.

6 CONCLUSIONS

In this study we postulated that miRSNPs in the 3'UTR of genes associated with glomerular function can be regarded as phenotype modifiers in monogenic diseases manifesting with proteinuria and hematuria, such as TBMN and CFHR5 nephropathy. We demonstrated the direct interaction between miRSNP C1936T on the 3'UTR of HBEGF and microRNA hsa-miR-1207-5p. The T1936 allele reduced normal translational regulation of HBEGF by miR-1207-5p and was found to be underrepresented in patients with mild course of CFHR5 nephropathy. In addition, elevated levels of MPO in the normal population were found to be statistically associated with the same allele, thus suggesting a potential interaction between HBEGF and MPO. This is the first time where such a SNP is correlated with the progression of a hereditary glomerulopathy.

Furthermore, after performing prediction analysis in search for miRNA binding sites on candidate gene promoter regions (10kb upstream their 5'UTR), we managed to spot a target sequence for miR-548c-5p located more than 8kb away from the transcription start point of the *FOXC2* transcription factor gene. In addition, we proceeded in a bioinformatic investigation of the miR-548 family, in which miR-548c-5p belongs to, and found that members of this family have more predicted targets on sequences upstream of genes, rather than in any other region. Direct interaction between the miRNA and its target sequence were sequentially demonstrated by encompassing luciferase reporter constructs, while we succeeded in isolating both the DNA target region and miR-548c-5p from AB8/13 undifferentiated podocytes using a modified ChIP protocol. Hence, we reported for the first time the use of luciferase reporter constructs in such experiments, as well as provided evidence for the direct interaction of miR-548c-5p with a DNA sequence located 8kb upstream of the *FOXC2* gene transcription start point.

REFERENCES

1. Underwood JC (2004) General and Systematic Pathology. Edinburgh: Churchill Livingstone.

2. Berne RM, Levy MN (1996) Principles of Physiology. St. Louis: Mosby-Year Book, Inc.

3. Hildebrandt F (2010) Genetic kidney diseases. Lancet 375: 1287-1295.

4. Deltas C, Papagregoriou G (2010) Cystic diseases of the kidney: molecular biology and genetics. Arch Pathol Lab Med 134: 569-582.

5. Greka A, Mundel P (2011) Cell Biology and Pathology of Podocytes. Annu Rev Physiol.

6. Patrakka J, Tryggvason K (2010) Molecular make-up of the glomerular filtration barrier. Biochem Biophys Res Commun 396: 164-169.

7. Miner JH (2012) The glomerular basement membrane. Exp Cell Res.

8. Ross MH, Reith LJ, Romrell LJ (1989) Histology: A text and atlas. Baltimore: Williams and Wilkins.

9. Ronco P (2007) Proteinuria: is it all in the foot? J Clin Invest 117: 2079-2082.

10. Abrahamson DR, Hudson BG, Stroganova L, Borza DB, St John PL (2009) Cellular origins of type IV collagen networks in developing glomeruli. J Am Soc Nephrol 20: 1471-1479.

11. St John PL, Abrahamson DR (2001) Glomerular endothelial cells and podocytes jointly synthesize laminin-1 and -11 chains. Kidney Int 60: 1037-1046.

12. Haraldsson B, Nystrom J, Deen WM (2008) Properties of the glomerular barrier and mechanisms of proteinuria. Physiol Rev 88: 451-487.

13. Miner JH (1999) Renal basement membrane components. Kidney Int 56: 2016-2024.

14. Van Agtmael T, Bruckner-Tuderman L (2010) Basement membranes and human disease. Cell Tissue Res 339: 167-188.

15. Dalla Vestra M, Arboit M, Bruseghin M, Fioretto P (2009) The kidney in type 2 diabetes: focus on renal structure. Endocrinol Nutr 56 Suppl 4: 18-20.

16. Tryggvason K, Patrakka J (2006) Thin basement membrane nephropathy. J Am Soc Nephrol 17: 813-822.

17. Jefferson JA, Alpers CE, Shankland SJ (2011) Podocyte biology for the bedside. Am J Kidney Dis 58: 835-845.

18. Holthofer H (2007) Molecular architecture of the glomerular slit diaphragm: lessons learnt for a better understanding of disease pathogenesis. Nephrol Dial Transplant 22: 2124-2128.

19. Sawada H, Stukenbrok H, Kerjaschki D, Farquhar MG (1986) Epithelial polyanion (podocalyxin) is found on the sides but not the soles of the foot processes of the glomerular epithelium. Am J Pathol 125: 309-318.

20. Huang TW, Langlois JC (1985) Podoendin. A new cell surface protein of the podocyte and endothelium. J Exp Med 162: 245-267.

21. Rodewald R, Karnovsky MJ (1974) Porous substructure of the glomerular slit diaphragm in the rat and mouse. J Cell Biol 60: 423-433.

22. Philippe A, Nevo F, Esquivel EL, Reklaityte D, Gribouval O, et al. (2008) Nephrin mutations can cause childhood-onset steroid-resistant nephrotic syndrome. J Am Soc Nephrol 19: 1871-1878.

23. Reiser J, Kriz W, Kretzler M, Mundel P (2000) The glomerular slit diaphragm is a modified adherens junction. J Am Soc Nephrol 11: 1-8.

24. Schwarz K, Simons M, Reiser J, Saleem MA, Faul C, et al. (2001) Podocin, a raft-associated component of the glomerular slit diaphragm, interacts with CD2AP and nephrin. J Clin Invest 108: 1621-1629.

25. Gerke P, Sellin L, Kretz O, Petraschka D, Zentgraf H, et al. (2005) NEPH2 is located at the glomerular slit diaphragm, interacts with nephrin and is cleaved from podocytes by metalloproteinases. J Am Soc Nephrol 16: 1693-1702.

26. Kestila M, Lenkkeri U, Mannikko M, Lamerdin J, McCready P, et al. (1998) Positionally cloned gene for a novel glomerular protein--nephrin--is mutated in congenital nephrotic syndrome. Mol Cell 1: 575-582.

27. Asanuma K, Mundel P (2003) The role of podocytes in glomerular pathobiology. Clin Exp Nephrol 7: 255-259.

28. Kim JM, Wu H, Green G, Winkler CA, Kopp JB, et al. (2003) CD2-associated protein haploinsufficiency is linked to glomerular disease susceptibility. Science 300: 1298-1300.

29. Kaplan JM, Kim SH, North KN, Rennke H, Correia LA, et al. (2000) Mutations in ACTN4, encoding alpha-actinin-4, cause familial focal segmental glomerulosclerosis. Nat Genet 24: 251-256.

30. Winn MP, Conlon PJ, Lynn KL, Farrington MK, Creazzo T, et al. (2005) A mutation in the TRPC6 cation channel causes familial focal segmental glomerulosclerosis. Science 308: 1801-1804.

31. Voskarides K, Makariou C, Papagregoriou G, Stergiou N, Printza N, et al. (2008) NPHS2 screening with SURVEYOR in Hellenic children with steroid-resistant nephrotic syndrome. Pediatr Nephrol 23: 1373-1375.

32. Gigante M, Piemontese M, Gesualdo L, Iolascon A, Aucella F (2011) Molecular and genetic basis of inherited nephrotic syndrome. Int J Nephrol 2011: 792195.

33. Wiggins RC (2007) The spectrum of podocytopathies: a unifying view of glomerular diseases. Kidney Int 71: 1205-1214.

34. Barisoni L, Schnaper HW, Kopp JB (2007) A proposed taxonomy for the podocytopathies: a reassessment of the primary nephrotic diseases. Clin J Am Soc Nephrol 2: 529-542.

35. Caridi G, Trivelli A, Sanna-Cherchi S, Perfumo F, Ghiggeri GM (2010) Familial forms of nephrotic syndrome. Pediatr Nephrol 25: 241-252.

36. Lowik MM, Groenen PJ, Levtchenko EN, Monnens LA, van den Heuvel LP (2009) Molecular genetic analysis of podocyte genes in focal segmental glomerulosclerosis--a review. Eur J Pediatr 168: 1291-1304.

37. Cohen RA, Brown RS (2003) Clinical practice. Microscopic hematuria. N Engl J Med 348: 2330-2338.

38. Voskarides K, Damianou L, Neocleous V, Zouvani I, Christodoulidou S, et al. (2007) COL4A3/COL4A4 mutations producing focal segmental glomerulosclerosis and renal failure in thin basement membrane nephropathy. J Am Soc Nephrol 18: 3004-3016.

39. Gale DP, de Jorge EG, Cook HT, Martinez-Barricarte R, Hadjisavvas A, et al. (2010) Identification of a mutation in complement factor H-related protein 5 in patients of Cypriot origin with glomerulonephritis. Lancet 376: 794-801.

40. Farazi TA, Juranek SA, Tuschl T (2008) The growing catalog of small RNAs and their association with distinct Argonaute/Piwi family members. Development 135: 1201-1214.

41. Wu L, Fa J, Belasco GJ (2006) MicroRNAs direct rapid deadenylation of mRNA. PNAS Vol. 103: 4034-4039.

42. Reinhart BJ, Slack FJ, Basson M, Pasquinelli AE, Bettinger JC, et al. (2000) The 21-nucleotide let-7 RNA regulates developmental timing in Caenorhabditis elegans. Nature 403: 901-906.

43. Chen K, Song F, Calin GA, Wei Q, Hao X, et al. (2008) Polymorphisms in microRNA targets: a gold mine for molecular epidemiology. Carcinogenesis 29: 1306-1311.

44. Lal A, Navarro F, Maher CA, Maliszewski LE, Yan N, et al. (2009) miR-24 Inhibits cell proliferation by targeting E2F2, MYC, and other cell-cycle genes via binding to "seedless" 3'UTR microRNA recognition elements. Mol Cell 35: 610-625.

45. Landgraf P, Rusu M, Sheridan R, Sewer A, Iovino N, et al. (2007) A mammalian microRNA expression atlas based on small RNA library sequencing. Cell 129: 1401-1414.

46. Lee Y, Kim M, Han J, Yeom KH, Lee S, et al. (2004) MicroRNA genes are transcribed by RNA polymerase II. EMBO J 23: 4051-4060.

47. Lee Y, Jeon K, Lee JT, Kim S, Kim VN (2002) MicroRNA maturation: stepwise processing and subcellular localization. EMBO J 21: 4663-4670.

48. Liu X, Fortin K, Mourelatos Z (2008) MicroRNAs: biogenesis and molecular functions. Brain Pathol 18: 113-121.

49. Zeng Y, Yi R, Cullen BR (2003) MicroRNAs and small interfering RNAs can inhibit mRNA expression by similar mechanisms. Proc Natl Acad Sci U S A 100: 9779-9784.

50. Lee Y, Ahn C, Han J, Choi H, Kim J, et al. (2003) The nuclear RNase III Drosha initiates microRNA processing. Nature 425: 415-419.

51. Lund E, Guttinger S, Calado A, Dahlberg JE, Kutay U (2004) Nuclear export of microRNA precursors. Science 303: 95-98.

52. Bartel DP (2004) MicroRNAs: genomics, biogenesis, mechanism, and function. Cell 116: 281-297.

53. Ketting RF, Fischer SE, Bernstein E, Sijen T, Hannon GJ, et al. (2001) Dicer functions in RNA interference and in synthesis of small RNA involved in developmental timing in C. elegans. Genes Dev 15: 2654-2659.

54. Peters L, Meister G (2007) Argonaute proteins: mediators of RNA silencing. Mol Cell 26: 611-623.

55. Engels BM, Hutvagner G (2006) Principles and effects of microRNA-mediated post-transcriptional gene regulation. Oncogene 25: 6163-6169.

56. Mourelatos Z, Dostie J, Paushkin S, Sharma A, Charroux B, et al. (2002) miRNPs: a novel class of ribonucleoproteins containing numerous microRNAs. Genes Dev 16: 720-728.

57. Sasaki T, Shiohama A, Minoshima S, Shimizu N (2003) Identification of eight members of the Argonaute family in the human genome small star, filled. Genomics 82: 323-330.

58. Kim VN (2005) MicroRNA biogenesis: coordinated cropping and dicing. Nat Rev Mol Cell Biol 6: 376-385.

59. Mencia A, Modamio-Hoybjor S, Redshaw N, Morin M, Mayo-Merino F, et al. (2009) Mutations in the seed region of human miR-96 are responsible for nonsyndromic progressive hearing loss. Nat Genet 41: 609-613.

60. Lewis MA, Quint E, Glazier AM, Fuchs H, De Angelis MH, et al. (2009) An ENU-induced mutation of miR-96 associated with progressive hearing loss in mice. Nat Genet 41: 614-618.

61. Abelson JF, Kwan KY, O'Roak BJ, Baek DY, Stillman AA, et al. (2005) Sequence variants in SLITRK1 are associated with Tourette's syndrome. Science 310: 317-320.

62. Beetz C, Schule R, Deconinck T, Tran-Viet KN, Zhu H, et al. (2008) REEP1 mutation spectrum and genotype/phenotype correlation in hereditary spastic paraplegia type 31. Brain 131: 1078-1086.

63. Zuchner S, Wang G, Tran-Viet KN, Nance MA, Gaskell PC, et al. (2006) Mutations in the novel mitochondrial protein REEP1 cause hereditary spastic paraplegia type 31. Am J Hum Genet 79: 365-369.

64. Xu J, Hu Z, Xu Z, Gu H, Yi L, et al. (2009) Functional variant in microRNA-196a2 contributes to the susceptibility of congenital heart disease in a Chinese population. Hum Mutat 30: 1231-1236.

65. Sun G, Yan J, Noltner K, Feng J, Li H, et al. (2009) SNPs in human miRNA genes affect biogenesis and function. RNA 15: 1640-1651.

66. Jazdzewski K, Liyanarachchi S, Swierniak M, Pachucki J, Ringel MD, et al. (2009) Polymorphic mature microRNAs from passenger strand of pre-miR-146a contribute to thyroid cancer. Proc Natl Acad Sci U S A 106: 1502-1505.

67. Saunders MA, Liang H, Li WH (2007) Human polymorphism at microRNAs and microRNA target sites. Proc Natl Acad Sci U S A 104: 3300-3305.

68. Georges M, Clop A, Marcq F, Takeda H, Pirottin D, et al. (2006) Polymorphic microRNA-target interactions: a novel source of phenotypic variation. Cold Spring Harb Symp Quant Biol 71: 343-350.

69. Hariharan M, Scaria V, Brahmachari SK (2009) dbSMR: a novel resource of genome-wide SNPs affecting microRNA mediated regulation. BMC Bioinformatics 10: 108.

70. Bao L, Zhou M, Wu L, Lu L, Goldowitz D, et al. (2007) PolymiRTS Database: linking polymorphisms in microRNA target sites with complex traits. Nucleic Acids Res 35: D51-54.

71. Harvey SJ, Jarad G, Cunningham J, Goldberg S, Schermer B, et al. (2008) Podocyte-specific deletion of dicer alters cytoskeletal dynamics and causes glomerular disease. J Am Soc Nephrol 19: 2150-2158.

72. Shi S, Yu L, Chiu C, Sun Y, Chen J, et al. (2008) Podocyte-selective deletion of dicer induces proteinuria and glomerulosclerosis. J Am Soc Nephrol 19: 2159-2169.

73. Ho J, Ng KH, Rosen S, Dostal A, Gregory RI, et al. (2008) Podocyte-specific loss of functional microRNAs leads to rapid glomerular and tubular injury. J Am Soc Nephrol 19: 2069-2075.

74. Carpena MP, Rados DV, Sortica DA, Souza BM, Reis AF, et al. (2010) Genetics of diabetic nephropathy. Arq Bras Endocrinol Metabol 54: 253-261.

75. Kato M, Zhang J, Wang M, Lanting L, Yuan H, et al. (2007) MicroRNA-192 in diabetic kidney glomeruli and its function in TGF-beta-induced collagen expression via inhibition of E-box repressors. Proc Natl Acad Sci U S A 104: 3432-3437.

76. Wang Q, Wang Y, Minto AW, Wang J, Shi Q, et al. (2008) MicroRNA-377 is up-regulated and can lead to increased fibronectin production in diabetic nephropathy. FASEB J 22: 4126-4135.

77. Zhang Z, Peng H, Chen J, Chen X, Han F, et al. (2009) MicroRNA-21 protects from mesangial cell proliferation induced by diabetic nephropathy in db/db mice. FEBS Lett 583: 2009-2014.

78. Wang G, Kwan BC, Lai FM, Choi PC, Chow KM, et al. (2010) Intrarenal expression of miRNAs in patients with hypertensive nephrosclerosis. Am J Hypertens 23: 78-84.

79. Wang G, Kwan BC, Lai FM, Choi PC, Chow KM, et al. (2010) Intrarenal expression of microRNAs in patients with IgA nephropathy. Lab Invest 90: 98-103.

80. Lee SO, Masyuk T, Splinter P, Banales JM, Masyuk A, et al. (2008) MicroRNA15a modulates expression of the cell-cycle regulator Cdc25A and affects hepatic cystogenesis in a rat model of polycystic kidney disease. J Clin Invest 118: 3714-3724.

81. Pandey P, Brors B, Srivastava PK, Bott A, Boehn SN, et al. (2008) Microarray-based approach identifies microRNAs and their target functional patterns in polycystic kidney disease. BMC Genomics 9: 624.

82. Morris KV (2005) siRNA-mediated transcriptional gene silencing: the potential mechanism and a possible role in the histone code. Cell Mol Life Sci 62: 3057-3066.

83. Hamilton A, Voinnet O, Chappell L, Baulcombe D (2002) Two classes of short interfering RNA in RNA silencing. EMBO J 21: 4671-4679.

84. Matzke M, Aufsatz W, Kanno T, Daxinger L, Papp I, et al. (2004) Genetic analysis of RNA-mediated transcriptional gene silencing. Biochim Biophys Acta 1677: 129-141.

85. Verdel A, Jia S, Gerber S, Sugiyama T, Gygi S, et al. (2004) RNAi-mediated targeting of heterochromatin by the RITS complex. Science 303: 672-676.

86. Schramke V, Sheedy DM, Denli AM, Bonila C, Ekwall K, et al. (2005) RNA-interference-directed chromatin modification coupled to RNA polymerase II transcription. Nature 435: 1275-1279.

87. Corey DR (2005) Regulating mammalian transcription with RNA. Trends Biochem Sci 30: 655-658.

88. Kim DH, Saetrom P, Snove O, Jr., Rossi JJ (2008) MicroRNA-directed transcriptional gene silencing in mammalian cells. Proc Natl Acad Sci U S A 105: 16230-16235.

89. Younger ST, Corey DR (2011) Transcriptional regulation by miRNA mimics that target sequences downstream of gene termini. Mol Biosyst 7: 2383-2388.

90. Janowski BA, Younger ST, Hardy DB, Ram R, Huffman KE, et al. (2007) Activating gene expression in mammalian cells with promoter-targeted duplex RNAs. Nat Chem Biol 3: 166-173.

91. Hwang HW, Wentzel EA, Mendell JT (2007) A hexanucleotide element directs microRNA nuclear import. Science 315: 97-100.

92. Weinmann L, Hock J, Ivacevic T, Ohrt T, Mutze J, et al. (2009) Importin 8 is a gene silencing factor that targets argonaute proteins to distinct mRNAs. Cell 136: 496-507.

93. Janowski BA, Huffman KE, Schwartz JC, Ram R, Nordsell R, et al. (2006) Involvement of AGO1 and AGO2 in mammalian transcriptional silencing. Nat Struct Mol Biol 13: 787-792.

94. Kim DH, Villeneuve LM, Morris KV, Rossi JJ (2006) Argonaute-1 directs siRNA-mediated transcriptional gene silencing in human cells. Nat Struct Mol Biol 13: 793-797.

95. Deltas C (2009) Thin basement membrane nephropathy: is there genetic predisposition to more severe disease? Pediatr Nephrol 24: 877-879.

96. Collins AJ, Gilbertson DT, Snyder JJ, Chen SC, Foley RN (2010) Chronic kidney disease awareness, screening and prevention: rationale for the design of a public education program. Nephrology (Carlton) 15 Suppl 2: 37-42.

97. Vernon KA, Gale DP, Goicoechea de Jorge E, McLean AG, Galliford J, et al. (2010) Recurrence of Complement Factor H-Related Protein 5 Nephropathy in a Renal Transplant. Am J Transplant.

98. Pierides A, Voskarides K, Athanasiou Y, Ioannou K, Damianou L, et al. (2009) Clinico-pathological correlations in 127 patients in 11 large pedigrees, segregating one of three heterozygous mutations in the COL4A3/ COL4A4 genes associated with familial haematuria and significant late progression to proteinuria and chronic kidney disease from focal segmental glomerulosclerosis. Nephrol Dial Transplant 24: 2721-2729.

99. Noto T, Kurth HM, Kataoka K, Aronica L, DeSouza LV, et al. (2010) The Tetrahymena argonaute-binding protein Giw1p directs a mature argonaute-siRNA complex to the nucleus. Cell 140: 692-703.

100. Foldes-Papp Z, Konig K, Studier H, Buckle R, Breunig HG, et al. (2009) Trafficking of mature miRNA-122 into the nucleus of live liver cells. Curr Pharm Biotechnol 10: 569-578.

101. Khraiwesh B, Arif MA, Seumel GI, Ossowski S, Weigel D, et al. (2010) Transcriptional control of gene expression by microRNAs. Cell 140: 111-122.

102. Athanasiou Y, Voskarides K, Gale DP, Damianou L, Patsias C, et al. (2011) Familial C3 Glomerulopathy Associated with CFHR5 Mutations: Clinical Characteristics of 91 Patients in 16 Pedigrees. CJASN In Press.

103. Panayiotou A. (2008) Biomarkers and subclinical atherosclerosis [PhD Thesis]. Nicosia: University of Cyprus.

104. Zoccali C, Bode-Boger S, Mallamaci F, Benedetto F, Tripepi G, et al. (2001) Plasma concentration of asymmetrical dimethylarginine and mortality in patients with end-stage renal disease: a prospective study. Lancet 358: 2113-2117.

105. Grone HJ, Grone EF, Malle E (2002) Immunohistochemical detection of hypochlorite-modified proteins in glomeruli of human membranous glomerulonephritis. Lab Invest 82: 5-14.

106. Dweep H, Sticht C, Pandey P, Gretz N (2011) miRWalk--database: prediction of possible miRNA binding sites by "walking" the genes of three genomes. J Biomed Inform 44: 839-847.

107. Lewis BP, Burge CB, Bartel DP (2005) Conserved seed pairing, often flanked by adenosines, indicates that thousands of human genes are microRNA targets. Cell 120: 15-20.

108. Enright AJ, John B, Gaul U, Tuschl T, Sander C, et al. (2003) MicroRNA targets in Drosophila. Genome Biol 5: R1.

109. Wang X (2008) miRDB: a microRNA target prediction and functional annotation database with a wiki interface. RNA 14: 1012-1017.

110. Miranda KC, Huynh T, Tay Y, Ang YS, Tam WL, et al. (2006) A pattern-based method for the identification of MicroRNA binding sites and their corresponding heteroduplexes. Cell 126: 1203-1217.

111. Hall TA (1999) BioEdit: a user-friendly biological sequence alignment editor and analysis program for Windows 95/98/NT. Nucl Acids Symp Ser 41: 95-98.

112. Saleem MA, O'Hare MJ, Reiser J, Coward RJ, Inward CD, et al. (2002) A conditionally immortalized human podocyte cell line demonstrating nephrin and podocin expression. J Am Soc Nephrol 13: 630-638.

113. Lydersen S, Fagerland MW, Laake P (2009) Recommended tests for association in 2 x 2 tables. Stat Med 28: 1159-1175.

114. Barnard GA (1947) Significance tests for 2 X 2 tables. Biometrika 34: 123-138.

115. Mehta CR, Hilton LF (1993) Exact power of conditional and unconditional tests: Going beyond the 2×2 contingency table. Am Stat 47: 91-98.

116. Mehta CR (1991) StatXact: A Statistical Package for Exact Nonparametric Inference. Am Stat 45: 74-75.

117. Ludbrook J (2008) Analysis of 2 x 2 tables of frequencies: matching test to experimental design. Int J Epidemiol 37: 1430-1435.

118. Deltas C, Pierides A, Voskarides K (2011) The role of molecular genetics in diagnosing familial hematuria(s). Pediatr Nephrol Epub 21 Jun 2011 - DOI: 10.1007/s00467-011-1935-5.

119. Liu M, Shi S, Senthilnathan S, Yu J, Wu E, et al. (2010) Genetic variation of DKK3 may modify renal disease severity in ADPKD. J Am Soc Nephrol 21: 1510-1520.

120. Persu A, Stoenoiu MS, Messiaen T, Davila S, Robino C, et al. (2002) Modifier effect of ENOS in autosomal dominant polycystic kidney disease. Hum Mol Genet 11: 229-241.

121. Lamnissou K, Zirogiannis P, Trygonis S, Demetriou K, Pierides A, et al. (2004) Evidence for association of endothelial cell nitric oxide synthase gene polymorphism with earlier progression to end-stage renal disease in a cohort of Hellens from Greece and Cyprus. Genet Test 8: 319-324.

122. Iwai N, Naraba H (2005) Polymorphisms in human pre-miRNAs. Biochem Biophys Res Commun 331: 1439-1444.

123. Lv K, Guo Y, Zhang Y, Wang K, Jia Y, et al. (2008) Allele-specific targeting of hsa-miR-657 to human IGF2R creates a potential mechanism underlying the association of ACAA-insertion/deletion polymorphism with type 2 diabetes. Biochem Biophys Res Commun 374: 101-105.

124. Tan Z, Randall G, Fan J, Camoretti-Mercado B, Brockman-Schneider R, et al. (2007) Allele-specific targeting of microRNAs to HLA-G and risk of asthma. Am J Hum Genet 81: 829-834.

125. Wang G, van der Walt JM, Mayhew G, Li YJ, Zuchner S, et al. (2008) Variation in the miRNA-433 binding site of FGF20 confers risk for Parkinson disease by overexpression of alpha-synuclein. Am J Hum Genet 82: 283-289.

126. Martin MM, Buckenberger JA, Jiang J, Malana GE, Nuovo GJ, et al. (2007) The human angiotensin II type 1 receptor +1166 A/C polymorphism attenuates microrna-155 binding. J Biol Chem 282: 24262-24269.

127. Song F, Zheng H, Liu B, Wei S, Dai H, et al. (2009) An miR-502-binding site single-nucleotide polymorphism in the 3'-untranslated region of the SET8 gene is associated with early age of breast cancer onset. Clin Cancer Res 15: 6292-6300.

128. Mulder GM, Nijboer WN, Seelen MA, Sandovici M, Bos EM, et al. Heparin binding epidermal growth factor in renal ischaemia/reperfusion injury. J Pathol 221: 183-192.

129. Smith JP, Pozzi A, Dhawan P, Singh AB, Harris RC (2009) Soluble HB-EGF induces epithelial-to-mesenchymal transition in inner medullary collecting duct cells by upregulating Snail-2. Am J Physiol Renal Physiol 296: F957-965.

130. Luo CC, Ming YC, Chao HC, Chu SM, Pang ST Heparin-Binding Epidermal Growth Factor-Like Growth Factor Downregulates Expression of Activator Protein-1 Transcription Factor after Intestinal Ischemia-Reperfusion Injury. Neonatology 99: 241-246.

131. Flamant M, Bollee G, Henique C, Tharaux PL (2012) Epidermal growth factor: a new therapeutic target in glomerular disease. Nephrol Dial Transplant 27: 1297-1304.

132. Zhuang S, Kinsey GR, Rasbach K, Schnellmann RG (2008) Heparin-binding epidermal growth factor and Src family kinases in proliferation of renal epithelial cells. Am J Physiol Renal Physiol 294: F459-468.

133. Takemura T, Murata Y, Hino S, Okada M, Yanagida H, et al. (1999) Heparin-binding EGF-like growth factor is expressed by mesangial cells and is involved in mesangial proliferation in glomerulonephritis. J Pathol 189: 431-438.

134. Paizis K, Kirkland G, Khong T, Katerelos M, Fraser S, et al. (1999) Heparin-binding epidermal growth factor-like growth factor is expressed in the adhesive lesions of experimental focal glomerular sclerosis. Kidney Int 55: 2310-2321.

135. Uchiyama-Tanaka Y, Matsubara H, Mori Y, Kosaki A, Kishimoto N, et al. (2002) Involvement of HB-EGF and EGF receptor transactivation in TGF-beta-mediated fibronectin expression in mesangial cells. Kidney Int 62: 799-808.

136. Malle E, Buch T, Grone HJ (2003) Myeloperoxidase in kidney disease. Kidney Int 64: 1956-1967.

137. Winterbourn CC, Vissers MC, Kettle AJ (2000) Myeloperoxidase. Curr Opin Hematol 7: 53-58.

138. Daugherty A, Dunn JL, Rateri DL, Heinecke JW (1994) Myeloperoxidase, a catalyst for lipoprotein oxidation, is expressed in human atherosclerotic lesions. J Clin Invest 94: 437-444.

139. Hillegass LM, Griswold DE, Brickson B, Albrightson-Winslow C (1990) Assessment of myeloperoxidase activity in whole rat kidney. J Pharmacol Methods 24: 285-295.

140. Granger DN, Benoit JN, Suzuki M, Grisham MB (1989) Leukocyte adherence to venular endothelium during ischemia-reperfusion. Am J Physiol 257: G683-688.

141. Vissers MC, Winterbourn CC (1986) The effect of oxidants on neutrophil-mediated degradation of glomerular basement membrane collagen. Biochim Biophys Acta 889: 277-286.

142. Besner G, Higashiyama S, Klagsbrun M (1990) Isolation and characterization of a macrophage-derived heparin-binding growth factor. Cell Regul 1: 811-819.

143. Rocourt DV, Mehta VB, Wu D, Besner GE (2007) Heparin-binding EGF-like growth factor decreases neutrophil-endothelial cell interactions. J Surg Res 141: 262-266.

144. Gale DP, Pickering MC (2011) Regulating complement in the kidney: insights from CFHR5 nephropathy. Dis Model Mech 4: 721-726.

145. Huppi K, Volfovsky N, Runfola T, Jones TL, Mackiewicz M, et al. (2008) The identification of microRNAs in a genomically unstable region of human chromosome 8q24. Mol Cancer Res 6: 212-221.

146. Alvarez ML, DiStefano JK (2011) Functional characterization of the plasmacytoma variant translocation 1 gene (PVT1) in diabetic nephropathy. PLoS One 6: e18671.

147. Guan Y, Kuo WL, Stilwell JL, Takano H, Lapuk AV, et al. (2007) Amplification of PVT1 contributes to the pathophysiology of ovarian and breast cancer. Clin Cancer Res 13: 5745-5755.

148. Graham M, Adams JM (1986) Chromosome 8 breakpoint far 3' of the c-myc oncogene in a Burkitt's lymphoma 2;8 variant translocation is equivalent to the murine pvt-1 locus. EMBO J 5: 2845-2851.

149. Enciso-Mora V, Broderick P, Ma Y, Jarrett RF, Hjalgrim H, et al. (2010) A genome-wide association study of Hodgkin's lymphoma identifies new susceptibility loci at 2p16.1 (REL), 8q24.21 and 10p14 (GATA3). Nat Genet 42: 1126-1130.

150. Hanson RL, Craig DW, Millis MP, Yeatts KA, Kobes S, et al. (2007) Identification of PVT1 as a candidate gene for end-stage renal disease in type 2 diabetes using a pooling-based genome-wide single nucleotide polymorphism association study. Diabetes 56: 975-983.

151. Millis MP, Bowen D, Kingsley C, Watanabe RM, Wolford JK (2007) Variants in the plasmacytoma variant translocation gene (PVT1) are associated with end-stage renal disease attributed to type 1 diabetes. Diabetes 56: 3027-3032.

152. Papagregoriou G, Erguler K, Dweep H, Voskarides K, Koupepidou P, et al. (2012) A miR-1207-5p Binding Site Polymorphism Abolishes Regulation of HBEGF and Is Associated with Disease Severity in CFHR5 Nephropathy. PLoS One 7: e31021.

153. Piriyapongsa J, Jordan IK (2007) A family of human microRNA genes from miniature inverted-repeat transposable elements. PLoS One 2: e203.

154. Obbard DJ, Gordon KH, Buck AH, Jiggins FM (2009) The evolution of RNAi as a defence against viruses and transposable elements. Philos Trans R Soc Lond B Biol Sci 364: 99-115.

155. van der Weyden L, Adams DJ (2007) The Ras-association domain family (RASSF) members and their role in human tumourigenesis. Biochim Biophys Acta 1776: 58-85.

156. Stitt-Cavanagh E, MacLeod L, Kennedy C (2009) The podocyte in diabetic kidney disease. ScientificWorldJournal 9: 1127-1139.

157. Qin YH, Zhou TB, Su LN, Lei FY, Huang WF, et al. (2011) Association between ACE polymorphism and risk of IgA nephropathy: a meta-analysis. J Renin Angiotensin Aldosterone Syst 12: 215-223.

158. Mizuiri S, Hemmi H, Arita M, Aoki T, Ohashi Y, et al. (2011) Increased ACE and decreased ACE2 expression in kidneys from patients with IgA nephropathy. Nephron Clin Pract 117: c57-66.

159. Shiota A, Yamamoto K, Ohishi M, Tatara Y, Ohnishi M, et al. (2010) Loss of ACE2 accelerates time-dependent glomerular and tubulointerstitial damage in streptozotocin-induced diabetic mice. Hypertens Res 33: 298-307.

160. Groffen AJ, Ruegg MA, Dijkman H, van de Velden TJ, Buskens CA, et al. (1998) Agrin is a major heparan sulfate proteoglycan in the human glomerular basement membrane. J Histochem Cytochem 46: 19-27.

161. Gallego PH, Shephard N, Bulsara MK, van Bockxmeer FM, Powell BL, et al. (2008) Angiotensinogen gene T235 variant: a marker for the development of persistent microalbuminuria in children and adolescents with type 1 diabetes mellitus. J Diabetes Complications 22: 191-198.

162. Buraczynska M, Grzebalska A, Spasiewicz D, Orlowska G, Ksiazek A (2002) Genetic polymorphisms of renin-angiotensin system and progression of interstitial nephritis. Ann Univ Mariae Curie Sklodowska Med 57: 330-336.

163. Doria A, Onuma T, Warram JH, Krolewski AS (1997) Synergistic effect of angiotensin II type 1 receptor genotype and poor glycaemic control on risk of nephropathy in IDDM. Diabetologia 40: 1293-1299.

164. Lewis EJ, Lewis JB (2003) Treatment of diabetic nephropathy with angiotensin II receptor antagonist. Clin Exp Nephrol 7: 1-8.

165. Wehbi GJ, Zimpelmann J, Carey RM, Levine DZ, Burns KD (2001) Early streptozotocin-diabetes mellitus downregulates rat kidney AT2 receptors. Am J Physiol Renal Physiol 280: F254-265.

166. Satchell SC, Harper SJ, Tooke JE, Kerjaschki D, Saleem MA, et al. (2002) Human podocytes express angiopoietin 1, a potential regulator of glomerular vascular endothelial growth factor. J Am Soc Nephrol 13: 544-550.

167. Yasui M, Kwon TH, Knepper MA, Nielsen S, Agre P (1999) Aquaporin-6: An intracellular vesicle water channel protein in renal epithelia. Proc Natl Acad Sci U S A 96: 5808-5813.

168. Dendooven A, van Oostrom O, van der Giezen DM, Leeuwis JW, Snijckers C, et al. (2011) Loss of endogenous bone morphogenetic protein-6 aggravates renal fibrosis. Am J Pathol 178: 1069-1079.

169. Wang S, Chen Q, Simon TC, Strebeck F, Chaudhary L, et al. (2003) Bone morphogenic protein-7 (BMP-7), a novel therapy for diabetic nephropathy. Kidney Int 63: 2037-2049.

170. Morrissey J, Hruska K, Guo G, Wang S, Chen Q, et al. (2002) Bone morphogenetic protein-7 improves renal fibrosis and accelerates the return of renal function. J Am Soc Nephrol 13 Suppl 1: S14-21.

171. Lehtonen S, Ryan JJ, Kudlicka K, Iino N, Zhou H, et al. (2005) Cell junction-associated proteins IQGAP1, MAGI-2, CASK, spectrins, and alpha-actinin are components of the nephrin multiprotein complex. Proc Natl Acad Sci U S A 102: 9814-9819.

172. Gigante M, Pontrelli P, Montemurno E, Roca L, Aucella F, et al. (2009) CD2AP mutations are associated with sporadic nephrotic syndrome and focal segmental glomerulosclerosis (FSGS). Nephrol Dial Transplant 24: 1858-1864.

173. Shih NY, Li J, Cotran R, Mundel P, Miner JH, et al. (2001) CD2AP localizes to the slit diaphragm and binds to nephrin via a novel C-terminal domain. Am J Pathol 159: 2303-2308.

174. Rastaldi MP, Candiano G, Musante L, Bruschi M, Armelloni S, et al. (2006) Glomerular clusterin is associated with PKC-alpha/beta regulation and good outcome of membranous glomerulonephritis in humans. Kidney Int 70: 477-485.

175. Herbach N, Schairer I, Blutke A, Kautz S, Siebert A, et al. (2009) Diabetic kidney lesions of GIPRdn transgenic mice: podocyte hypertrophy and thickening of the GBM precede glomerular hypertrophy and glomerulosclerosis. Am J Physiol Renal Physiol 296: F819-829.

176. Kalluri R, Shield CF, Todd P, Hudson BG, Neilson EG (1997) Isoform switching of type IV collagen is developmentally arrested in X-linked Alport syndrome leading to increased susceptibility of renal basement membranes to endoproteolysis. J Clin Invest 99: 2470-2478.

177. Heidet L, Arrondel C, Forestier L, Cohen-Solal L, Mollet G, et al. (2001) Structure of the human type IV collagen gene COL4A3 and mutations in autosomal Alport syndrome. J Am Soc Nephrol 12: 97-106.

178. Marcocci E, Uliana V, Bruttini M, Artuso R, Silengo MC, et al. (2009) Autosomal dominant Alport syndrome: molecular analysis of the COL4A4 gene and clinical outcome. Nephrol Dial Transplant 24: 1464-1471.

179. Slajpah M, Gorinsek B, Berginc G, Vizjak A, Ferluga D, et al. (2007) Sixteen novel mutations identified in COL4A3, COL4A4, and COL4A5 genes in Slovenian families with Alport syndrome and benign familial hematuria. Kidney Int 71: 1287-1295.

180. Demosthenous P, Voskarides K, Stylianou K, Hadjigavriel M, Arsali M, et al. (2012) X-linked Alport syndrome in Hellenic families: Phenotypic heterogeneity and mutations near interruptions of the collagen domain in COL4A5. Clin Genet 81: 240-248.

181. Mothes H, Heidet L, Arrondel C, Richter KK, Thiele M, et al. (2002) Alport syndrome associated with diffuse leiomyomatosis: COL4A5-COL4A6 deletion associated with a mild form of Alport nephropathy. Nephrol Dial Transplant 17: 70-74.

182. Uliana V, Marcocci E, Mucciolo M, Meloni I, Izzi C, et al. (2011) Alport syndrome and leiomyomatosis: the first deletion extending beyond COL4A6 intron 2. Pediatr Nephrol 26: 717-724.

183. Teixeira JE, Costa RS, Lachmann PJ, Wurzner R, Barbosa JE (1996) CR1 stump peptide and terminal complement complexes are found in the glomeruli of lupus nephritis patients. Clin Exp Immunol 105: 497-503.

184. Verma J, Arora V, Marwaha V, Kumar A, Das N (2005) Association of leukocyte CR1 gene transcription with the disease severity and renal involvement in systemic lupus erythematosus. Lupus 14: 273-279.

185. Nystrom J, Hultenby K, Ek S, Sjolund J, Axelson H, et al. (2009) CRIM1 is localized to the podocyte filtration slit diaphragm of the adult human kidney. Nephrol Dial Transplant 24: 2038-2044.

186. Roestenberg P, van Nieuwenhoven FA, Wieten L, Boer P, Diekman T, et al. (2004) Connective tissue growth factor is increased in plasma of type 1 diabetic patients with nephropathy. Diabetes Care 27: 1164-1170.

187. Besse-Eschmann V, Le Hir M, Endlich N, Endlich K (2004) Alteration of podocytes in a murine model of crescentic glomerulonephritis. Histochem Cell Biol 122: 139-149.

188. Sayyed SG, Hagele H, Kulkarni OP, Endlich K, Segerer S, et al. (2009) Podocytes produce homeostatic chemokine stromal cell-derived factor-1/CXCL12, which contributes to glomerulosclerosis, podocyte loss and albuminuria in a mouse model of type 2 diabetes. Diabetologia 52: 2445-2454.

189. Asanuma K, Campbell KN, Kim K, Faul C, Mundel P (2007) Nuclear relocation of the nephrin and CD2AP-binding protein dendrin promotes apoptosis of podocytes. Proc Natl Acad Sci U S A 104: 10134-10139.

190. Asanuma K, Akiba-Takagi M, Kodama F, Asao R, Nagai Y, et al. (2011) Dendrin location in podocytes is associated with disease progression in animal and human glomerulopathy. Am J Nephrol 33: 537-549.

191. Hashimoto T, Karasawa T, Saito A, Miyauchi N, Han GD, et al. (2007) Ephrin-B1 localizes at the slit diaphragm of the glomerular podocyte. Kidney Int 72: 954-964.

192. Ciani L, Patel A, Allen ND, ffrench-Constant C (2003) Mice lacking the giant protocadherin mFAT1 exhibit renal slit junction abnormalities and a partially penetrant cyclopia and anophthalmia phenotype. Mol Cell Biol 23: 3575-3582.

193. Fliser D, Kollerits B, Neyer U, Ankerst DP, Lhotta K, et al. (2007) Fibroblast growth factor 23 (FGF23) predicts progression of chronic kidney disease: the Mild to Moderate Kidney Disease (MMKD) Study. J Am Soc Nephrol 18: 2600-2608.

194. Cancilla B, Ford-Perriss MD, Bertram JF (1999) Expression and localization of fibroblast growth factors and fibroblast growth factor receptors in the developing rat kidney. Kidney Int 56: 2025-2039.

195. Castelletti F, Donadelli R, Banterla F, Hildebrandt F, Zipfel PF, et al. (2008) Mutations in FN1 cause glomerulopathy with fibronectin deposits. Proc Natl Acad Sci U S A 105: 2538-2543.

196. Takemoto M, He L, Norlin J, Patrakka J, Xiao Z, et al. (2006) Large-scale identification of genes implicated in kidney glomerulus development and function. EMBO J 25: 1160-1174.

197. Zhang X, Chen X, Wu D, Liu W, Wang J, et al. (2006) Downregulation of connexin 43 expression by high glucose induces senescence in glomerular mesangial cells. J Am Soc Nephrol 17: 1532-1542.

198. Sawai K, Mukoyama M, Mori K, Yokoi H, Koshikawa M, et al. (2006) Redistribution of connexin43 expression in glomerular podocytes predicts poor renal prognosis in patients with type 2 diabetes and overt nephropathy. Nephrol Dial Transplant 21: 2472-2477.

199. Dai C, Saleem MA, Holzman LB, Mathieson P, Liu Y (2010) Hepatocyte growth factor signaling ameliorates podocyte injury and proteinuria. Kidney Int 77: 962-973.

200. Esposito C, Parrilla B, De Mauri A, Cornacchia F, Fasoli G, et al. (2005) Hepatocyte growth factor (HGF) modulates matrix turnover in human glomeruli. Kidney Int 67: 2143-2150.

201. Ruotsalainen V, Ljungberg P, Wartiovaara J, Lenkkeri U, Kestila M, et al. (1999) Nephrin is specifically located at the slit diaphragm of glomerular podocytes. Proc Natl Acad Sci U S A 96: 7962-7967.

202. Ihalmo P, Schmid H, Rastaldi MP, Mattinzoli D, Langham RG, et al. (2007) Expression of filtrin in human glomerular diseases. Nephrol Dial Transplant 22: 1903-1909.

203. Rinta-Valkama J, Aaltonen P, Lassila M, Palmen T, Tossavainen P, et al. (2007) Densin and filtrin in the pancreas and in the kidney, targets for humoral autoimmunity in patients with type 1 diabetes. Diabetes Metab Res Rev 23: 119-126.

204. Patrie KM, Drescher AJ, Goyal M, Wiggins RC, Margolis B (2001) The membrane-associated guanylate kinase protein MAGI-1 binds megalin and is present in glomerular podocytes. J Am Soc Nephrol 12: 667-677.

205. Hayashi K, Horikoshi S, Osada S, Shofuda K, Shirato I, et al. (2000) Macrophage-derived MT1-MMP and increased MMP-2 activity are associated with glomerular damage in crescentic glomerulonephritis. J Pathol 191: 299-305.

206. Hayashi K, Osada S, Shofuda K, Horikoshi S, Shirato I, et al. (1998) Enhanced expression of membrane type-1 matrix metalloproteinase in mesangial proliferative glomerulonephritis. J Am Soc Nephrol 9: 2262-2271.

207. Marson BP, Lacchini R, Belo V, Dickel S, da Costa BP, et al. (2012) Matrix Metalloproteinase (MMP)-2 Genetic Variants Modify the Circulating MMP-2 Levels in End-Stage Kidney Disease. Am J Nephrol 35: 209-215.

208. Zeisberg M, Khurana M, Rao VH, Cosgrove D, Rougier JP, et al. (2006) Stage-specific action of matrix metalloproteinases influences progressive hereditary kidney disease. PLoS Med 3: e100.

209. Srichai MB, Colleta H, Gewin L, Matrisian L, Abel TW, et al. (2011) Membrane-type 4 matrix metalloproteinase (MT4-MMP) modulates water homeostasis in mice. PLoS One 6: e17099.

210. He W, Tan RJ, Li Y, Wang D, Nie J, et al. (2012) Matrix Metalloproteinase-7 as a Surrogate Marker Predicts Renal Wnt/beta-Catenin Activity in CKD. J Am Soc Nephrol 23: 294-304.

211. Ebihara I, Nakamura T, Shimada N, Koide H (1998) Increased plasma metalloproteinase-9 concentrations precede development of microalbuminuria in non-insulin-dependent diabetes mellitus. Am J Kidney Dis 32: 544-550.

212. Jones N, Blasutig IM, Eremina V, Ruston JM, Bladt F, et al. (2006) Nck adaptor proteins link nephrin to the actin cytoskeleton of kidney podocytes. Nature 440: 818-823.

213. Nakayama K, Natori Y, Sato T, Kimura T, Sugiura A, et al. (2004) Altered expression of NDST-1 messenger RNA in puromycin aminonucleoside nephrosis. J Lab Clin Med 143: 106-114.

214. Salmivirta K, Talts JF, Olsson M, Sasaki T, Timpl R, et al. (2002) Binding of mouse nidogen-2 to basement membrane components and cells and its expression in embryonic and adult tissues suggest complementary functions of the two nidogens. Exp Cell Res 279: 188-201.

215. Cheng HT, Kopan R (2005) The role of Notch signaling in specification of podocyte and proximal tubules within the developing mouse kidney. Kidney Int 68: 1951-1952.

216. Niranjan T, Bielesz B, Gruenwald A, Ponda MP, Kopp JB, et al. (2008) The Notch pathway in podocytes plays a role in the development of glomerular disease. Nat Med 14: 290-298.

217. Denhez F, Wilcox-Adelman SA, Baciu PC, Saoncella S, Lee S, et al. (2002) Syndesmos, a syndecan-4 cytoplasmic domain interactor, binds to the focal adhesion adaptor proteins paxillin and Hic-5. J Biol Chem 277: 12270-12274.

218. Eitner F, Ostendorf T, Kretzler M, Cohen CD, Eriksson U, et al. (2003) PDGF-C expression in the developing and normal adult human kidney and in glomerular diseases. J Am Soc Nephrol 14: 1145-1153.

219. Matsumoto K, Hiraiwa N, Yoshiki A, Ohnishi M, Kusakabe M (2002) PDGF receptor-alpha deficiency in glomerular mesangial cells of tenascin-C knockout mice. Biochem Biophys Res Commun 290: 1220-1227.

220. Beck KF, Guder G, Schaefer L, Pleskova M, Babelova A, et al. (2005) Nitric oxide upregulates induction of PDGF receptor-alpha expression in rat renal mesangial cells and in anti-Thy-1 glomerulonephritis. J Am Soc Nephrol 16: 1948-1957.

221. Matsui K, Breitender-Geleff S, Soleiman A, Kowalski H, Kerjaschki D (1999) Podoplanin, a novel 43-kDa membrane protein, controls the shape of podocytes. Nephrol Dial Transplant 14 Suppl 1: 9-11.

222. Schmid H, Henger A, Cohen CD, Frach K, Grone HJ, et al. (2003) Gene expression profiles of podocyte-associated molecules as diagnostic markers in acquired proteinuric diseases. J Am Soc Nephrol 14: 2958-2966.

223. Narita I, Kondo D, Goto S, Saito N, Watanabe Y, et al. (2001) Association of gene polymorphism of polymeric immunoglobulin receptor and IgA nephropathy. Intern Med 40: 867-872.

224. Neophytou P, Constantinides R, Lazarou A, Pierides A, Deltas CC (1996) Detection of a novel nonsense mutation and an intragenic polymorphism in the PKD1 gene of a Cypriot family with autosomal dominant polycystic kidney disease. Hum Genet 98: 437-442.

225. Mochizuki T, Wu G, Hayashi T, Xenophontos SL, Veldhuisen B, et al. (1996) PKD2, a gene for polycystic kidney disease that encodes an integral membrane protein. Science 272: 1339-1342.

226. Boyer O, Benoit G, Gribouval O, Nevo F, Pawtowski A, et al. (2010) Mutational analysis of the PLCE1 gene in steroid resistant nephrotic syndrome. J Med Genet 47: 445-452.

227. Hinkes B, Wiggins RC, Gbadegesin R, Vlangos CN, Seelow D, et al. (2006) Positional cloning uncovers mutations in PLCE1 responsible for a nephrotic syndrome variant that may be reversible. Nat Genet 38: 1397-1405.

228. Shimizu-Hirota R, Sasamura H, Kuroda M, Kobayashi E, Saruta T (2004) Functional characterization of podocan, a member of a new class in the small leucine-rich repeat protein family. FEBS Lett 563: 69-74.

229. Ross MD, Bruggeman LA, Hanss B, Sunamoto M, Marras D, et al. (2003) Podocan, a novel small leucine-rich repeat protein expressed in the sclerotic glomerular lesion of experimental HIV-associated nephropathy. J Biol Chem 278: 33248-33255.

230. Kono K, Kamijo Y, Hora K, Takahashi K, Higuchi M, et al. (2009) PPAR{alpha} attenuates the proinflammatory response in activated mesangial cells. Am J Physiol Renal Physiol 296: F328-336.

231. Miglio G, Rosa AC, Rattazzi L, Grange C, Collino M, et al. (2011) The subtypes of peroxisome proliferator-activated receptors expressed by human podocytes and their role in decreasing podocyte injury. Br J Pharmacol 162: 111-125.

232. Ozaltin F, Ibsirlioglu T, Taskiran EZ, Baydar DE, Kaymaz F, et al. (2011) Disruption of PTPRO causes childhood-onset nephrotic syndrome. Am J Hum Genet 89: 139-147.

233. Hirakawa M, Tsuruya K, Yotsueda H, Tokumoto M, Ikeda H, et al. (2006) Expression of synaptopodin and GLEPP1 as markers of steroid responsiveness in primary focal segmental glomerulosclerosis. Life Sci 79: 757-763.

234. Tian J, Wang HP, Mao YY, Jin J, Chen JH (2007) Reduced glomerular epithelial protein 1 expression and podocyte injury in immunoglobulin A nephropathy. J Int Med Res 35: 338-345.

235. Yoo TH, Li JJ, Kim JJ, Jung DS, Kwak SJ, et al. (2007) Activation of the renin-angiotensin system within podocytes in diabetes. Kidney Int 71: 1019-1027.

236. Rops AL, Gotte M, Baselmans MH, van den Hoven MJ, Steenbergen EJ, et al. (2007) Syndecan-1 deficiency aggravates anti-glomerular basement membrane nephritis. Kidney Int 72: 1204-1215.

237. Cevikbas F, Schaefer L, Uhlig P, Robenek H, Theilmeier G, et al. (2008) Unilateral nephrectomy leads to up-regulation of syndecan-2- and TGF-beta-mediated glomerulosclerosis in syndecan-4 deficient male mice. Matrix Biol 27: 42-52.

238. Greene DK, Tumova S, Couchman JR, Woods A (2003) Syndecan-4 associates with alpha-actinin. J Biol Chem 278: 7617-7623.

239. Kaufman L, Potla U, Coleman S, Dikiy S, Hata Y, et al. (2010) Up-regulation of the homophilic adhesion molecule sidekick-1 in podocytes contributes to glomerulosclerosis. J Biol Chem 285: 25677-25685.

240. Brady HR, Spertini O, Jimenez W, Brenner BM, Marsden PA, et al. (1992) Neutrophils, monocytes, and lymphocytes bind to cytokine-activated kidney glomerular endothelial cells through L-selectin (LAM-1) in vitro. J Immunol 149: 2437-2444.

241. Inagi R, Nangaku M, Miyata T, Kurokawa K (2003) Mesangial cell-predominant functional gene, megsin. Clin Exp Nephrol 7: 87-92.

242. Ohtomo S, Nangaku M, Izuhara Y, Yamada N, Dan T, et al. (2008) The role of megsin, a serine protease inhibitor, in diabetic mesangial matrix accumulation. Kidney Int 74: 768-774.

243. Xia Y, Li Y, Du Y, Yang N, Li C, et al. (2006) Association of MEGSIN 2093C-2180T haplotype at the 3' untranslated region with disease severity and progression of IgA nephropathy. Nephrol Dial Transplant 21: 1570-1574.

244. Lee HB, Ha H (2005) Plasminogen activator inhibitor-1 and diabetic nephropathy. Nephrology (Carlton) 10 Suppl: S11-13.

245. Taneda S, Hudkins KL, Muhlfeld AS, Kowalewska J, Pippin JW, et al. (2008) Protease nexin-1, tPA, and PAI-1 are upregulated in cryoglobulinemic membranoproliferative glomerulonephritis. J Am Soc Nephrol 19: 243-251.

246. Okamoto N, Aruga S, Matsuzaki S, Takahashi S, Matsushita K, et al. (2007) Associations between renal sodium-citrate cotransporter (hNaDC-1) gene polymorphism and urinary citrate excretion in recurrent renal calcium stone formers and normal controls. Int J Urol 14: 344-349.

247. Toyohara T, Suzuki T, Morimoto R, Akiyama Y, Souma T, et al. (2009) SLCO4C1 transporter eliminates uremic toxins and attenuates hypertension and renal inflammation. J Am Soc Nephrol 20: 2546-2555.

248. Beltcheva O, Hjorleifsdottir EE, Kontusaari S, Tryggvason K (2010) Sp1 specifically binds to an evolutionarily conserved DNA segment within a region necessary for podocyte-specific expression of nephrin. Nephron Exp Nephrol 114: e15-22.

249. Ristola M, Arpiainen S, Saleem MA, Mathieson PW, Welsh GI, et al. (2009) Regulation of Neph3 gene in podocytes--key roles of transcription factors NF-kappaB and Sp1. BMC Mol Biol 10: 83.

250. Nicholas SB, Liu J, Kim J, Ren Y, Collins AR, et al. (2010) Critical role for osteopontin in diabetic nephropathy. Kidney Int 77: 588-600.

251. Endlich N, Sunohara M, Nietfeld W, Wolski EW, Schiwek D, et al. (2002) Analysis of differential gene expression in stretched podocytes: osteopontin enhances adaptation of podocytes to mechanical stress. FASEB J 16: 1850-1852.

252. Mundel P, Heid HW, Mundel TM, Kruger M, Reiser J, et al. (1997) Synaptopodin: an actin-associated protein in telencephalic dendrites and renal podocytes. J Cell Biol 139: 193-204.

253. Srivastava T, Garola RE, Whiting JM, Alon US (2001) Synaptopodin expression in idiopathic nephrotic syndrome of childhood. Kidney Int 59: 118-125.

254. Quaggin SE, Vanden Heuvel GB, Igarashi P (1998) Pod-1, a mesoderm-specific basic-helix-loop-helix protein expressed in mesenchymal and glomerular epithelial cells in the developing kidney. Mech Dev 71: 37-48.

255. Cui S, Schwartz L, Quaggin SE (2003) Pod1 is required in stromal cells for glomerulogenesis. Dev Dyn 226: 512-522.

256. Wu DT, Bitzer M, Ju W, Mundel P, Bottinger EP (2005) TGF-beta concentration specifies differential signaling profiles of growth arrest/differentiation and apoptosis in podocytes. J Am Soc Nephrol 16: 3211-3221.

257. Iglesias-de la Cruz MC, Ziyadeh FN, Isono M, Kouahou M, Han DC, et al. (2002) Effects of high glucose and TGF-beta1 on the expression of collagen IV and vascular endothelial growth factor in mouse podocytes. Kidney Int 62: 901-913.

258. McLennan SV, Wang XY, Moreno V, Yue DK, Twigg SM (2004) Connective tissue growth factor mediates high glucose effects on matrix degradation through tissue

inhibitor of matrix metalloproteinase type 1: implications for diabetic nephropathy. Endocrinology 145: 5646-5655.

259. Han SY, Jee YH, Han KH, Kang YS, Kim HK, et al. (2006) An imbalance between matrix metalloproteinase-2 and tissue inhibitor of matrix metalloproteinase-2 contributes to the development of early diabetic nephropathy. Nephrol Dial Transplant 21: 2406-2416.

260. Kassiri Z, Oudit GY, Kandalam V, Awad A, Wang X, et al. (2009) Loss of TIMP3 enhances interstitial nephritis and fibrosis. J Am Soc Nephrol 20: 1223-1235.

261. Camp TM, Smiley LM, Hayden MR, Tyagi SC (2003) Mechanism of matrix accumulation and glomerulosclerosis in spontaneously hypertensive rats. J Hypertens 21: 1719-1727.

262. Schnabel E, Anderson JM, Farquhar MG (1990) The tight junction protein ZO-1 is concentrated along slit diaphragms of the glomerular epithelium. J Cell Biol 111: 1255-1263.

263. Santin S, Ars E, Rossetti S, Salido E, Silva I, et al. (2009) TRPC6 mutational analysis in a large cohort of patients with focal segmental glomerulosclerosis. Nephrol Dial Transplant 24: 3089-3096.

264. Guo JK, Menke AL, Gubler MC, Clarke AR, Harrison D, et al. (2002) WT1 is a key regulator of podocyte function: reduced expression levels cause crescentic glomerulonephritis and mesangial sclerosis. Hum Mol Genet 11: 651-659.

265. Bockenhauer D, van't Hoff W, Chernin G, Heeringa SF, Sebire NJ (2009) Membranoproliferative glomerulonephritis associated with a mutation in Wilms' tumour suppressor gene 1. Pediatr Nephrol 24: 1399-1401.

APPENDIX I

Table 19: List of genes that are considered candidates for miRNA targeting predictions. The list is comprised of a variety of genes; some are implicated in glomerular diseases, while others have podocyte, glomerular basement membrane or glomerular endothelium specific expression.

Gene	Name	Chromosome	Information
ACE	Angiotensin I converting enzyme 1	17q23.3	Associated with diabetic and IgA nephropathy [156,157,158]
ACE2	Angiotensin converting enzyme 2	Xp22	Associated with diabetic and IgA nephropathy [158,159]
AGRN	Agrin	1p36.33	Principal component of the glomerular basement membrane [160]
AGT	Angiotensinogen	1q42.2	Variants confer to susceptibility for diabetic nephropathy and interstitial nephritis [161,162]
AGTR1	Angiotensin II receptor, type 1	3q24	Associated with diabetic nephropathy and its inhibitors are used for therapeutic purposes [163,164]
AGTR2	Angiotensin II receptor, type 2	Xq23	Implicated in diabetic nephropathy[165]
ANGPT1	Angiopoietin 1	8q23.1	Expressed by podocytes [166]
AQP6	Aquaporin 6	12q13.13	Expressed and localized in podocytes [167]
BMP6	Bone morphogenetic protein 6	6p24.3	Involved in diabetic nephropathy and exacerbates renal fibrosis after injury[168]
BMP7	Bone morphogenetic protein 7	20q13.31	Proposed as a therapeutic agent for diabetic nephropathy, as it improves the fibrotic image and kidney's return to normal function [169,170]
CASK	Calcium/calmodulin-dependent serine protein kinase	Xp11.4	Member of the nephrin interacting complex, activated at slit diaphragms and tight junctions of the podocyte[171]
CD2AP	CD2-associated protein	6p12.3	Slit diaphragm protein that its mutations cause Focal Segmental Glomerulosclerosis 3[172,173]
CFHR5	Complement factor H-related 5	1q22-q23	Mutations cause CFHR5 nephropathy[39]
CLU	Clusterin	8p21.1	Adjusts inflammation reactions in podocytes during membranous glomerulonephritis[174]

Gene	Name	Chromosome	Information
COL4A1	Collagen, IV, alpha 1	13q34	Deposes in the mesangium of mice with diabetic nephropathy and an early component of the GBM which remains in XL Alport syndrome [175,176]
COL4A2	Collagen, IV, alpha 2	13q34	Forms a trimer with COL4A1 (α1α1α2) in fetal GBM and is not substituted by α3α4α5 in XL Alport[176]
COL4A3	Collagen, IV, alpha 3	2q36.3	Mutations cause TBMN or AR Alport syndrome [38,177]
COL4A4	Collagen, IV, alpha 4	2q36.3	Mutations cause TBMN or AR Alport syndrome [38,178]
COL4A5	Collagen, IV, alpha 5	Xq22	Mutations cause XL Alport syndrome [179,180]
COL4A6	Collagen, IV, alpha 6	Xq22.3	Mutations cause alport syndrome with diffuse leiomyomatosis [181,182]
CR1	Complement component	1q32	Associated with SLE nephropathy and diffuse proliferative glomerulonephritis as its levels of expression fall in the damaged glomerulus [183,184]
CRIM1	Cystein rich transmembrane BMP regulator 1	2p21	Expressed in podocytes and found on slit diaphragms[185]
CTGF	Connective tissue growth factor	6q23.2	Increased in diabetic nephropathy and are correlated with proteinuria and increased creatinine clearance[186]
CTTN	Cortactin	11q13.3	Normally expressed in podocyte foot processes but dislocated to the cell body, the cytoplasm and the apical cell membrane [187]
CXCL12	Chemokine (C-X-C motif) ligand 12	10q11.21	Expressed by podocytes and contributes in glomerular sclerosis, proteinuria and loss of podocytes in diabetic mice[188]
DDN	Dendrin	12q13.11	Interacts with CD2AP to promote apoptosis in glomerulopathy podocytes, by relocating from the slit diaphragm to the nucleus, and is associated with podocyte injury in glomerulopathies [189,190]
EFNB1	Ephrin-B1	Xq13.1	Expressed in podocytes and found on slit diaphragms[191]
FAT1	FAT tumor suppressor homolog 1	4q35.2	Expressed predominantly in podocytes and FAT1 knockout mice exhibit loss of slit diaphragms and podocyte fusion [192]
FGF23	Fibroblast growth factor 23	12p13.32	Marker of progression of renal disease in patients with non-diabetic CKD[193]
FGFR3	Fibroblast growth factor receptor 3	4p16.3	Expressed in the mature glomerulus of rats and involved in kidney development [194]

Gene	Name	Chromosome	Information
FN1	Fibronectin 1	2q35	Mutations cause fibronectin deposits at the glomerulus leading to ESKD[195]
FOXC2	Forkhead box C2	16q24.1	Controls the differentiation of podocytes and the expression of genes such as Col4a3, Col4a4 and Nphs2. [196]
GJA1	Gap junction protein, alpha 1 (Connexin 43)	6q22.31	Downregulated by elevated glycose and is possibly involved in diabetic nephropathy[197,198]
HBEGF	Heparin-binding EGF-like growth factor	5q31.3	Expressed in mesangial cells, where it is involved in their proliferation in glomerulonephritis and contributes to lesion formation in focal glomerulosclerosis via site specific mitogen stimulation.[133,134]
HGF	Hepatocyte growth factor	7q21.1	Has a protective effect in podocytes against proteinuria and fibrosis, while it preserves the normal turnover of mesangial matrix in the glomerulus [199,200]
KIRREL	Nephrin related 1 (NEPH1)	1q23.1	Localizes at slit diaphragms of podocytes [201]
KIRREL2	Filtrin (NEPH3)	19q13.12	Expressed at the glomerulus and its levels are reduced in FSGS [202]
KIRREL3	Nephrin-like protein 2 (NEPH2)	11q24.2	Expressed at the glomerular slit diaphragm and interacts with nephrin[25]
LRRC7	Leucine rich repeat containing 7 (Densin)	1p31.1	Expressed in podocytes and is associated with nephrin and its interaction complex at the slit diaphragm[203]
MAGI1	Membrane associated guanylate kinase, WW and PDZ domain containing 1	3p14.1	Expressed in podocytes, is member of the nephrin complex and interacts with various podocyte specific proteins[171,204]
MMP1	Matrix metalloproteinase 1	11q22.2	Found with MMP2 to be associated with crescentic nephropathy and is enhanced in mesangial glomerulonephritis[205,206]
MMP2	Matrix metalloproteinase 2	16q12.2	Polymorphisms are associated with ESKD and activated in the damaged glomeruli of crescentic nephropathy. [205,207]
MMP3	Matrix metalloproteinase 3	11q22.2	Responsible for GBM collagen degradation [208]
MMP4	Matrix metalloproteinase 4	12q24.33	Expressed in the early stages of kidney development and is involved in branching morphogenesis[209]
MMP7	Matrix metalloproteinase 7	11q22.2	Marker of CKD as it was found to be co-activated with the Wnt/β-catenin signaling[210]
MMP9	Matrix metalloproteinase 9	20q13.12	Responsible for the extracellular matrix accumulation in diabetic nephropathy and enhances the pathological phenotype of Alport Syndrome. [208,211]
NCK1	NCK adaptor protein 1	3q22	Expressed in podocytes where it connects nephrin to the actin cytoskeleton [212]
NDST1	N-deacetylase/N-sulfotransferase (heparin glucosamyl) 1	5q33.1	Involved in puromycin aminonucleoside nephrosis by influencing heparan sulfate assembly in GBM [213]
NID1	Nidogen 1	1q43	Part of the glomerular basement membrane [214]

Gene	Name	Chromosome	Information
NID2	Nidogen 2	14q22.1	Part of the glomerular basement membrane [214]
NOTCH1	Notch 1	9q34.3	Involved in kidney development and its increasingly expressed in podocytes during diabetic nephropathy and FSGS [215,216]
NPHS1	Nephrin	19q13.12	Nephrotic syndrome (Finnish type) [22]
NPHS2	Podocin	1q25.2	Steroid resistant nephrotic syndrome 1, minimal change nephritis, FSGS [31]
NUDT16L1	Nucleoside diphosphate linked moiety X-type motif 16-like 1 (nudix, syndesmos)	16p13.3	Member of focal adhesion complexes and interacts with syndecan-4 [217]
PDGFC	Platelet derived growth factor C	4q32.1	Elevated expression in podocytes of patients with IgA nephropathy, membranous nephropathy, minimal change disease and transplant glomerulopathy[218]
PDGFRA	Platelet derived growth factor receptor, alpha polypeptide	4q12	Expressed at the mesangium in glomerulonephritis and is reduced in anti-Thy-1 glomerulonephritis [219,220]
PDPN	Podoplanin	1p36.21	Expressed by the podocyte and is believed to have a value as a diagnostic marker in glomerular diseases manifesting with proteinuria [221,222]
PIGR	Polymeric immunoglobulin receptor	1q32.2	Gene variants associated with IgA nephropathy [223]
PKD1	Polycystic kidney disease 1	16p13.3	AD Polycystic kidney disease type 1 [224]
PKD2	Polycystic kidney disease 2	4q22.1	AD Polycystic kidney disease type 2 [225]
PLCE1	Phospholipase C, epsilon 1	10q23.33	Steroid-resistant nephrotic syndrome type 3, Childhood nephrotic syndrome [226,227]
PODN	Podocan	1p32.3	Secreted from podocytes to the glomerular extracellular matrix and appears in glomerular sclerotic lesions caused by HIV-associated glomerulopathy [228,229]
PPARA	Peroxisome proliferative activated receptor, alpha	22q13.3	Proposed as a therapeutic agent in mesangial glomerulonephritis against inflammation and podocyte apoptosis [230,231]
PTPRO	Protein tyrosine phosphatase, receptor type, O (GLEPP1)	12p13-p12	Glomerular epithelial podocyte membrane protein that is responsible for childhood-onset nephrotic syndrome, is suggested as a marker for FSGS steroid therapy outcome and has reduced expression in IgA nephropathy [232,233,234]
REN	Renin	1q32.1	Elevated expression by podocytes in diabetic nephropathy [235]

Gene	Name	Chromosome	Information
SDC1	Syndecan 1	2p24.1	Heparan sulfate proteoglycan of the GBM, where in knockout mice causes basement membrane nephritis by the influx and accumulation of immune complexes [236]
SDC2	Syndecan 2	8q22.1	In syndecan-4 knockout mice, nephrectomy causes the up-regulation of syndecan-2 and eventually glomerulosclerosis[237]
SDC4	Syndecan 4	20q13.12	Expressed in podocytes and associates with focal adhesions and alpha-actinin cytoskeleton[238]
SDK1	Sidekick homolog 1, cell adhesion molecule	7p22.2	Overexpressed in podocytes in FSGS [239]
SELL	Selectin L	1q24.2	Promotes binding of leukocytes to kidney glomerular epithelial cells [240]
SERPINB7	Serine (or cysteine) proteinase inhibitor, clade B (ovalbumin), member 7 (megsin)	18q21.33	The most abundant protein of the mesangium.[241] It is overexpressed in diabetic nephropathy and promotes mesangial expansion, while SNPs on its 3'UTR have been associated with IgA nephropathy.[242,243]
SERPINE1	Serpine peptidase inhibitor, clade E, (Nexin, plasminogen activator inhibitor type 1), member 1	7q22.1	Expression is induced in the mesangium due to diabetic nephropathy or renal fibrosis in general [244]
SERPINE2	Serpine peptidase inhibitor, clade E, (Nexin, plasminogen activator inhibitor type 1), member 2	2q36.1	Found to be increased during cryoglobulinemic membraniproliferative glomerulonephritis and influence glomerulosclerosis[245]
SLC13A2/ NADC1	Solute carrier family 1, member 2	17p13.2	Influences the excretion of urinary citrate in kidneys and is responsible for calcium urolithiasis.[246]
SLCO4C1/ OATPX	Solute carrier organic anion transporter family, member 4C1	5q21.2	Transports uremic toxins accumulated in chronic kidney disease.[247]
SP1	SP1 transcription factor	12q13.13	Regulator of NEPH3 and NPHS1 expression in podocytes. [248,249]
SPP1	Secreted phosphoprotein	4q22.1	Important mediator of proteinuria, implicated in diabetic nephropathy and is highly expressed in stressed podocytes[250,251]
SYNPO	Synaptopodin	5q33.1	Expressed in podocytes and interacts with actin to regulate the shape and motility of podocyte foot processes. Synaptopodin levels are dramatically reduced in idiopathic nephrotic syndrome.[252,253]
TCF21/POD1	Transcription factor 21	6q23-q24	Responsible for glomerulogenesis in mice and podocyte differentiation.[254,255]
TGFB1	Transforming growth factor beta 1	19q13.2	Involved in podocyte differentiation and apoptosis, while it is elevated in hyperglycemic conditions causing diabetic nephropathy. [256,257]

Gene	Name	Chromosome	Information
TIMP1	Tissue inhibitor of metallopeptidase 1	Xp11.23	Inhibits MMPs and is elevated in diabetic nephropathy, thus influencing extracellular matrix accumulation. [258]
TIMP2	Tissue inhibitor of metallopeptidase 2	17q25.3	Inhibitor of MMP2 and implicated in extracellular matrix accumulation in diabetic nephropathy. [259]
TIMP3	Tissue inhibitor of metallopeptidase 3	22q12.3	TIMP3 knocked out mice developed chronic fibrosis in kidney proximal tubules. [260]
TIMP4	Tissue inhibitor of metalloproteinase 4	3p25	Found to interact with MMP2 and MMP9 in matrix accumulation and glomerulosclerosis observed in hypertensive rat models. [261]
TJP1	Tight junction protein 1 (zona occludens 1)	15q13.1	Expressed at the slit diaphragms of the glomerular epithelium [262]
TRPC6	Transient receptor potential cation channel, subfamily C, member 6	11q22.1	Focal segmental glomerulosclerosis type 2 (FSGS2) [263]
WT1	Wilms Tumor 1	11p13	Regulates the functionality of podocytes and is found to be reduced in glomerulonephritis and mesangial sclerosis, while a mutation in WT1 causes membranoproligerative glomerulonephritis. [264,265]

APPENDIX II

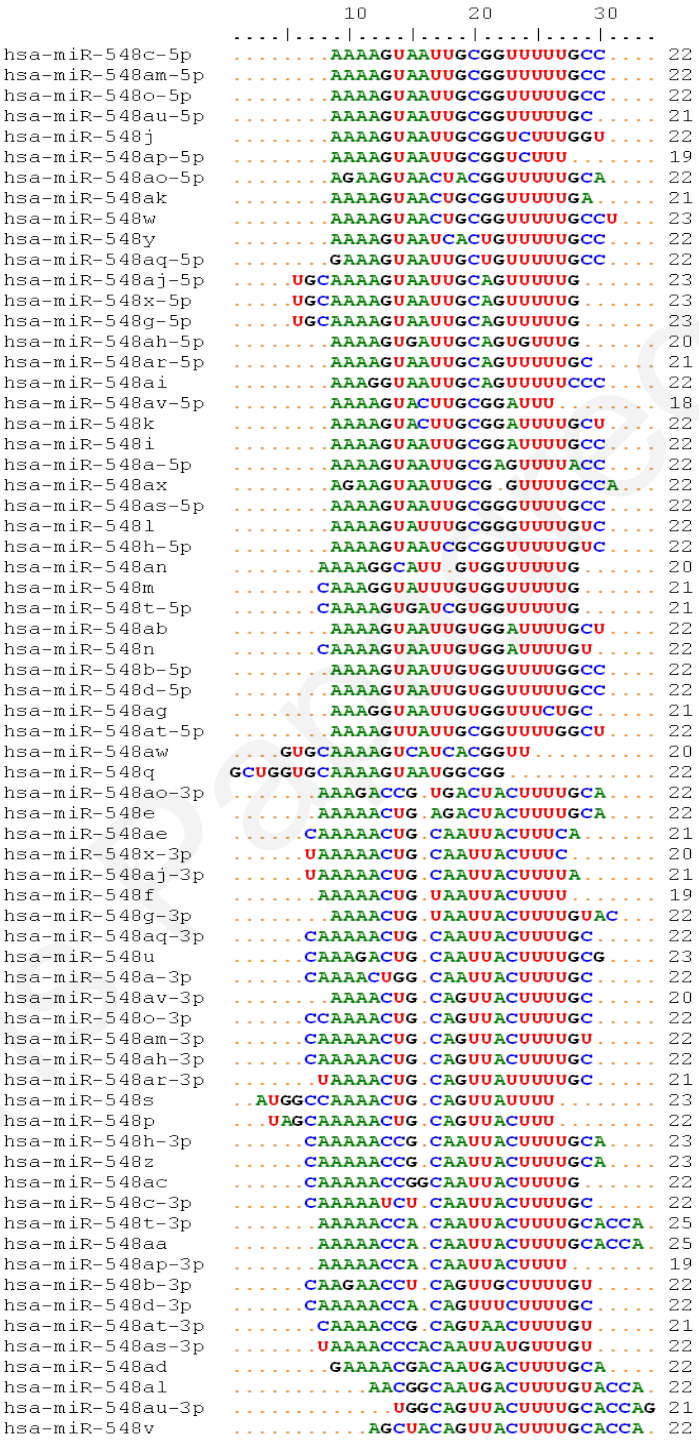

Figure 24: Multiple sequence alignment of all miR-548 family members.